STUDY OF THE DEVELOPMENT OF PLASTIC HINGES IN COMPOSITE STEEL-CONCRETE STRUCTURAL MEMBERS SUBJECTED TO SHEAR AND/OR BENDING

Teză destinată obţinerii
titlului ştiinţific de doctor inginer
la
Universitatea "Politehnica" din Timişoara
în domeniul Inginerie Civilă
de către

Ing. DANKU GELU

Conducător ştiinţific: Prof.Dr.Ing.Dr.H.C. Dan DUBINA,
    M.c. al Academiei Române
Referenţi ştiinţifici: Prof.Dr.Ing. Luis Simoes DA SILVA
    Prof.Dr.Ing. Cosmin CHIOREAN
    Conf.Dr.Ing. Adrian CIUTINA

Ziua susţinerii tezei: **22.07.2011**

Acknowledgements

Timişoara, July 2011   Eng. Danku Gelu

Danku Gelu

STUDY OF THE DEVELOPMENT OF PLASTIC HINGES IN COMPOSITE STEEL-CONCRETE STRUCTURAL MEMBERS SUBJECTED TO SHEAR AND/OR BENDING

Abstract:
The accuracy of concentrated plasticity models applied in dissipative zones of composite steel-concrete beams in case of joints from Moment Resisting Frames (MRF), and in case of links from Eccentric Braced Frames (EBF) is still a matter of discussions. To simplify the problem, a quite current practice, is to not install connectors in the expected plastic zones, and to consider having symmetric moment or shearing plastic hinges, which occurs in the steel beam or link only. However, since the reinforcing bars still remain active, even if the connectors have been suppressed , and also due to some friction contact between concrete slab and beam or link flange the assumption of the "nominal "symmetric" plastic hinge could be false.

Intensive experimental research on composite beam-to-column MR joints and portal EBFs, accompanied by advanced numerical simulations were carried out in the CEMSIG Research Centre (http://cemsig.ct.upt.ro) of PU Timisoara in order to check the validity of this assumption. Reference single steel specimens and then composite ones, with and without headed connectors, have been tested under monotonic and cyclic loading.

Based on test results and accompanied by numerical simulation, potential multi-linear models for time-history analyses are suggested and discussed. The thesis summarizes the experimental and numerical investigation and presents the main conclusions of the research.

TABLE OF CONTENTS

List of figures

List of tables

Notations, abbreviations & acronyms

Notations

Chapter 2

q	Behaviour factor (Europe)
e	Length of link
$M_{pl,link}$	Plastic resisting moment of link
$V_{pl,link}$	Plastic resisting shear force of link
N_{Rd}	Axial strength
M_{Ed}	Design bending moment
V_{Ed}	Design shear force
γ_{ov}	Factor with accounts for supplied material
Ω	Overstrength factor - accounts for the strength reserve in main dissipative elements
b_{eff}	Effective width of concrete slab
$I_{equivalent}$	Equivalent moment of inertia of the composite cross section

Chapter 3

f_y	yield limit
f_u	ultimate strength
P_{rd}	strength of a shear connector
h	height of connector
d	diameter of connector
e_y	Yield displacement (ECCS)
Tc	Corner period
a_g	Peak ground acceleration
F_i	Seismic level force
F_b	Base shear force
s_i	Level height
λ	Ground motion intensity factor
D_y	Yield displacement
S_{ini}	Initial rigidity
F_y	Yield force
$S_{j,link}$	Initial link rigidity
V_{max}	Maximum shear force
γ_{RBS}	Rotation of the reduced beam section
γ_{weld}	Rotation at the welds' level
$\gamma_{col.web}$	Rotation of the column web plate
h_c	Height of the column section
h_b	Height of the beam section
t_{fb}	Thickness of the beam's flange
t_w	Thickness of the web
η	Seismic capacity factor

Abbreviations & acronyms

AISC	American Institute of Steel Constructions (http://www.aisc.org/)
CEMSIG	Research Centre for Mechanics of Materials and Structural Safety - CEMSIG is a RTD (Research and Technical Development) unit of the "Politehnica" University of Timisoara, at the Faculty of Civil Engineering, Department of Steel Structures and Structural Mechanics (http://cemsig.ct.upt.ro/cemsig/index.php)
FEMA	Federal Emergency Management Agency is an agency of the United States Department of Homeland Security (http://www.fema.gov/)
MRF	Moment resisting frame
EBF	Eccentrically braced frame
CBF	Centrically braced frame
FEM	Finite element method
RBS	Reduced beam section
DUAL	Dual frame - generally involves a combination of a braced frame and an unbraced moment resisting frame
FE	Finite element
IDA	Incremental Dynamic Analysis
PGA	Peak ground acceleration
ULS	Ultimate limit state
SLS	Serviceability limit state
CPLS	Collapse prevention limit state
IO	Immediate occupancy
LS	Life safety
CP	Collapse prevention
CWP	Column web panel

REZUMAT

Teza de doctorat îşi propune să studieze comportamentul articulaţiilor plastice din grinzile compuse. Acurateţea modelelor pentru articulaţiile plastice din zonele disipative ale grinzilor compuse oţel-beton (mai precis o grindă din oţel care conlucrează cu placa din beton prin intermediul unor conectori) care fac parte din configuraţia cadrelor necontravântuite MRF (Moment Resisting Frames) sau contravântuite excentric, cu link scurt, EBF (Eccentrically Braced Frame) este un subiect controversat. Pentru a simplifica problema, în practica curentă nu se dispun conectori în zonele potenţial plastice şi se mizează pe un comportament simetric de încovoiere sau forfecare. Totuşi, datorită prezenţei armăturilor din placă şi datorită forţelor de frecare care apar la interfaţa dintre cele două materiale, ipoteza în care se consideră dezvoltarea unei articulaţii plastice simetrice în secţiunea din oţel s-ar putea dovedi a fi falsă.

În vederea evaluării acestor probleme, în cadrul centrului de cercetare CEMSIG (http://cemsig.ct.upt.ro) din Universitatea „Politehnica" Timişoara s-au efectuat teste experimentale pe noduri grindă-stâlp şi cadre contravântuite excentric. S-au încercat atât specimene din oţel, care au servit ca referinţă, cât şi specimene compuse, cu sau fără conectori, în regim monoton şi ciclic.

Pe baza rezultatelor experimentale şi a calibrărilor numerice, modele multilineare pentru articulaţiile plastice sunt propuse şi analizate. Teza prezintă rezultatele experimentale şi numerice obţinute, precum şi concluziile principale ale cercetării.

Capitolul I: Introducere
Se încadrează subiectul tezei în tematica actuală, este descris scopul tezei şi obiectivele tezei (justificate). Se prezintă cadrul în care s-a desfăşurat teza – participarea doctorandului la contracte de cercetare şi încadrarea în contextul programelor de cercetare naţionale.

Capitolul II: Comportamentul grinzilor compuse în zonele plastice
Se tratează stadiul actual de cunoaştere a problematicii din teză. Se descriu (structurat, sub formă de review) rezultatele obţinute cu privire la probleme similare, conexe, în lume (publicaţii, rapoarte de cercetare). Sunt amintite studiile lui James Ricles, Michael Engelhardt, Andre Plumier & Catherine Doneaux, ş.a.

Sunt comentate rezultatele obţinute în studiile existente şi se subliniază eventualele aspecte din norme, în special EC4 şi EC8 care tratează subiectul zonelor disipative din grinzile compuse.

În cadrul concluziilor se exprimă aspectele ce nu sunt rezolvate sau lasă loc pentru alte abordări, respectiv sunt tratate necorespunzător.

Capitolul III: Program experimental
Se prezintă programul propriu-zis de încercări experimentale, pe două ramuri principale: cadre EBF cu link scurt şi noduri grindă-stâlp cu dog-bone.

Proiectarea programului experimental are la bază proiectarea cadrului structurii de bază duale (împreună cu toate analizele efectuate), inclusiv simularea comportării specimenelor în condiţii experimentale, cu modelarea în programe de calcul (SAP2000, Abaqus).

Este prezentat în detaliu standul experimental, instrumentarea şi parametrii monitorizaţi, precum şi protocoalele de încărcare utilizate. Testele cuprind atât specimene cu grinzi din oţel (profile europene) cât şi specimene cu grinzi compuse (profil plus placa din beton de 12 cm). Au fost încercate un număr de 8 cadre EBF şi 6 noduri grindă-stâlp în diverse configuraţii.

Încercările experimentale sunt descrise în ordinea efectuării lor. Se prezintă rezultatele primare aşa cum au rezultat din înregistrarea încercărilor, inclusiv observaţiile privind comportarea specimenelor în timpul testelor. Se evidenţiază interpretarea rezultatelor experimentale pe curbe forţă tăietoare-rotire şi moment-rotire şi curbe înfăşurătoare. Se arată gradul de participare a componentelor şi energia disipată/ciclu şi energiile cumulate. Concluzii.

Capitolul IV: Program de simulări numerice

Sunt evidenţiate modelele existente pentru articulaţiile plastice, modul lor de definire şi implementarea lor în programele de calcul mai uzuale. Se prezintă calibrarea unui model experimental pentru bara disipativă scurtă şi pentru zona adiacentă îmbinării grindă-stâlp în următoarele tipologii:

- element din oţel
- element compus

Scopul capitolului este de a se arăta influenţa conexiunii oţel-beton asupra performanţelor cadrelor analizate.

Este prezentată proiectarea cadrelor – 8 tipuri de cadre (fiecare cu câte 3 deschideri): cadru dual P+4, cadru dual P+12, cadru necontravântuit P+5, cu 3 deschideri de 8m, cadru necontravântuit P+5, cu 3 deschideri de 6m, cadru contravântuit excentric P+6, cadru contravântuit excentric P+8, cadru dual P+8.

Cadrele folosite în analizele numerice au fost simulate în 2 variante de grinzi: oţel şi compuse. Se consideră pentru analizele incremental dinamice, cutremurele Vrâncene din '77, '86 si '90. (7 accelerograme). Se enumeră apoi rezultatele analizelor de tip push-over şi TH.

În concluzie se prezintă importanţa modelării elementelor mixte în zonele plastice în funcţie de interacţiune şi modelele propuse. Se arată dacă se confirmă sau nu ipotezele iniţiale şi metodologia care se propune în acest scop.

Capitolul V: Metodologie şi prescripţii de proiectare

Se prezintă o metodologie de proiectare propusă de autor, împreună cu câteva prescripţii care asigură un comportament corespunzător al structurilor cu grinzi compuse sub acţiunea cutremurelor. Metodologia este mai apoi demonstrată pe un studiu de caz.

Capitolul VI: Concluziile şi contribuţiile tezei

Capitolul sintetizează concluziile tezei şi prezintă principalele contribuţii ale tezei cu privire la tematica subiectului.

SUMMARY

The accuracy of concentrated plasticity model to be applied in dissipative zones in composite steel concrete beams (e.g. steel beam cooperating with reinforced concrete slab) in case of Moment Resisting joints, in MR Frames (MRF), and in case of links, from Eccentric Braced Frames (EBF) still is matter of discussion. To simplify the problem, a quite current practice, is to not install connectors in the expected plastic zones, and to consider having symmetric moment or shearing plastic hinges, which occurs in the steel beam or link only. However, since the reinforced bars still remain active, even the connectors have been suppressed , and also due to some friction contact between concrete slab and beam or link flange the assumption of the "nominal "symmetric" plastic hinge could be far enough from reality.

Intensive experimental research on composite beam-to-column MR joints and portal EBF, accompanied by advanced numerical simulations were carried out in the CEMSIG Research Centre (http://cemsig.ct.upt.ro) of PU Timisoara in order to check the validity of this assumption. Reference single steel specimens and then composite ones, with and without headed connectors, have been tested under monotonic and cyclic loading.

Based on test results and accompanied by numerical simulation, potential multi-linear models for time-history analyses are suggested and discussed. The thesis summarizes the experimental and numerical investigation and presents the main conclusions of the research.

Chapter I: Introduction

The thesis is considering the subject in the framework of current research, worldwide. The scope and main points of the thesis are explained and justified. The thesis was part of a larger research grant, through which its author was involved in a number of research programs.

Chapter II: Behaviour of composite sections in plastic zones

Second chapter presents worldwide similar studies, their conclusions and main ideas. The chapter contains a review of the most important existing data regarding the research of composite beams under cyclic loads. The research of James Ricles, Michael Engelhardt, Andre Plumier & Catherine Doneaux are mentioned here.

The obtained results of the previous studies are commented upon, while the problems which still have issues are pointed out. The current European norms and provisions related to the subject are discussed.

Chapter III: Experimental program

The experimental program designed and conducted by the author is presented, on its two main directions: EBF frames and beam-to-column joints with RBS.

The design of the experimental program started with a full size dual frame, on which nonlinear analyses were also performed. The test specimens' behaviour was simulated in advanced numerical programs (such as SAP2000, Abaqus).

The experimental setup is presented in detail, together with all of the monitored parameters and loading protocols. The tests comprise of single steel specimens (European hot rolled profiles) and composite beam specimens (steel

profile plus a 12 cm concrete slab). A number of 8 EBFs and 6 beam-to-column joints were tested in various configurations.

The specimens are described in the order they were tested. The primary results are shown, including the observations regarding specimens' behaviour during the tests. The main differences are pointed out through shear force vs. rotation curves in the case of EBFs and moment-rotation curves in case of the tested joints. The dissipated energies are also compared together with close consideration of the degree of interaction between components. Conclusions are stated.

Chapter IV: Numerical study

Existing models are discussed, considering both their theoretical approach and implementation in design software. The calibration of an experimental model is presented for the short link and also for the reduced section of the beam, adjacent to the column. The subject is considered by two approaches:
- Steel element
- Composite element

Conclusions of the modelling are presented.

The main target of this chapter is to underline the influence of steel-concrete interaction towards the performance of analyzed frames.

The design of the frames is presented (each is a facade frame from a full-size building) and their configurations: dual 4 story frame, dual 8 story frame, dual 12 story frame, 5 story moment resisting frame (one with 3 spans of 8m and one with 3 spans of 6m), eccentrically braced frame with 6 and 8 stories.

These structures were used in numerical analyses and were modelled using two approaches: with steel beams and with composite beams. A number of 7 earthquake recordings were used for the IDA (incremental dynamic analyses). In the later part of this chapter, the results of push-over and time-history analyses are presented and discussed.

The conclusions reveal the importance of the correct modelling of the composite elements in the plastic zones of frames and the proposed models. The initial hypotheses are shown to be true or false, and a design methodology is proposed.

Chapter V: Design approach and proposed provisions

The chapter presents a design methodology proposed by the author, together with some prescriptions that are meant to ensure a correct behaviour of structures with composite beams subjected to earthquakes. The methodology is then exemplified on a case study.

Chapter VI: Conclusions and contributions of the thesis

The chapter shows the main conclusions of the study and presents the main contributions of the thesis towards the subject.

1. INTRODUCTION

1.1 Generals

The accuracy of plastic hinge models used in the dissipative zones of composite beams (in case of joints in Moment Resisting Frames and links in Eccentrically Braced Frames) is an up-to-date subject, the advantages of using composite solution being at the moment under investigation. The current practice in using composite beams in MRFs and EBFs advises not to install shear connectors in the zones where the plastic hinge is expected to develop and to consider a symmetric plastic behaviour for the beam, just as for the steel only section. However, due to the presence of the reinforced concrete slab (even if there are no connectors installed) and the friction between the steel profile and slab, the plastic hinge on beams will not have a symmetric behaviour under hogging and sagging moments, as it happens in case of current steel sections. This fact rises questions regarding the specific design criteria, and, very important, what values to be used for behaviour and overstrength factors.

The thesis summarizes the research carried out at the Department of Steel Structures of „Politehnica" University of Timisoara, aiming to answer these questions. Both experimental and numerical studies have been developed to observe and characterise the mechanism of plastic hinges for composite steel-concrete sections under predominant bending moments or shear.

Research is based on observing the behaviour of composite hinges of shear and bending, analysed as part of DUAL frame systems, consisting of MRF and EBF.

MRFs are widely used for structures of low and medium height. These frames are capable to offer a sufficient dissipation capacity through the relatively big number of plastic zones (at the ends of beams). In this way the requirements for preventing collapse are satisfied even in the case of severe earthquakes. Although, it is quite difficult to limit the damage in case of serviceability limit states (by limiting the lateral deformations), once the height of the building is increasing. This is mainly due to the fact that the lateral rigidity reduces once the height increases, even if the global number of hinges is increased.

On the other hand, EBFs offer high lateral rigidity, while the dissipation occurs in the link elements, by inelastic distortion.

By combining the two structural systems (moment resisting and braced frames), the DUAL configuration was obtained:
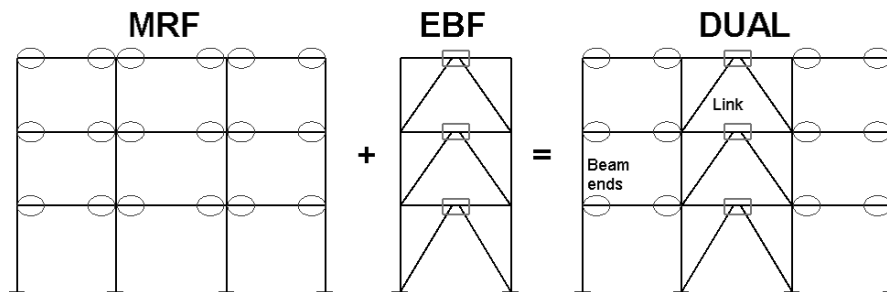
Fig. 1.1.   Plastic zones from MRF, EBF and DUAL configurations

The transmitting of lateral loads is achieved through the diaphragm effect of the floors, while the MRFs should be able to withstand 25% of the lateral forces in order for the DUAL system to function efficiently. The dissipative zones of the DUAL frames are considered at both ends of the MRF beams and in the link from the EBF (marked zones in Fig. 1.1).

Modelling of the plastic zones of these frames is quite difficult because it has to include the pinching effect and geometric nonlinearities. However, simplified models which characterise quite accurately the behaviour of either bending or shear hinges for steel elements already exist in literature.

1.2 Composite behaviour

The usage of composite beams within multi-storey steel structures is justified by their load-bearing efficiency and material savings. When considering a structure with composite elements which requires to be designed in a seismic area, certain ductility requirements arise, while the whole structure needs to attain prescribed performance levels. Much progress has been made, for example in Japan, where the structural steel/reinforced concrete frame is the standard system for tall buildings. The main reason for this preference is that the sections and members are best suited to resist repeated earthquake loadings, which require a high amount of resistance and ductility.
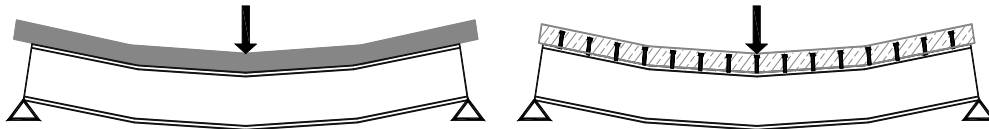
Fig. 1.2.   Non-composite and composite beams [1]

When discussing the behaviour of composite beams, it is known that for the non-composite beam the load will be sheared between the 2 parts (slab and steel profile) with each deforming in bending, generating separately the typical linear variation of elastic strain ε over its own depth.

The composite beams are more efficient structurally because they develop smaller deflections and strains than the non-composite beam. The deflection in the composite beam may be 25% smaller than the deflection in the non-composite beam. In composite beams the steel beam is designed to act with the slab, preventing the slip at the interface using the shear connectors. These are welded or shot-fired to the structural steel and enclosed by concrete.

While modelling of sections made of a single material has no more secrets for the structural engineer, when it comes to composite cross sections, the problems that arise regard both boundary conditions at the interface of the materials, the simultaneous definition of two or more materials and estimating the plastic behaviour of the resulting section.

1.3 Objective of the thesis

The main objective of the thesis is to study the hypothesis which states that when no connectors are disposed in the plastic zone of a composite beam, the behaviour of the plastic hinges resembles the model of the "pure" steel cross-section. In this idea, the influence of the interaction between the steel profile and concrete slab in the potentially plastic zones of composite beams from MR and EB frames is studied. As results of the study, multilinear hinge curves are proposed and conclusions regarding the seismic behaviour of composite beams are discussed, together with the proposal for a coherent numerical model (included in global analyses) based on experimental and simulation data. The key-points in the numerical simulation are the modelling of both plastic hinges (bending or shear) and composite behaviour of elements. This subject is tackled in the following relevant chapters, i.e. 3, 4 and 5 (in which a design methodology is proposed and tested).

2. HISTERETIC BEHAVIOUR OF STEEL-CONCRETE COMPOSITE SECTIONS

2.1 Introduction

The presence in the dissipative parts of the beams of two materials, out of which one is homogeneous (steel) while the other has a different behaviour in tension and in compression (the case of concrete), leads to a difficult calculus evaluation of the global plastic behaviour of such beams. In the dissipative zones it is generally essential to allow for the development of plastic hinges, with good rotation demands and high ductility.

Present chapter aims at providing the background of existing world-wide studies close to the subject and a brief review of existing code provisions in tight connection

2.2 Design concepts

Earthquake resistant composite structures must be designed according to one of the following concepts:

Concept a: Dissipative structural behaviour with composite plastic hinges
Concept b: Dissipative structural behaviour with steel plastic hinges
Concept c: Non-dissipative structural behaviour.

Concepts "a" and "b" consider the capacity of dissipative zones from the structures to develop and maintain plastic hinges. In these concepts, the value of the design behaviour factor "q" will be greater than 1.0.

In concept "b", only the steel section is considered in the process of seismic design, without considering the advantages or disadvantages that the concrete slab may bring in the dissipative zones; application of this concept is generally governed by measures which imply either disconnecting the concrete slab in the plastic zone, or assuring that the slab does not work together with the steel section. The composite structure needs to be designed according to EC4 and by considering the provisions of EC8 regarding the subject.

In concept "c", the seismic loads' effect on the structure is evaluated by elastic analyses, without even considering non-linear behaviour.

When lateral loads due to an earthquake are applied to a structure with composite beams cracks develop in the concrete slab under the action of negative moment. Cracking of the concrete slab has been found to decrease the strength of a composite beam under cyclic loading [2]. That is why it is generally assumed in design that the concrete slab has no tensile strength, the negative moment capacity of a composite beam is thus equal only to that of the steel section and longitudinal slab reinforcement.

There are relatively few tests that have been conducted on the behaviour of composite beams subjected to cyclic loading. Humar [3] conducted tests on composite beams with solid concrete slabs. The results of his studies have shown that if longitudinal reinforcement is placed in the slab and premature web buckling of the steel section is prevented then the steel-concrete composite sections exhibit

stable hysteretic loops when subjected to cyclic loading. It results that some degree of composite action can be maintained under cyclic loading.

Research [4][5] has provided data which shows that the effective width of composite beams under monotonic loading is influenced by several factors, among which we can mention load distribution along the span, cross sectional properties of the composite beam and boundary conditions. Experiments have proved that cracking of the slab results in a decrease of the effective width. Cyclic load tests on composite beams in Japan [6] have indicated that the effective width decreases as the inelastic range of testing commences, decreasing as the amplitude of the cyclic loading is increased. Based on the above issues, it seems that the degree of deterioration of the composite action is not only related to the loss of shear connection but also to the amount of slab cracking.

Tests involving vertical shear in continuous composite beams subjected to monotonic loads [7] indicate that if longitudinal reinforcement is provided in the slab and has not yielded, then this reinforcement will carry a portion of the vertical shear. Once the reinforcement yields, the steel section has to be able to take all vertical shear stresses. This gives an indication that under severe cyclic loading, where the concrete slab cracks and yielding of longitudinal reinforcement takes place, the steel section in a composite beam is likely to provide most of the vertical shear resistance.

At the beginning of the 80's, as part of a US-Japan research program [2], tests were conducted in Tsukuba, Japan on a K-braced EBF with a composite floor system. The results of the tests indicated that composite links performed well and were able to withstand a major earthquake with minor damage. The cracking and damage to the concrete slab was local and mostly in the region directly above the links which had experienced plastic deformations. The failure of the test structure occurred by a failure of a brace gusset place. Required axial brace forces were computed with the structure in its steel solution, ignoring the effects of composite floor slabs on the links' capacity. However, no general conclusions could be drawn, since the test program involved only one structure and one simulated earthquake.

Since the earthquakes of 1994 in Northridge and of 1995 in Kobe, intensive research and testing efforts have been underway to find better methods to design and construct seismic resistant steel frames. A number of improved beam-to-column connection design strategies have been proposed [8], many of which have shown to exhibit satisfactory levels of ductility in numerous tests. Two key concepts have been developed in order to provide highly ductile response and reliable performance: strengthening the connection and/or weakening the beam, in order to avoid damages of the respective column.

The final purpose of the research is to provide a beam-to-column connection that is stronger than the beam section. It is intended to force the plastic hinge away from the face of the column, and to develop the large stresses and inelastic strains further into the beam. Reinforcing the connection, however, increases its cost and also, if excessive reinforcement is used, new problems can result due to the need for very large welds and higher degrees of restraint. An alternative to reinforcing a moment connection that provides benefits similar to reinforcement, and may avoid some of the disadvantages, is the Reduced Beam Section (RBS) in the vicinity of the connection, also known as the `dog bone' moment connection. The concept of the RBS was proposed by Plumier, since 1990 [9][10]. However, the typology and the

technology of the RBS beam-to-column connection, as well as its behaviour under cyclic load conditions, were comprehensively investigated, in USA, after the Northridge earthquake [11].

The idea of weakening the beam relies on the fact that portions of the beam flanges are trimmed away in the region adjacent to the beam-to-column connection. Various shapes cut-outs are possible (constant, tapered or radius cut) to reduce the cross sectional area. The RBS can be viewed as a ductile fuse. It forces yielding to occur within the reduced section of the beam, an area that can sustain large inelastic strains, while at the same time, limiting stress at the less ductile region near the face of the column. Extensive experimental [12][13][14] and analytical [15][16][17] projects have been conducted proving the effectiveness of this solution. It is apparent that the tapered element shall not present any geometrical discontinuities, in order to avoid the trigger of cracks during inelastic excursions. To this end the RBS profile shape should be curved. Furthermore, experimental investigations have demonstrated that the curved RBS behaves with the highest rotational capacity with respect to polyline shaped solutions [18][19].

Concluding the research efforts of the SAC program [12], recommendations for the design and detailing of the RBS member were prescribed in FEMA 350 [8] and FEMA 351 [20] documents.

In Europe, also, following the spirit of the above mentioned recommendations, in Eurocode 8, Part 3, [21], the design of such type of connections are presented. In Fig. 2.1 proposals for radius cut from FEMA 350 [8], which prequalified this shape, and Eurocode 8 Part 3 are presented. One can remark that the a and b values from Eurocode 8, Part 3 are the average values compared to FEMA 350, while for g; s and r the same values were adopted. It is not worthwhile to highlight the difference between the US and European design practice; besides, there are no experimental studies that use the European Profiles, excepting the studies conducted by Plumier [9].

Geometrical characteristics of the reduced beam section	
FEMA 350 [1]/ 351 [13]	EC 8, Part 3 [14]
$a = 0.50 - 0.75b_f$	$a = 0.60b_f$
$b = 0.65 - 0.85d_b$	$b = 0.75d_b$
$c \leq 0.25b_f$	$g \leq 0.25b_f$
$s = a + b/2$	$s = a + b/2$
$r = (4c^2 + b^2)/8c$	$r = (4g^2 + b^2)/8g$

RBS with radius cut
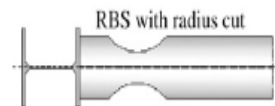
Fig. 2.1.   Prescribed values for the design of the RBS and frequent cut shapes [25]

2.3 Code provisions

MRFs should be designed as ductile structures which dissipate large amounts of energy during earthquakes, thus preserving the integrity of the structure. The dissipation is mainly obtained through inelastic deformation of elements, usually in beams or joints. Ductility of a MRF requires careful design of the beams and columns in order to meet the so-called "strong column – weak beam" concept, with proper details for the column joint. For usual design, reduced beam sections (RBS) solutions could be used. The RBS solution proved to be a very good solution for dissipating energy by avoiding the plasticization of the neighbouring connection (with a more complex behaviour). Although a high amount of research was conducted on RBS, the subject is still under development due to the need to find the

best suitable way to adjust the steel sections of beams adjacent to joints and the way in which the composite beam influences the formation of plastic hinges.
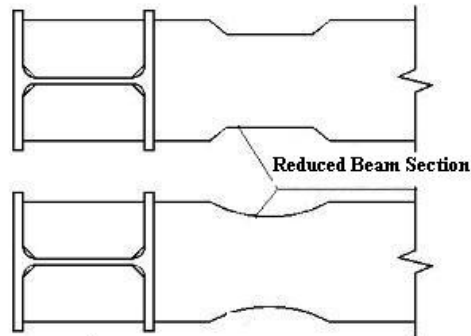
Fig. 2.2.   Examples of the Reduced Beam Section (solution known also as „dog-bone")

On the other hand, by design, the EBFs should posses both properties of high elastic lateral stiffness and good energy dissipation capacity.

The lateral deformation is generally limited by the presence of braces, while the high-dissipation character is accomplished by the „link" which by design should be the dissipative part of the structure. All the other elements should be designed as non-dissipative. Some typical configurations for such systems are shown in the picture below:
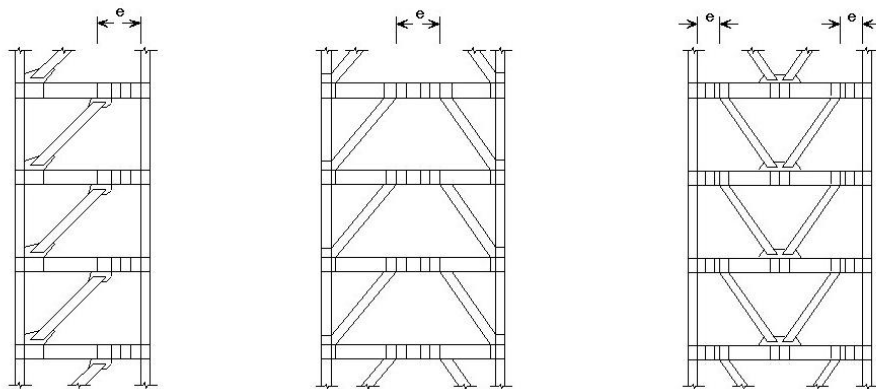
Fig. 2.3.   Types of eccentrically braced frames: "D" brace system, "K" brace system

and "V" brace system

Under severe seismic ground motion where inelastic behaviour is expected, the links act as fuses for dissipating energy. Depending on the length of the link, the seismic energy is dissipated through elastic-plastic cycles of shear (for short links), bending (for long links) or shear and bending (for intermediate links).

If we denote by „e" the length of the link, then:

- for short links: $e \leq 1.6 \cdot \dfrac{M_{pl,link}}{V_{pl,link}}$, pure shear hinge mechanism;

- for intermediate links: $1.6 \cdot \dfrac{M_{pl,link}}{V_{pl,link}} < e < 3.0 \cdot \dfrac{M_{pl,link}}{V_{pl,link}}$, bending and shear

                                                                  hinge mechanism

- for long links: $e \geq 3.0 \cdot \dfrac{M_{pl,link}}{V_{pl,link}}$, bending hinge mechanism

Links are known to be excellent energy dissipaters under cyclic loading, provided that the ultimate limit state of the link can be developed and maintained. According to the current Eurocode 8 provisions the other frame members must be designed and detailed by considering an overstrength (especially columns and braces). These members should be verified considering the most unfavourable combination of axial force and bending moment, such that :

$$N_{Rd}(M_{Ed}, V_{Ed}) \geq N_{Ed,G} + 1.1 \gamma_{ov} \Omega N_{Ed,E}$$

where,

$N_{Rd}(M_{Ed}, V_{Ed})$ is the axial resistance of the column or brace, considering the bending moment – shear force interaction, taken from the corresponding seismic design combination;

$N_{Ed,G}$ is the axial force from the column or brace due to non-seismic actions which are included in the seismic combinations;

$N_{Ed,E}$ is the axial force from the column or brace due to the design seismic action;

γ_{ov} is an amplification coefficient, taken from SR EN1998-1, par.6.1.3(2) and 6.2(3) (usually 1.25);

Ω is the overstrength factor, taken from SR EN1998-1, par. 6.8.3, as:

$$\Omega_i = 1.5(V_{pl,link}/V_{Ed}) \text{ for short links}$$

$$\Omega_i = 1.5(M_{pl,link}/M_{Ed}) \text{ for medium and long links}$$

2.3.1 Eurocode provisions

Composite action between steel beams and concrete slab is generally meant to improve the rigidity and resistance of the member, needing careful design and detailing according to specific sections of Eurocode 4 and Eurocode 8. A special attention is paid to the detailing of the shear connection between the two materials: steel and concrete (which have a very different elastic and post-elastic behaviour). However, when lateral loads such as earthquakes are acting on a structure having composite beams, the bending moment may suffer a cyclic reversal leading to cracks in the concrete slab due to tension efforts. Special detailing and requirements are given in the actual seismic design codes for composite beams subjected to seismic loads, such as:

- special requirements for the connecting devices (SR EN1998-1, par.7.6.2);

- special requirements for the detailing and positioning of the reinforcement of the beams adjacent to beam-to-column joints (SR EN1998-1, par. 7.6.2 and Annex C.3.1.2);

- special requirements for design as dissipative or non-dissipative elements.

In what concerns the use of composite RBS or composite links, the in-use norms are very poor in details and requirements, practically limiting the composite interaction up to the physical boundaries of the dissipative element. The following paragraphs extracted from Eurocode 8 show the considerations regarding the composite interaction on ductile elements:

„§7.6.2 Steel beams composite with slab

(1)P The design objective of this sub clause is to maintain the integrity of the concrete slab during the seismic event, while yielding takes place in the bottom part of the steel section and/or in the rebars of the slab.

(2)P If it is not intended to take advantage of the composite character of the beam section for energy dissipation, 7.7.5 shall be applied.

§7.7 Design and detailing rules for moment frames

§7.7.1 Specific criteria

(1)P 6.6.1(1)P applies.

(2)P The composite beams shall be designed for ductility and so that the integrity of the concrete is maintained.

§7.7.5 Conditions for disregarding the composite character of beams with slab.

(1)P The plastic resistance of a beam section composite with slab (lower or upper bound plastic resistance of dissipative zones) may be computed taking into account only the steel section (design in accordance with concept c) as defined in 7.1.2) if the slab is totally disconnected from the steel frame in a circular zone around a column of diameter $2b_{eff}$, with b_{eff} being the larger of the effective widths of the beams connected to that column.

(2) For the purposes of (1)P, "totally disconnected" means that there is no contact between slab and any vertical side of any steel element (e.g. columns, shear connectors, connecting plates, corrugated flange, steel deck nailed to flange of steel section).

(3) In partially encased beams, the contribution of concrete between the flanges of the steel section should be taken into account.

§7.9.3 Links

(1)P Links shall be made of steel sections, possibly composite with slabs. They may not be encased."

By 7.7.5(1) the plasticization is thought as for a steel element, ignoring the fact that the beam is composite up to the boundaries of the dissipative element. However, the adjacent composite beam has a certain influence on the behaviour of the dissipative element.

Up to this moment there is sufficient information about the behaviour of the composite beams under monotonic loads [23], but still there are some pressing issues when considering the behaviour of composite beams of EBF's and beam-to-column joints in MRF subjected to cyclic loads. These issues mainly regard the hysteretic behaviour of links when using composite beams, the influence of the presence of shear connectors in the expected plastic zones and whether the braces and columns posses enough overstrength in case of fully composite beams if the design is done by using bare steel guidelines.

Traditionally, due to the dual composition of the dissipative area in composite beams (steel – homogeneous material, characterized by buckling in

compression; concrete – different behaviour in tension and compression) it is engineering difficult to predict a behaviour law in case of cyclic loads. Thus in the dissipative zones it is essential to develop plastic hinges with a high degree of ductility and considerable plastic rotations. Generally this issue is achieved by steel sections only, but the concrete's presence could introduce an additional influence.

2.3.2 AISC 341/2005 provisions

The American document also gives some rules for the design of composite beams, but these are quite general and do not give specific information regarding the subject of plastic hinges in composite elements:

- In part II of the document, Section 14.3. – Links in C-EBF (composite eccentrically braced frames): *Links shall be unencased structural steel and shall meet the requirement for eccentrically braced frame (EBF) links in Part I Section 15. It is permitted to encase the portion of the beam outside of the link in reinforced concrete. Beams containing the link are permitted to act compositely with the floor slab using shear connectors along all or any portion of the beam if the composite action is considered when determining the nominal strength of the link.*

- In Section C6.3. Composite Beams: *These provisions apply only to composite beams that are part of the seismic load resisting system. While these Provisions permit the design of composite beams based solely upon the requirements in the Specification, the effects of reversed cyclic loading on the strength and stiffness of shear studs should be considered. This is particularly important for C-SMF (Composite-Special Moment Frames) where the design loads are calculated assuming large member ductility and toughness. In the absence of test data to support specific requirements in these Provisions, the following special measures should be considered in C-SMF: (1) implementation of an inspection and quality assurance plan to insure proper welding of shear stud connectors to the beams (see Sections 18 and 19); and (2) use of additional shear stud connectors beyond those required in the Specification immediately adjacent to regions of the beams where plastic hinging is expected.*

- In Section C 14: *Satisfactory behaviour of C-EBF (Composite-Eccentrically Braced Frame) is dependent on making the braces and columns strong enough to remain essentially elastic under loads generated by inelastic deformations of the links. Since this requires an accurate calculation of the shear link nominal strength, it is important that the shear region of the link not be encased in concrete. Portions of the beam outside of the link are permitted to be encased since overstrength outside the link would not reduce the effectiveness of the system. Shear links are permitted to be composite with the floor or roof slab since the slab has a minimal effect on the nominal shear strength of the link. The additional strength provided by composite action with the slab is important to consider, however, for long links whose nominal strength is governed by flexural yielding at the ends of the links (Ricles and Popov, 1989).*

2.4 Summary review of existing research

The current subchapter consists of a literature review of selected papers appreciated as relevant for the subject. Of course, such a review, based on author's selection, cannot be exhaustive.

2.4.1 Experiments on eccentrically braced frames with composite floors performed at EERC by Ricles, J. and Popov, E. [22]

James Ricles' and Edgar Popov's study [22] included eight tests which were performed on two-thirds scaled subassemblies consisting of floor beams of eccentrically braced steel frames. Two of these specimens were bare steel, with the remaining six consisting of steel sections with a composite floor slab. The observed behaviour of each specimen was documented, the results of each test was then analyzed and compared in order to determine the increase in cyclic link capacity due to composite action, whether cyclic web buckling in composite links can be inhibited using bare steel link design criteria, and the extent of participation and damage of the concrete slab under extreme loading.

(a) K-Braced EBF Subassembly, Test Series I
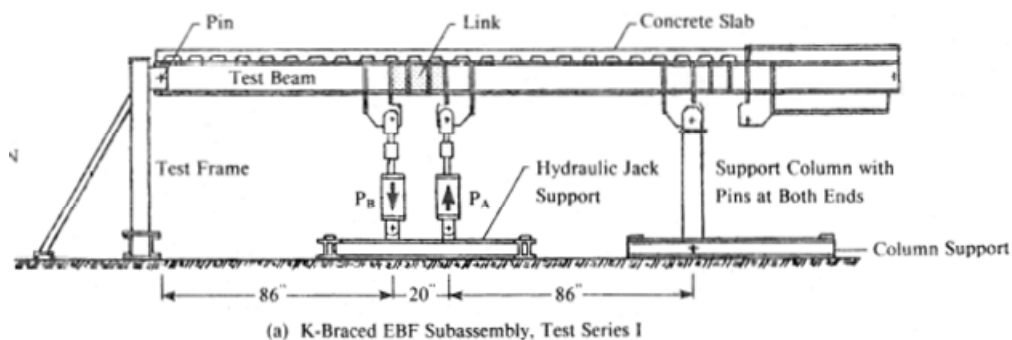
Fig. 2.4.   Ricles' Test set-up [22]

The conclusions of the study do not mention specifically the difference in plastic hinge behaviour between steel and composite beams. However, the conclusions stated in the study refer to the following points:
-   Initial elastic stiffness of the composite links has proven to be greater than that of bare steel links;
-   Composite links have a greater shear yield strength than bare steel links;
-   Energy dissipation was higher for the composite link;
-   The effective slab width based on stress distribution depends on beam spacing, loading conditions, beam span and orthotropic properties of the slab. The effective width of the slab varies along the beam of the EBF's, with minimum values at the ends of the link;
-   The floor slab and beam both contribute to the resistance of the applied loads. The force couple provides the largest contribution to the increase

in the composite section's capacity. The elastic shear force resisted by the floor slab at the link is from 8 to 12 percent of the total shear force. Floor slabs above an interior link offer larger contributions to the applied shear than the exterior links;

2.4.2 Cyclic Behaviour of Steel and Composite Beam-To-Column Joints, experimental research performed at a Civil Engineering Departments, Instituto Superior Técnico, Lisbon, Portugal and Universidade de Coimbra, Coimbra, Portugal, by L. Caladoa, L. Simões da Silva and R. Simões [31]

The study presents the results obtained from experimental research on two types of European joint solutions, namely steel and composite beam-to-column connections. Steel joints were designed in order to investigate the influence of the connection detail (fully welded and top and seat with web angle) and the column size, while the composite ones were designed to analyze the influence of the slab, the internal and external localization of the joint and the type of the column, steel and composite. An experimental program on different types of steel and composite beam-to-column connections has been carried out. The experimental tests have been performed on specimens representative of frame structure beam-to-column joints close to the ones typical of European design practice.
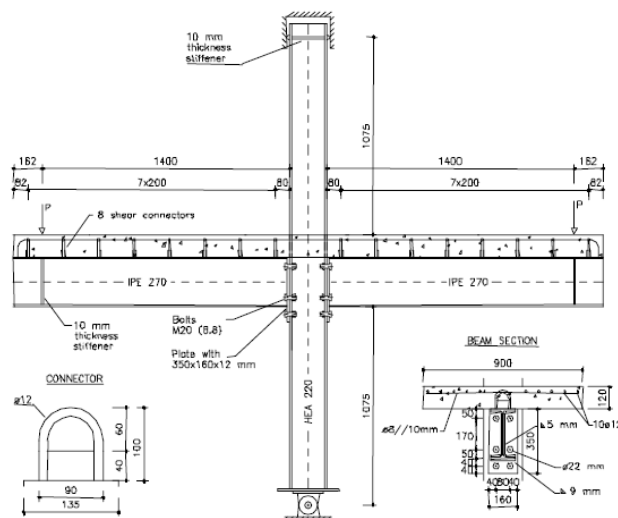
Fig. 2.5.   Setup of the composite joints tested at University of Coimbra [31]

The results have shown that for welded steel joints the behaviour of the connection is strongly affected by the panel zone, which is directly related to the column size. On the contrary, for top and seat with web angle steel connections the panel zone does not affect the behaviour of the joint, which instead is mainly, related to the tension angle geometry and strength properties. Concerning composite joints, the experimental tests performed have evidenced that the influence of the type of the column, steel or composite occurred only in the first cycles when the concrete is not cracked. In the plastic phase the behaviour of the

joints was similar. On the contrary, the localization of the joint, internal or external, has influence on the cyclic behaviour of the connection. External joints have exhibited some pinched hysteretic loops while for internal nodes the cyclic behaviour was more regular and stable.

2.4.3 Bi-directional cyclic testing of a 3-d frame at the JRC – ISPRA, A. Plumier, C. Doneaux, J.G. Bouwkamp, H. Parung [37]

A test of a full-scale structure has been run in the ELSA reaction-wall facility of the European Joint Research Centre at Ispra, Italy (Bouwkamp 1998) (Plumier 1998). The structure, a 3 storey 3 bay by 3 bay moment frame, has been conceived in order to test design hypothesis. The full-scale specimen is an assembly of various zones characterized by variations of parameters like the density of devices connecting the slab to the beams, the density of the reinforcement of the slab, the proportions of the composite sections, the effectiveness of the stress transfer from the slab to the columns. From the test, moment rotation curves at every connection have been derived.
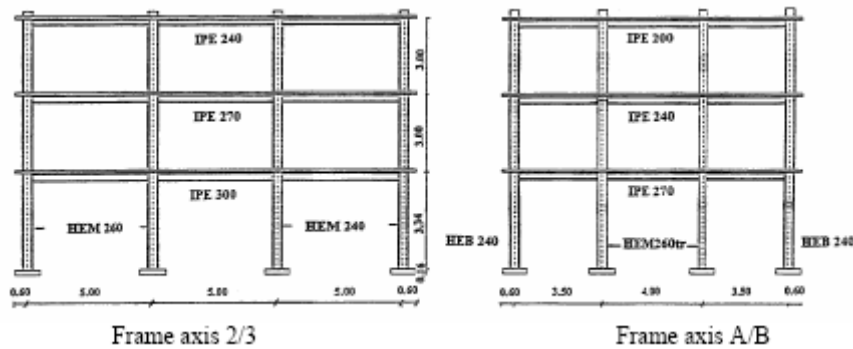
Fig. 2.6.   Frame views of the tested 3D structure [37]

Fig. 2.7.   Test in-progress [37]

The following test program has been executed: cyclic loading in X direction up to 2% drift and Y direction up to 2% drift; pseudo Dynamic Test ; cyclic loading in X-direction until failure; max. top-floor displacement +/- 400 mm (4.5% drift).

The summary of conclusions of the experimental tests are:

- the design relations of the reinforcements of the slab of composite beams conducted to a layout that maintained the intended integrity of the concrete during the cyclic testing.

- the effective widths of slab deduced from Eurocode 4 provide correct estimates of the real plastic moments of composite beams.

- Paulay's definition of effective width gives slightly better results for capacity design.

- the plastic moments of beams must be computed taking into account all the re-bars present, welded mesh and simple re-bars.

- considering the steel sections only in the design of composite frames is totally inaccurate; it is also unsafe for what concerns the capacity design of columns.

- disconnecting the slab from the beams ends and from the columns in a narrow zone does not prevent bending moment values higher than those of the steel sections to be realized in the plastic hinges.

- the global overstrength of the structure has been assessed on the basis of the global base shear – top displacement curves of test phase 1 and 5; the overstrength is the ratio of maximum resistance to first yield load: $\alpha_{max} / \alpha_1 = 2400 / 1100 = 2.2$. Considering that failure is reached after a resistance drop of 20 % of the maximal load, a reliable structural overstrength is:

$\alpha_u / \alpha_1 = 0.8*(2400 / 1100) = 1.75$.

Numerical studies have also been performed.

Beam to-column connection zones at either end of the beams were modelled with DRAIN-2D as linear-non-linear fibre models capable of representing the non-linear cyclic response of the composite beams in those regions. Columns and beams were modelled as steel and, respectively, composite linear beam-column elements.

Numerical results show agreement with the experimental results. Considering the test performance of the 3-D frame and this correlation with numerical results, the composite moment resistant structure would perform well under an actual design earthquake. In fact, using the Ballio method to determine the behaviour factor q, the results for the test frame with a thickness of the slab of 15 cm, indicated a q =4.5.

2.4.4 Cyclic tests on beam-column sub-assemblages at T.U.Darmstadt, C. Doneaux, H. Parung [37]

Three full-size interior composite beam-to-column joint assemblies of a composite building frame with floor slabs were tested under cyclic loading. Several particular design concepts were considered, such as different layout and concentration of studs and reinforcements, and the influence of a transverse beam in the composite beam-to-column moment force transfer (Doneux 1998). The three sub-assemblages were replicas of parts of a 3D structure tested at JRC Ispra. The main goal of the research project was to study the role of the slab on moment transfer in earthquake resistant composite frames.
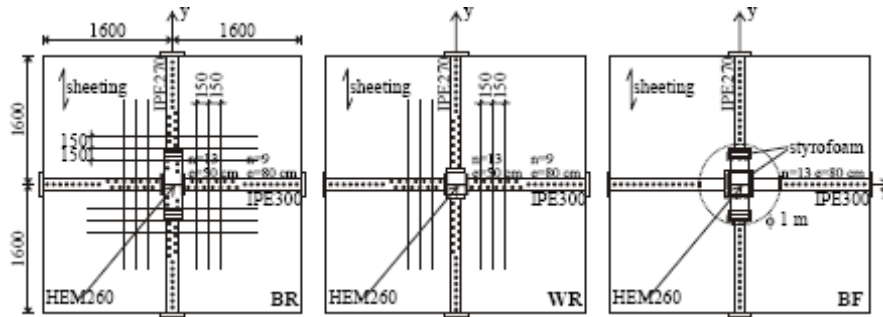
Fig. 2.8.   Overview of the tested specimens from TU Darmstadt [37]

The main results of the tests are:
- the measures taken to maximize the effective width are effective.
- the design relations presented in (Plumier 1998) gave a safe design, bringing the intended yielding scheme for a value of bending moment which can rather accurately be computed.
- the positive plastic moments are as well estimated on the basis of the Eurocode 4 definition of effective width as on the basis of the Plumier's mechanisms (direct compression and inclined struts).
- the negative plastic moments are underestimated on the basis of the "old Eurocode 4 definition" of effective width, but overestimated on the basis of the new Eurocode 4 definition of effective width.
- the transverse beam is not really activated in the case of a rigid slab. This mechanism is too flexible in comparison with the high stiffness of the direct compression of the concrete on the column.
- the behaviour of the slab as a tension or compression flange of a beam carrying membrane forces is a complex phenomenon.

2.4.5 Shaking table tests on beam-column sub-assemblages at NTUA [37]

To evaluate the difference in responses between cyclic quasi static and real dynamic tests, beam-column sub-assemblages have been tested on the shaking table at the National Technical University at Athens, Greece. Two shear interactions have been considered. The tests also provided data on the low cycle fatigue resistance of the headed studs connecting the steel sections and the concrete: it was demonstrated that the low cycle fatigue resistance may be the critical aspect of design once partial shear connection is realized.

2.4.6 Low cycle fatigue test of a plane composite frame at CEA SACLAY, M.R. Agatino, C. Doneux, A. Plumier [37]

A 3 bay plane composite frame has been tested under constant amplitude of displacements at the CEA Saclay, France. The parameters considered are the degree of shear connection between steel and concrete and an original detailing of the connection between slab and facade steel beam.
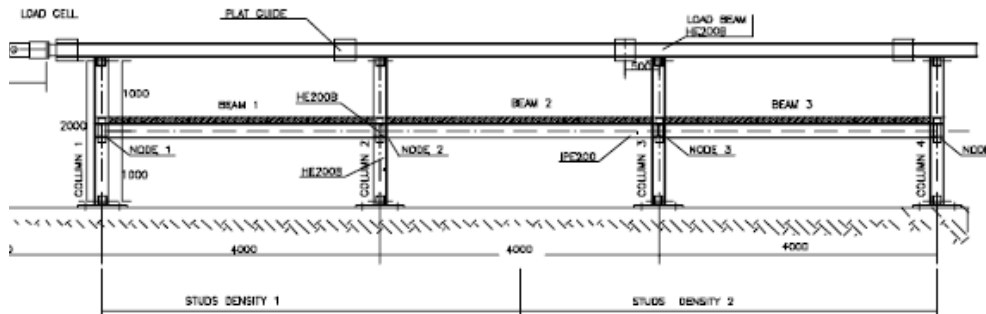
Fig. 2.9.   Reinforcement of the slab and anchoring on the transverse beam [37]

The test intended to set forward the peculiar aspects of behaviour of composite beams in low cycle fatigue and to study the redistribution of bending moments during the applied force reversals as well as to provide the usual data on elastic stiffness and plastic resistances of beams of different design. The tests concluded to the following:

- the bottom fibres of composite sections follow the same fatigue curve as the steel section used; however, given the higher strains at equal rotation in a composite beam with reference to a steel beam, the fatigue life is reduced by a factor of at least 2;

- the test has demonstrated the effectiveness of the anchorage of the re-bars to the studs of the external transverse beam, under negative bending, and of bearing of compression of the concrete on the transverse beam under positive bending;

- as far as the inertia is concerned, the provisory b_{eff} proposed in the ICONS-EC8 1998 draft version overestimates the positive moment of inertia, but on the contrary, the b_{eff} proposed in the same document underestimates the negative moments of inertia;

- these two results have to be considered to define the values of b_{eff} finally proposed for Eurocode 8; these ones should give the best possible estimate of the response of the structure, because in seismic design, lower bound values can be on the safe side for some aspects of the response and on the unsafe side for other aspects: typically safe side for resistance and unsafe side for displacements, meaning seismic forces and P-D effects;

- the $I_{equivalent}$, proposed by the ICONS-EC8 1998 document gives the best estimate of the moment distribution along the composite beam.

2.4.7 Experimental evaluation of behaviour factors at Bristol [37]

A series of shaking table tests, realized at Bristol University, UK, (Tsujii 1999) have been dedicated to the experimental evaluation of behaviour factors of composite steel concrete structures made of partially encased sections without slab. A comparison of the composite frames with bare steel frames was conducted. This study, coupled with numerical dynamic analysis using the ADAPTIC software, came to the conclusion that behaviour factors of the composite frames were slightly larger than that of the bare steel frame, while higher values of overstrength and dynamic ductility were also observed. In parallel, other purely numerical work was also

performed in order to handle better the context of the behaviour factors of composite structures. In particular, a study was dedicated to the definition of the correct way to evaluate q factors, because it had appeared that in past studies many different definitions of such critical parameters as "first yield" or "plastic redistribution factor" had been used, sometimes bringing apparent high discrepancies in results, which in fact were only related to the methodology. (Sanchez 1999)

2.4.8 Seismic response of composite frames – Calculation of behaviour factors, A. S. Elnashai, B.M. Broderick [37]

A series of dynamic analyses have been performed to determine the response of moment-resisting composite frames to a selection of earthquake ground motions. Structural behaviour factors evaluated from the demands determined for seismic events of various intensities were found to be significantly greater than those recommended by Eurocode 8 (up to $7\alpha_u/\alpha_i$). While inter-story drift was commonly the most severe response parameter, when the variability caused by the elastic response of individual structures to different earthquake loads is taken into account, the inelastic rotation of composite beams under negative moment more usually determined the identified behaviour factors. Sufficient differences in the seismic behaviour of composite and steel frames have been identified to justify the use of separate behaviour factors in either case, and as such, the code provisions for composite structures can be amended to reflect the more accurate behaviour factors identified in the study.

In the design of composite frames to resist gravity loading, a large proportion of the negative beam moments are redistributed to positive moment regions. However, as seismic design is normally based on elastic analysis, this is not possible when earthquake loads are to be resisted. To properly reflect the characteristics of composite frames, plastic design procedures should be employed. The use of local behaviour factors to reduce the design forces in selected locations may allow this to be achieved without contradicting current seismic design philosophies.

Overall, the enhanced rotation ductility capacities of composite members in general and the asymmetric behaviour of composite beams in particular, greatly improves the energy dissipation capabilities of moment-resisting composite frames over that of their bare steel equivalents; leading directly to the identified higher behaviour factors.

While the work detailed in this study constitutes a comprehensive assessment of the class of structure under investigation, it would nevertheless be enhanced through comparison with similar studies on both steel frames and composite frames with different lateral resistance systems (such as braced frames). In this manner, the identified characteristics which most affect the specific behaviour of moment-resisting composite frames under seismic actions could be confirmed and the suggestions for improved design guidance given in the study, extended to a wider range of structures.

2.4.9 Behaviour of eccentrically braced structures having active links connected or not with r.c. slab, Paul IOAN and Serban DIMA, TUCB, Bucharest [42]

The study analyses a 10 story DUAL structure, in various configurations. The building has three spans of 8.0m and seven bays of 6.0m. The level height (4.0m) is constant along the whole height of the building. The dual solution in this case consists of eccentrically braced frames and moment resisting frames on transverse direction, and concentrically braced frames (X-shape) and moment resisting frames on longitudinal direction (Fig. 2.10).The columns have a double T symmetrically section, which varies along their height.
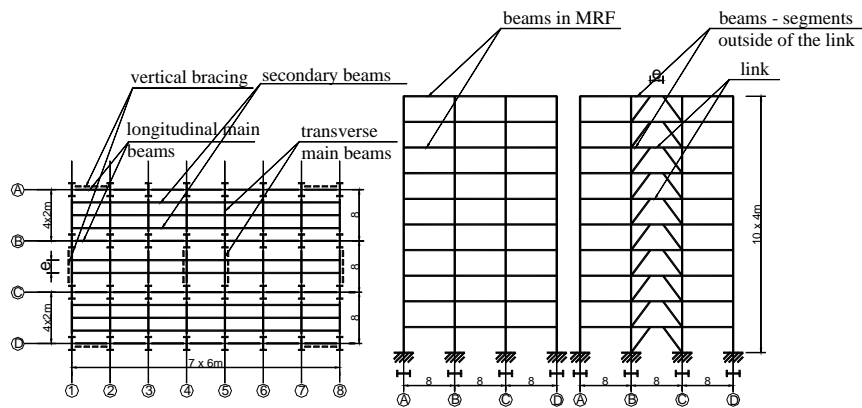
Fig. 2.10. The 10 story structure used in the numerical analysis at TUCB [42]

Time-history nonlinear numerical simulations were performed on the structure, using the recordings of the following earthquakes: Vrancea 1977, El Centro 1940, Northridge 1994, Mexico City 1995. The composite beams were modelled by an equivalent cross-section, as seen in the following figure:
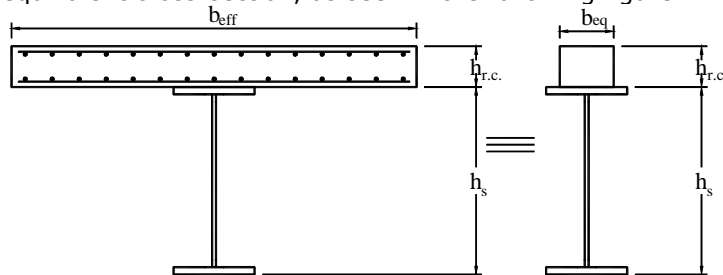
Fig. 2.11. Equivalent all-steel cross-section [42]

The conclusions of the numerical study regard the following aspects:
- By replacing the homogeneous beams (resulted from design) with the equivalent composite beams, the calculation methodology leads to a major simplification of the design effort as well as a rational conformation of the structural elements.
- The short, intermediary or long links must not be directly loaded (by gravitational loads) in order to allow the development of the plastic

hinges due to the seismic action and to avoid the uncontrolled stresses combination, produced by gravitational loads. The combination of the stresses corresponding to different loads may restraint the development of the rotations in the elastic-plastic range. The loads can be applied on secondary beams which intentionally delimitate the link and which assure the overall stability.

-    By the chosen constructive system, the links shall work in the structure only as homogenous elements. The reinforced concrete slab shall be separated (Fig. 2.12) by the top flange of the link or by the dissipative zone. The separation shall be performed by creating a gap between the top flange and the reinforced concrete slab. No connectors shall be provided on this zone. The reinforced concrete slab shall be supported by secondary beams, which delimitate the link. Along the secondary beams will be created expansion joints provided with dowels in order to assure the diaphragm effect. The dowels shall allow the rotation in vertical plane.
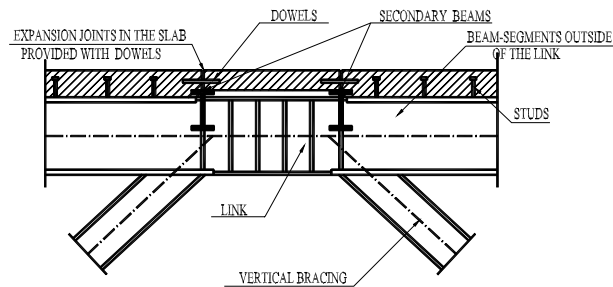
Fig. 2.12. Proposed detailing solution for the link element [42]

2.4.10 Seismic design and performance of composite frames, G. Thermou, A.S. Elnashai, A. Plumier [43]

In this study, the seismic design and performance of composite steel-concrete frames are studied. The provisions of Eurocode 4 and Eurocode 8, which were in a preliminary stage at that time, are employed for the design of six composite steel-concrete frames. The deficiencies of the codes and the clauses that cause difficulties to the designer are discussed. The inelastic static pushover analysis is employed for obtaining the response of the frames and the overstrength factors. The evaluation of the response modification factor takes place by performing incremental time-history analysis up to collapse limit states in order to investigate the conservatism of the code. The last purpose of this study is to investigate if elastically designed structures can behave in a dissipative mode.

The composite beams were modelled in the simulated structures, first in SAP2000 as „general" cross-sections with the input data for the definition of cross-sections specified by the user (no methods for defining a „real" composite CS were available at that time in SAP2000). Then, in a second step the same structures were modelled in the FE software INDYAS (developed at the Imperial College, London), using a model that implies a steel CS and a composite slab connected by rigid „links" (Fig. 2.13).
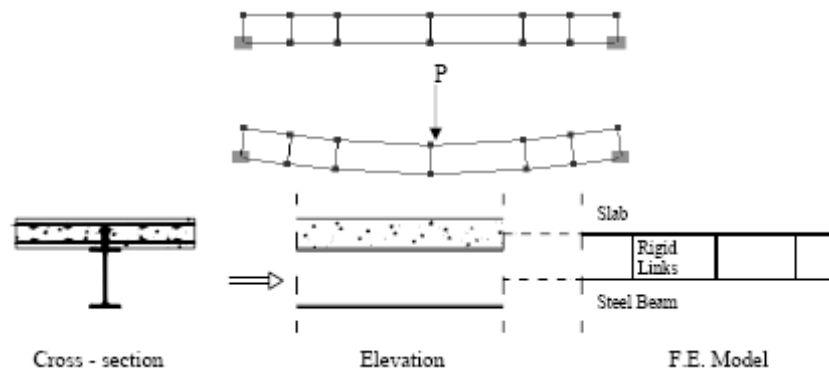
Fig. 2.13. Modelling of the composite beams in the INDYAS software [43]

The analyses performed involve the use of 4 artificial recordings and also capacity design using push-over analysis. The main conclusions of the study regard the following aspects:

- The study underlines that the frames exhibited high overstrength values;
- The calculated force reduction factors exhibit higher values compared to the code suggested values (q). The design „q" factor was considered as 4, but this conclusion should be limited to the current study, as the authors imply;
- It is noteworthy that the frame designed elastically (q=1) and without capacity design exhibited a reduction factor greater than 1;

2.4.11 Cyclic tests on bolted steel and composite double-sided beam-to-column joints, D. Dubina, A. L. Ciutina, A. Stratan [24][47]

The study summarises the research performed in the CEMSIG laboratory of the "Politehnica" University in Timisoara, in order to evaluate the performance of beam-to-column extended end plate connections for steel and composite joints. The study comprises both laboratory tests (performed on steel and composite joints) and numerical models (calibrated in DRAIN 2DX program).

The conducted tests included 12 specimens. Out of these, 6 were steel, three joints tested under symmetrical loading, and three joints under anti-symmetrical loading. The first specimen from each series was tested monotonically, in order to determine the yield displacement D_y. The 6 composite specimens were also tested in the same manner, both monotonic and cyclic.

The numerical analyses used the so-called "element 14", developed for DRAIN 2DX (Prakash et al. 1993) at the University of Ljubljana, Slovenia. This element allows for a sophisticate modelling of joint behaviour, starting from known characteristics obtained in experimental tests. It is a non-linear spring and allows a tri-linear non-symmetrical envelope behaviour.
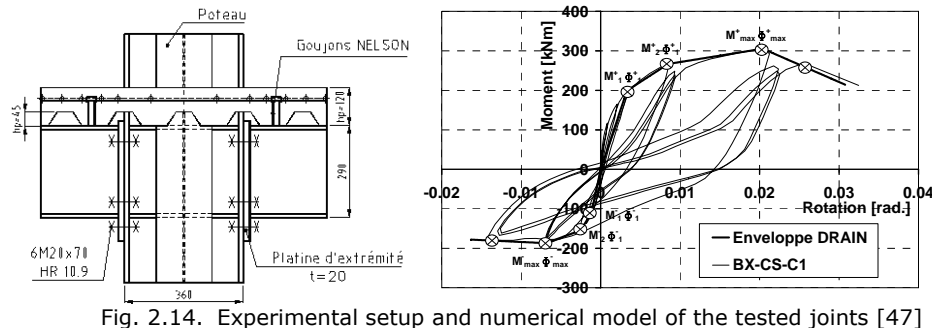
Fig. 2.14. Experimental setup and numerical model of the tested joints [47]

The conclusions of the tests and numerical simulations refer to the following main ideas:

- The use of X-shaped columns facilitates the design for three- and four-way connections for spatial moment resisting frames;
- Cyclic loading introduces differences between the type of failure for both bare steel and composite joints. While for the monotonic tests the failure was characterised by the breakage of the bolts and deformations in the column flange/end plate, in case of the cyclic tests failure of the fillet welds occured. Thus, weld quality is of great importance;
- Composite action of the concrete slab has been noticed to have a positive effect on the ductile behaviour of the symmetrically loaded joints under negative moments;
- In the case of composite joints with partially extended end-plate, the steel reinforcement in the slab is not able to compensate for the missing bolt row;
- The joint modelling in DRAIN 2DX can offer solutions for the verification of structuctural beam-to-column joints. These models have been proven to give results close to reality, for an accurate structural analysis.

2.4.12 Analysis of steel–concrete composite beam-to-column joints: bolted solutions, O. S. Bursi, F. Ferrario, R. Pucinotti, R. Zandonini [48]

In this study, an advanced design methodology is proposed for steel-concrete composite moment-resisting frames. The research activity mainly focused on the design of the beam-to-column joints under seismic-induced fire loading together with the definition of adequate structural details for composite columns. Thermal analyses of cross sections were performed in order to obtain internal temperature distribution; structural analyses were then performed on the whole frame to assess the global behavior under the combined action of static and fire loadings.

Results of the numerical analyses were used in order to derive information about the mechanical and numerical behavior of joints. The experimental program was carried out on four beam-to-column joints. Numerical simulations showed a satisfactory performance of joints under seismic-induced fire loading.
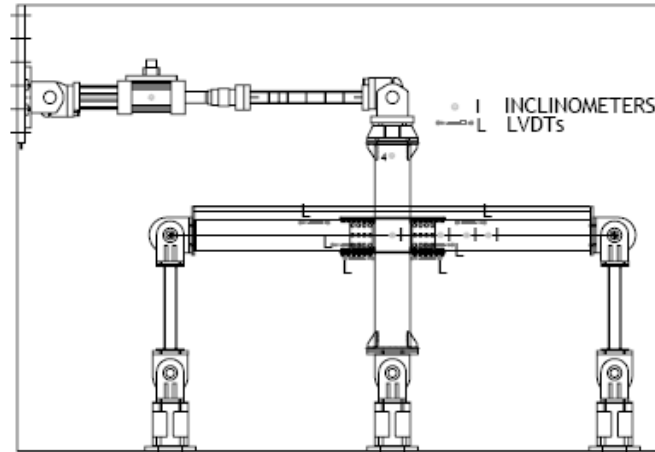
Fig. 2.15. Assemblies tested at Department of Mechanical and Structural Engineering,
University of Trento, Italy [48]

All sub-assemblages exhibited rigid behaviour for the designed composite joints and good performance in terms of resistance, stiffness, energy dissipation and local ductility; as expected plastic hinges developed in beams as a consequence of the capacity design. Moreover, a behaviour factor of about 4 has been observed for the composite frames analysed. As a result, the joint can be used in Ductility Class M structures. Numerical fire simulations have shown that the joint is able to carry the internal action for a maximum time of 15 minutes without any passive fire protection: this time interval is enough to quit the building after a severe earthquake. Moreover, joints endowed with prefabricated slab exhibit a better behaviour compared to the joint with a composite slab.

2.4.13 Development of a Phenomenological Model for Beam-To-Column Connections in Moment Resisting Frames subjected to Seismic Loads, P. N. N. S. Kumar (PhD Thesis) [49]

Phenomenological models are based on some characteristic curves of the experimental behavior; using pre-determined rules, they are capable of simulating the whole experimental response.

The proposed phenomenological model is based on the model proposed by Noé et al., (1996). The model realised by Kumar is based on a base cycle formulation rules with modified rules. New envelope curves are identified and incorporated in the model for addressing the
decreasing loading cycles observed as part of seismic loads. New hysteresis rules are proposed to address all three types of loading commonly used by the researchers in the experimental studies of the beam-to-column connections. In order to address the low cycle fatigue behavior commonly observed in the beam-to-column connections, two degradation functions are proposed. The model is validated against nine test cases from different types of connections.
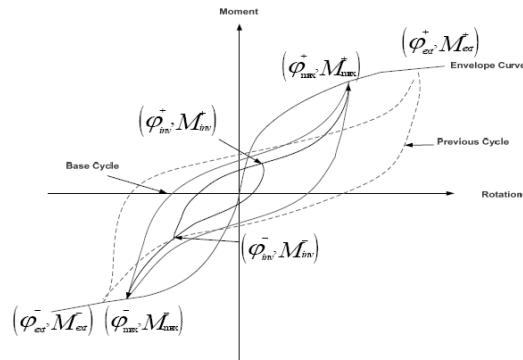
Fig. 2.16. Theoretical approach of the proposed model [49]

Phenomenological models demand careful observation of the existing experimental results, identifying the ways and means to predict the behavior, formulation of set rules for identified behavior, implementing the rules in the appropriate programs and validating the set rules.

The study indicated that phenomenological models are able to predict the cyclic and/or seismic behavior precisely.

Seismic analysis of frames studied indicated that the elastic-perfectly plastic connection behavior is underestimating the moments produced in the beam-to-column connections and lateral displacements produced in the beams.

2.4.14 Seismic behaviour of eccentrically braced frames, M. Bosco, P. P. Rossi [51]

The analysis of the seismic behaviour of eccentrically braced frames designed in fulfilment of capacity design principles has highlighted the significant role of the link overstrength factor. The link overstrength factor is, however, unable to explain many seismic responses because it is defined on the basis of the sole elastic behaviour of structures. To achieve thorough comprehension of the seismic behaviour of eccentrically braced systems, this study proposes a new parameter, called damage distribution capacity factor. The proposed parameter is calculated on the basis of the inelastic structural behaviour and is intended to evaluate the effect of premature yielding of links on the ability of structures to develop significant inelastic behaviour of all links prior to link failure.

Finally, an analytical relation is defined between overstrength factor of links, damage distribution capacity factor and plastic rotation of links in order to obtain quantitative evaluation of the structural damage of eccentrically braced structures upon first failure of links.

$$DDC_i = \frac{\dfrac{1}{n_s-1} \cdot \left(\displaystyle\sum_{j=1}^{n_s} \frac{\Delta u_j}{\Delta u_j^{\lim}} \right)_{j \neq i}}{\left(\dfrac{\Delta u_i}{\Delta u_i^{\lim}} \right)}$$
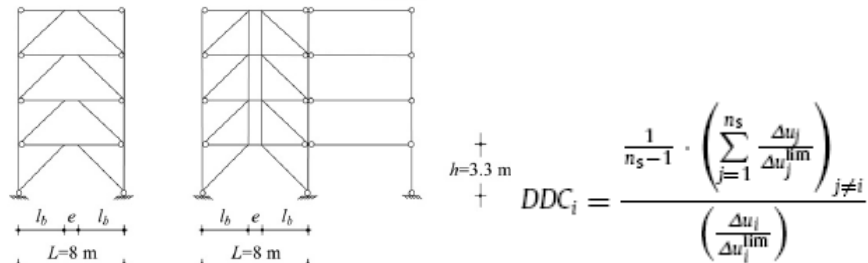
Fig. 2.17. Analysed frames and expression of the proposed damage parameter [51]

The proposed factor is calculated as the ratio of the mean value of the normalized interstorey displacements at the storeys where links are hypothesised to be elastic with respect to the normalized displacement at the storey where links have yielded. In the above expression, Δ_u is the interstorey displacement demand and Δ_{ulim} the ultimate value of the plastic interstorey displacement (in both parameters the symbol Δ indicates that the interstorey displacements are evaluated from deformed structural configurations).

The main conclusions of the above mentioned study are:
- The analysis of the normalized overstrength factor of links only sometimes allows reliable evaluation, of the seismic behaviour of eccentrically braced structures. This is not surprising because the overstrength factor of links is based on the elastic behaviour which immediately precedes first yielding of links and, thus, does not depend on the inelastic behaviour of structures.
- The damage distribution capacity factor allows substantial improvement in the prediction of the seismic response of generic eccentrically braced structures.
- Design procedures generally suggested by seismic codes (e.g. Eurocode 8) for traditional eccentrically braced structures do not ensure wide spread of the plastic behaviour of links among all storeys prior to link failure. Particularly in moderate and high-rise buildings, the design of traditional eccentrically braced frames according to capacity design principles, leads to low and non-uniform values of the damage distribution capacity factor. This design deficiency may negatively affect the seismic response of eccentrically braced structures, in terms of exploitation of their dissipative capacity.

2.4.15 Behavior of exterior partial-strength composite beam-to-column connections: Experimental study and numerical simulations, G. Vasdravellis, M. Valente , C.A. Castiglioni [52]

The experimental tests and numerical analyses were carried out to study the seismic behavior of semi-rigid partial-strength steel–concrete composite beam-to-column joints at the Laboratory of the Politecnico di Milano.

Four full-size sub-assemblages representing exterior composite beam-to-column joints were tested under cyclic loading. The specimens exhibited large dissipative capacities and very stable and ductile behavior without significant reduction in strength and stiffness.

The hysteretic behavior and the dominant failure modes of the tested sub-assemblages, the contribution of the column web panel to the overall joint rotations and the mechanisms which may describe the force transfer between concrete slab and column are analyzed and discussed within the study. Then, finite element models of the tested specimens were developed and numerical analyses were carried out in order to further investigate the stress state in the composite sub-assemblages and to study the influence of various parameters on the joint behavior. The influence of the slab contribution, the mechanisms of force transfer in the slab in the connection zone, the effect of the degree of partial interaction and the stress field existing in the slab for various layout of seismic rebars were studied.
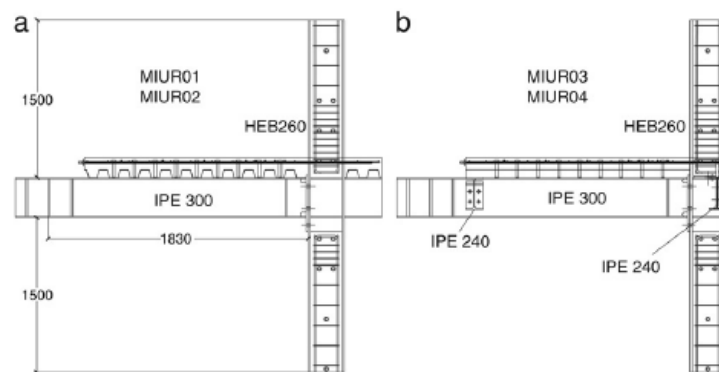
Fig. 2.18. Exterior composite beam-to-column sub-assemblages tested in the laboratory [52]

The numerical simulations involved Abaqus analyses, that modelled the composite joints using solid elements (C3D8R). At least two elements were employed in the thickness of steel flanges, end-plate and stiffeners to reproduce accurately the bending behavior. The materials used for modelling (structural and reinforcing steel) were assumed to behave as elasto-plastic material with hardening both in compression and in tension, using von Mises plasticity. Modulus of elasticity, yield stress and ultimate stress were taken from the laboratory tests performed on the materials of the tested specimens. The concrete was defined by using the „concrete damaged plasticity" model from Abaqus, that provides a realistic inelastic behaviour, even if it is computationally more expensive.

The main results of this study may be summarised as follows:

- Experimental tests demonstrated that the specimens exhibited high ductility and large dissipative capacities, achieving inelastic rotations far beyond the limit of EC8 for DCH moment-resisting frames.
- Stable and ductile behavior for positive and negative bending moment was observed for all the tested sub-assemblages. Plastic deformations were concentrated in the connection and in the column web panel and there was no evidence for plastic hinge formation or flange buckling in the steel beam.
- The contribution of the column web panel to the overall joint rotations was significant.
- The transverse seismic rebars near the column flange resulted in a ductile joint cyclic response, avoiding premature brittle failures.

- The experimental investigation showed that steel–concrete composite joints employing partial-strength beam-to-column connections and exploitation of the column web panel inelastic resources can guarantee a very efficient and highly dissipative seismic performance and they can represent an advantageous structural solution against their welded counterparts, eliminating the risk of brittle failures.
- The numerical models proved a useful tool to understand the complex behavior of bolted partial-strength composite joints with partial interaction and the complicated stress states resulting from positive or negative applied bending moments.
- The significant contribution of the slab to the joint performance was also appreciated, enhancing the initial stiffness and the ultimate moment capacity when composite action is developed.
- Numerical analyses showed that full-shear connection in sense of zero slip is an unrealistic case resulting in an over-estimation of the connection response and thus partial shear connection must be considered, as a small slip always exists. In addition, when plastic slip occurs, the ductility of the system increases with only a small compromise in resistance.

2.4.16 Behaviour of a semi-continuous beam-column connection for composite slim floors, Mikko Malaska (PhD Thesis) [53]

This study focuses on the behaviour of beam-column connections in a building frame consisting of slim floor beams. The principal purpose was to gain a better understanding of the engineering features of semi-continuous composite joints and to apply this knowledge in the design of structures frequently used in Finland.

A new advanced structural design connecting a slim floor beam to a tubular steel column section filled with concrete was designed using an application of the semicontinuous concept. The design was implemented and the construction tested in a thorough study. Experimental work included two tests on bare steel connections and four tests on composite connections with full-scale specimens. The two steel tests were used to demonstrate the joint behaviour during the erection and pouring stage. Four specimens of composite connections were then tested in order to learn the influence of the slab characteristics on the connection behaviour in terms of the amount of reinforcement used in the slab, the shear-to-moment ratio, and the concrete strength.

This thesis also proposes a mathematical model for predicting the moment-rotation characteristics of the joint. In the model formulation the basic mechanism of force transfer within the components of a composite connection was applied.
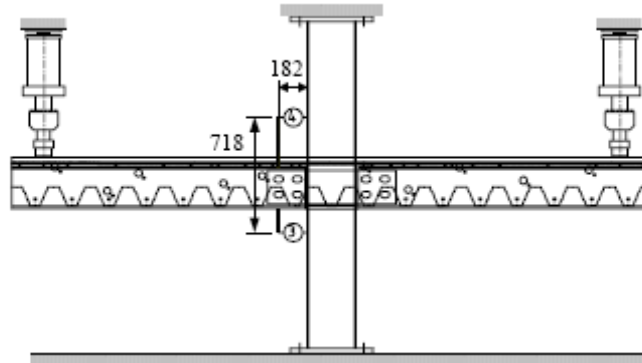
Fig. 2.19. Test setup with slim floor [53]

The author admits that the general form of the mechanical model proposed has to be studied in order to validate the model for cases when the exposed load in a joint is not symmetrical. The model proposed needs to be experimentally calibrated against the test results in which the joints are exposed to unbalanced loading. This work also leaves room for the experimental validation of the design methods proposed for the capacity of the column exposed to local and for the capacity of the compressed concrete core below the inserted shear flat slab.

From the experiments of this work, a general insight into the static behaviour of the shear flat slabs has been obtained. However, it is insufficient to understand all the detailed aspects of the distribution of stresses in the plate. For the load-slip behaviour of the shear connectors used in the joint specimens no test data is available. The experimental results indicated that in the specimens full shear connection between the steel beam and the concrete slab was achieved.

2.4.17 Behaviour and modelling of partial-strength beam-to-column composite joints for seismic applications, A. Braconi, W. Salvatore, R. Tremblay and O. S. Bursi [54]

The group of researchers from University of Pisa, Trento and Montreal proposed a refined component model to predict the inelastic monotonic response of exterior and interior beam-to-column joints for partial-strength composite steel–concrete moment-resisting frames. The joint typology is designed to exhibit ductile seismic response through plastic deformation developing simultaneously in the column web panel in shear, the bolted end-plate connection, the column flanges in bending and the steel reinforcing bars in tension. The model can handle the large inelastic deformations consistent with high ductility moment-resisting frames.

In order to model the concrete slab, a fibre representation was adopted, considered to capture the non-uniform stress distribution and progressive crushing of the concrete at the interface between the concrete slab and the column flange. The model is validated against results from full-scale subassemblages monotonic tests performed at the University of Pisa, Italy. A parametric study is presented to illustrate the capabilities of the model and the behaviour of the joints examined.
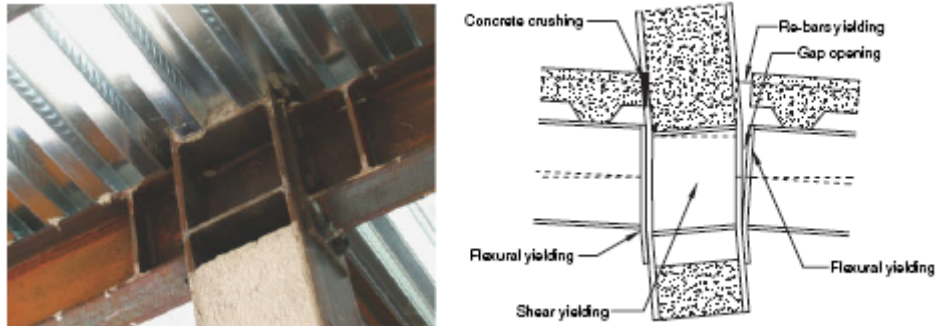
Fig. 2.20. The partial strength joint that has been studied [54]
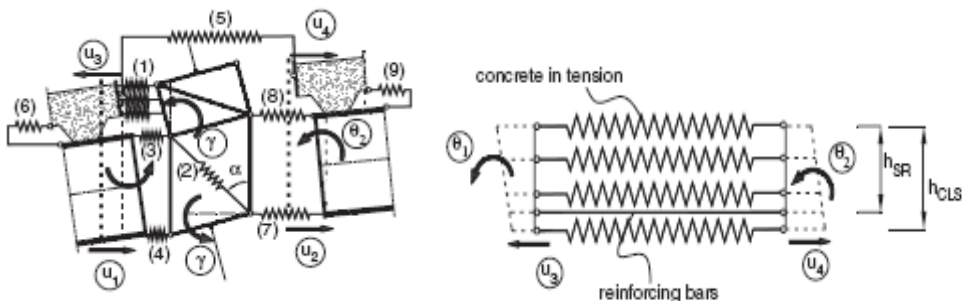
Fig. 2.21. Proposed component model [54]

A component model was developed in order to reproduce the observed response of the entire assemblies of beam-to-column test specimens. In the model, the connections between the beam end plates and the column flanges were represented by equivalent T-stubs located at top and bottom beam flanges. The model accounted for the response of: the concrete in compression, the column web panel in shear, the upper T-stub in compression under positive moment or in tension under negative moment, the lower T-stub in tension under positive moment or in compression under negative moment, the concrete slab in tension, and the shear connectors in the beam under positive moment and negative moment.

The conclusions obtained, as stated in the study involve the following aspects:

- Bearing failure of the concrete slab against the column flange was found to occur prematurely, which suggests that the Eurocode 8 methodology for determining the capacity of the compression force transfer mechanisms between the concrete slab and the column should be reviewed.
- The component model took into account plastic deformation developing in the beam end plate/column flange as well as in the column panel zone. The model was found to reproduce very accurately the observed response and experimental measurements for the joint configurations.

2.4.18 Experimental and numerical model for space steel and composite semi-rigid joints, M. A. Dabaon, M. H. El-Boghdadi, O. F. Kharoob [55]

An experimental investigation was conducted at the Faculty of Engineering in Gharbeya, Egypt, to study the behaviour of space steel and composite semi-rigid joints. The effect of loading from the minor direction on the main direction of semi-rigid joints was considered. Five full-scale tests were performed on semi-rigid space steel and composite extended endplates joints. A three-dimensional finite element model is proposed by the authors, using ANSYS software for the analytical investigation. A comparative study between the present numerical model and the experimental results is presented to establish the validity of the proposed model. Also, an application was made on a space frame to show the effect of joint rigidity using a beam-element model.
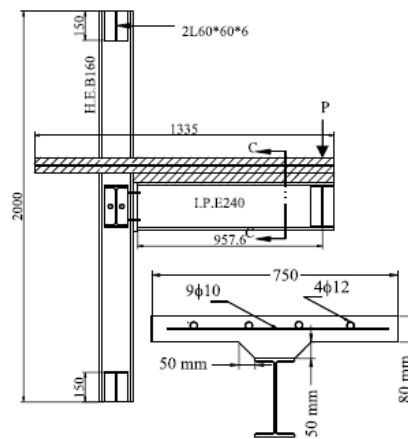
Fig. 2.22. Tests performed in Egypt [55]
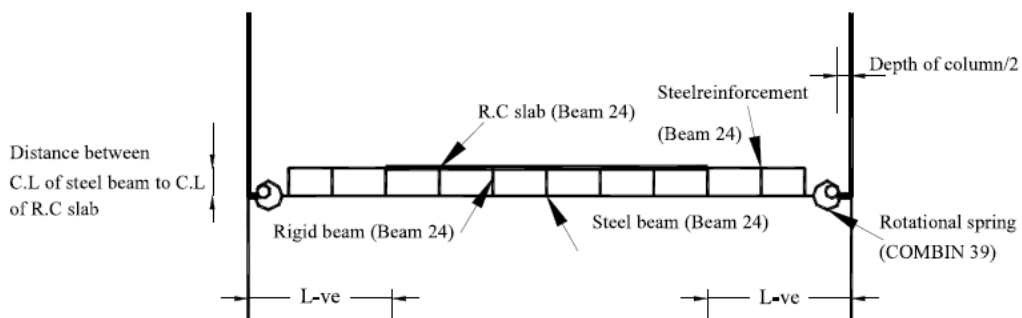
Fig. 2.23. Modelling of the composite beam [55]

The main ideas stated in the study:
-    It was found that a vertical force and/or bending moment, acting at the minor axis of a joint, reduces both the load bearing capacity and stiffness of the joint, with respect to its major axis. The moment capacity and the stiffness of joints subjected to vertical force only in

minor direction are less than those for joints subjected to both vertical force and bending moment.
- A 3-D finite element model was proposed using ANSYS for the analytical investigation. A comparative study was made between the current model and the experimental results.
- Finally, for simplicity, a beam-element model was proposed to model the global space steel and composite frames. Also, a verification of the beam-element model was made by comparing it with previous studies.

2.5 Conclusions

The review of the current norms and their respective provisions concerning the inelastic behaviour of composite beams has shown that there is insufficient data to guide the seismic design of such elements. Moreover, when considering the composite aspect, the structural designer is put in a position to choose whether to consider or not the steel and concrete as working together in order to achieve a high or medium dissipative capacity under severe seismic loads. In this case, the „pure" steel approach is simpler but conservative with respect to the desired results.

The existing experimental studies have shown some of the differences between steel and composite solutions, mostly when it comes to the design of beam-to-column joints. A wide spread of results indicated that when the beam is composite, the joints tend to dissipate energy not only by beam plasticization near column, but also in the column's web panel and in the bolted or welded connection. This is generally the less desired case when it comes to accepting structural damage after an earthquake. In conclusion, the subject needs precise design solutions to account for both the composite aspect and its modelling in current practice.

On the other hand, the subject of steel EBFs is fully comprehended worldwide. While steel beams with links have been proved to function very well under seismic loads, when it comes to estimating the dissipative capacity of EBFs with composite beams, the existing opinions recommend detaching the slab from the profile in the link zone. However, this does not necessarily lead to a "pure" steel behaviour of the plastic hinge, since the concrete slab is expected to have some influence in this zone. Few or no studies exist in this direction and there are no specific provisions that characterise the behaviour of composite links, which obviously cannot behave in the same manner as their steel counterparts.

Moreover, the distinction between the behaviour of composite beams with and without connectors over the plastic zones hasn't been underlined in almost none of the existing studies.

Therefore, there appears the need to obtain characteristic curves that best describe the phenomena occurring in plastic hinges of composite steel-concrete cross-sections under cyclic loads and some specific prescriptions that can be used in current design practice.

3. EXPERIMENTAL PROGRAM

3.1 Introduction

The behaviour of dissipative zones of composite steel-concrete beams in case of joints of Moment Resisting Frames (MRF), and in case of links of the Eccentric Braced Frames (EBF) is an issue subjected to controversy and represents a topic of interest in the research community. For this reason, the current seismic design provisions recommend (for a safe design of elements) to avoid installing connectors in the expected plastic zones, and to consider a symmetric plastic hinge for the steel beam or link only. However, since the reinforcing bars and the concrete slab are active although the connectors have been suppressed, accomplished by the friction contact between the concrete slab and beam or link flange, the assumption of the "nominal symmetric" plastic hinge could be false.

The composite action (by presence of the connectors in the plastic zones) could even more improve the structural behaviour, in elastic and post-elastic range. There is also a need to find the real response of the dissipative elements when the connectors are not installed. In this direction the existing studies have pointed out that the concrete slab has a considerable influence on the adjacent steel dissipative elements.

Based on the above open issues, an experimental program was developed within the research centre „CEMSIG" at the University „Politehnica" of Timisoara, focused on the study of the development of plastic hinges in steel dual MR – EB frames, with and without interaction with the concrete slab.

The experimental tests were performed in order to observe the steel dissipative elements, which are ideally considered to work independently from the adjacent concrete elements. The experimental tests were designed and calibrated based on numerical simulations with finite elements. The obtained results were used afterwards in global structural analyses of push-over and time-history types.

The first objective of the study was to have a basis of comparison. This was accomplished by testing purely steel specimens, whose behaviour was checked and compared with the existing provisions. Secondly, composite elements were tested, but without connection with the slab in the dissipative zones, in order to observe the influence of the concrete slab over the dissipative steel elements. Third, fully connected composite elements were tested and compared with the first two configurations in order to draw correct conclusions. The obtained experimental curves have been used as basis for the calibration of finite element analyses, described in Chapter 4, and numerical simulations on real structures, described in Chapter 5. These analyses are meant to ensure the use of composite cross-sections in the plastic zones from buildings located in seismic areas, such as Romania.

3.2 Design of the base structure for the experimental specimens

In order to design the experimental specimens, the initial step was to dimension a complete dual frame (MRF and EBF), according to up-to-date European norms. In order to check the structural behaviour and the plastic demand of the dissipative elements, there have been performed analyses by means of push-over and time-history incremental dynamic analysis (IDA) procedures. These had to

prove that the plastic demand limits requested by the standards are sufficient for the chosen dual frame.

In this direction, the experimental tests performed on the dissipative elements of the frames must, in turn, confirm a proper ductility just like the one resulting from the global frame analysis.

Initially, the base frame was considered to be made only of steel, and later on the analyses were conducted on the same frame with composite beams.

3.2.1 Initial design of the structure

The frame chosen for the study is part of a dual frame structure MRF+EBF, having 3 spans and 3 bays , as shown in the figures below:
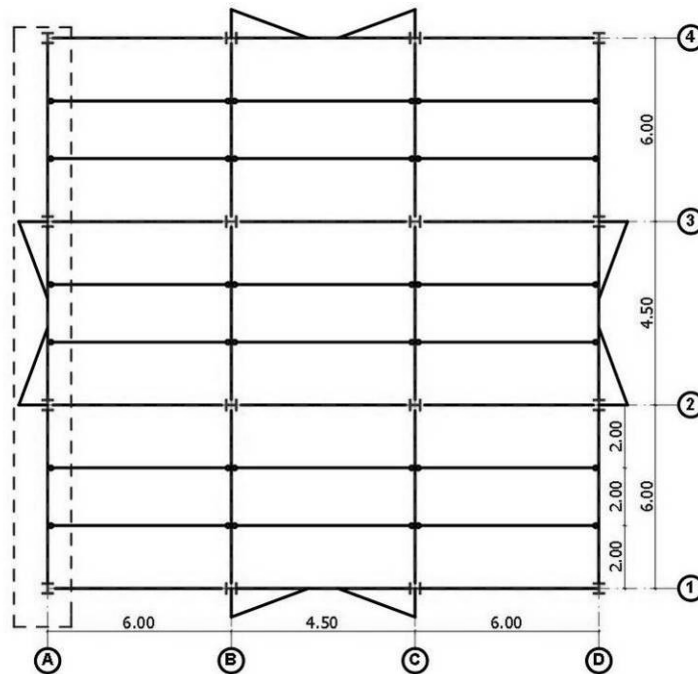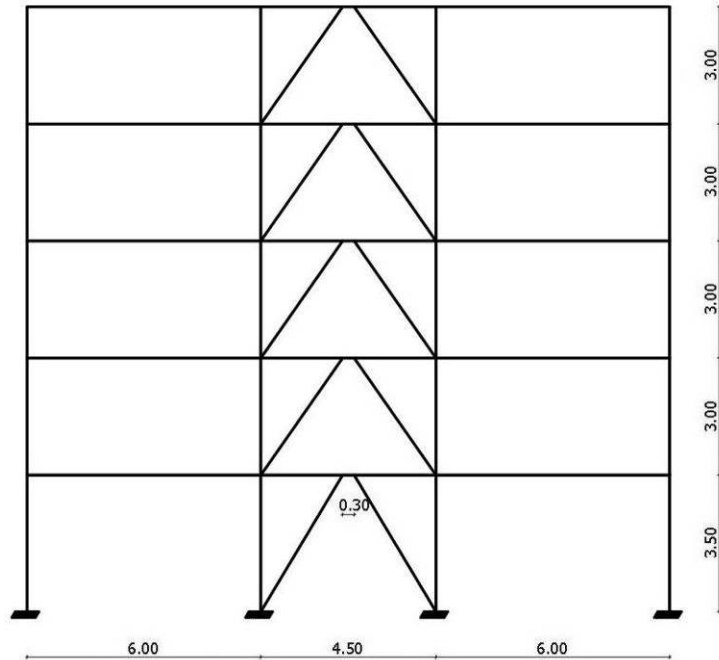
Fig. 3.1.   Plan view and section of the base structure

The structure was conceived as double-symmetrical with eccentric braced frames on mid-lateral spans. The study is focused on a facade frame, namely the frame from axis A, on the reason of carrying less gravitational loads. The frame has 5 stories and 3 spans, the central span being eccentrically braced, while the first and the last spans are moment resisting frames. The lateral MRF's spans have 6 m each, while the EBF span is 4.5 m and the story heights are 3.5 m for the ground floor and 3 m for the current floors. The dissipative element (the link) has the characteristics of a short link (a length of 0.3 m) and was modelled in 2 stages, first as a fixed link and then as a detachable link, by decreasing its shear rigidity. This hypothesis comes from the fact that in a detachable link the rigidity is affected by the effect of slip at the bolt holes (because of tolerances) – phenomenon known as "pinching effect" – and the rotations at the end of the link, which appear during a dynamic loading.
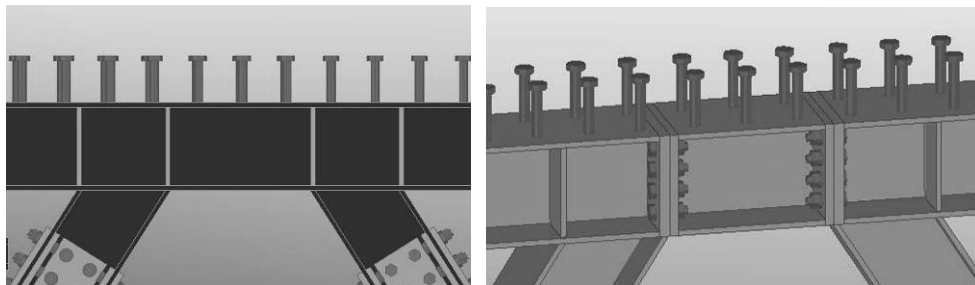
Fig. 3.2.   Beam with continuous and removable link configurations

The loads applied on the frame were computed using the valid Romanian norms. These loads included dead load, live load and nodal masses. It was considered from experience that wind load has no influence on design. The load combinations which were applied onto the structure are the following:

a) Fundamental combination:
ULS: 1.35G + 1.5Q+1.05S
SLS: 1.00G + 1.00Q+0.7S

b) Special combination:
ULS: G + E + 0.4Q   [dissipative]
ULS: G + ΩE + 0.4Q [non-dissipative]
SLS: G + q γ E + 0.4Q

where,

G – permanent load taken as 4.5 kN/m^2
Q – live load taken as 3 kN/m^2 (for an office building)
S – snow load taken as 1.6 kN/m^2
E – earthquake load

The earthquake load was introduced by seismic spectrum, taken from the Romanian Seismic Map for Bucharest, having the following characteristics:

- control period: T_c = 1.6 s
- ground acceleration a_g=0.24g

These characteristics are in accordance to the Romanian earthquake design code P100/1-2006. The design spectrum is shown in the figure:
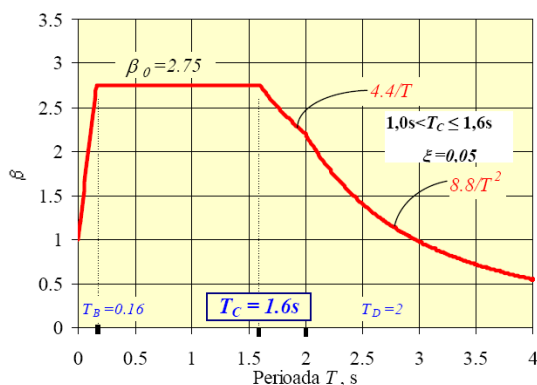
Fig. 3.3.   Elastic design spectrum for Bucharest [29]

The behaviour factor q was corresponding to a structure of high ductility , and taken as q=6 (according to P100- ch. 6/ table 6.3), considering a value a_u/a_y of 1.2. The design of non-dissipative elements was performed by considering an overstrength multiplication factor $1.1\gamma_{ov}\Omega$=2.5, value characteristic to dual frames, composed of eccentrically braced frames and moment resisting frames (according to annex F.4./P100-1/2006).

3.2.2 Design checking by non-linear push-over and time-history analyses

Pushover analysis [45] is a static, nonlinear procedure in which the magnitude of the structural loading is incrementally increased in accordance with a

certain predefined pattern. With the increase in the magnitude of the loading, weak links and failure modes of the structure are found. The loading is monotonic with the effects of the cyclic behaviour and load reversals being estimated by using a modified monotonic force-deformation criteria and with damping approximations. Static pushover analysis evaluates the real strength of the structure and can also be used as a tool for performance based design.

The level masses (computed from dead load and live load) were concentrated in the frame's nodes with the following values:
- marginal nodes: m1=13.2 kN
- central nodes: m2=23 kN

For the push-over analyses, level forces applied on the structure have a linear triangular distribution, with the values for the forces determined according to paragraphs 4.5.3.2.2 and 4.5.3.2.3 from P100-1/2006.

$$F_i = F_b \cdot \frac{m_i \cdot s_i}{\sum\limits_{i=1}^{n} m_i \cdot s_i} \text{ , where}$$

F_b – base shear force
m_i – level mass, calculated according to Annex C from P100-1/2006
s_i – current height for the level mass
n – number of levels

Thus, the following distribution resulted:
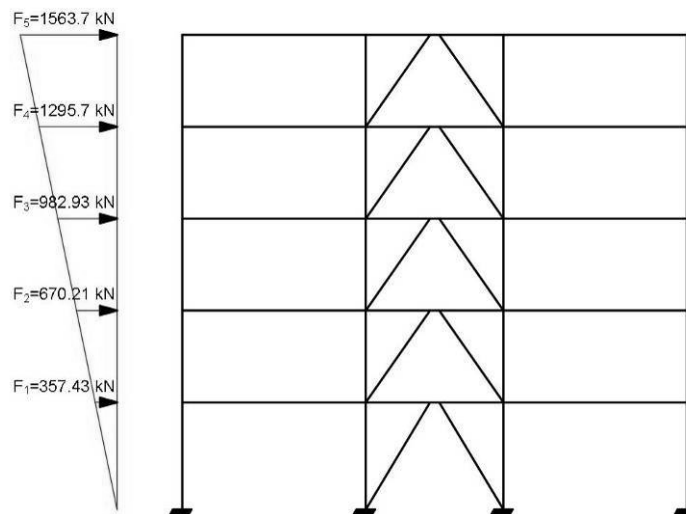
Fig. 3.4.   Applied level forces for push-over analyses

The design and check of structural elements was performed according to Eurocode 3, taking into account the provisions of P100, chapter 6 for the MRF and EBF. The checks were performed in different manners for the MRF beams and for the link under ULS conditions (fundamental and special combinations). The columns, braces and beams of the EBF were checked under the action of ULS (fundamental and special non-dissipative) combination of loads. As a general idea a mild steel

strength S235 was used for dissipative elements, while the non-dissipative elements were conceived of higher strength steel S355.

The following sections resulted for the structural elements:
- columns EBF – HEB260, S355
- columns MRF – HEB260, S355
- beam, including link EBF – HEA200, S355
- beams MRF – HEA260, S235
- braces EBF – HEA180, S355

The hinge limit states are shown as defined in the SAP2000 software, as follows:
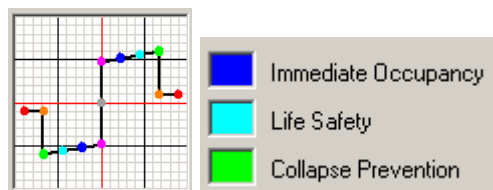
Fig. 3.5.   Plastic hinge's limit states as defined in SAP2000 [44]

The corresponding values for the above mentioned limit states were taken from the American norm FEMA356 [57], and represent the following levels of plastic rotation:

Element	Limit state	Maximum rot. Values [mrad]
Link	IO	50
	LS	110
	CP	140

Element	Limit state	Maximum rot. values [mrad]
RBS	IO	$12.5-0.1d^*$
	LS	$38-0.2d^*$
	CP	$50-0.3d^*$
*d – height of section in inches		

Table. 3.1.Allowed values for rotations in FEMA356 [57]

Further on we can observe the plastic hinge development by the push-over analyses:
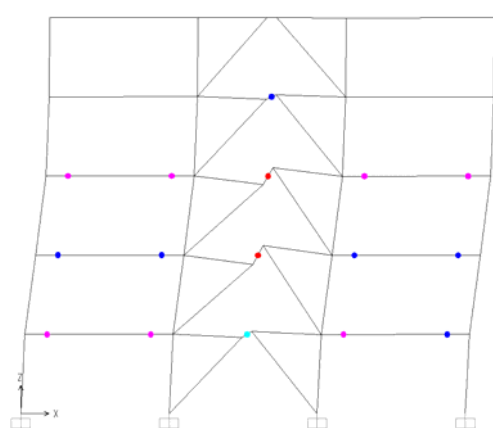
Fig. 3.6.   Development of plastic hinges during the push-over analisys

The incremental dynamic analyses of Time-history type (TH) were performed using the scaled recordings of 3 earthquakes from Vrancea region, from 1977, 1986 and 1990. The accelerograms used were recorded at INCERC Bucharest site. The earthquake with the highest intensity (Vrancea 1977, NS component) has the peak acceleration PGA=0.19g.
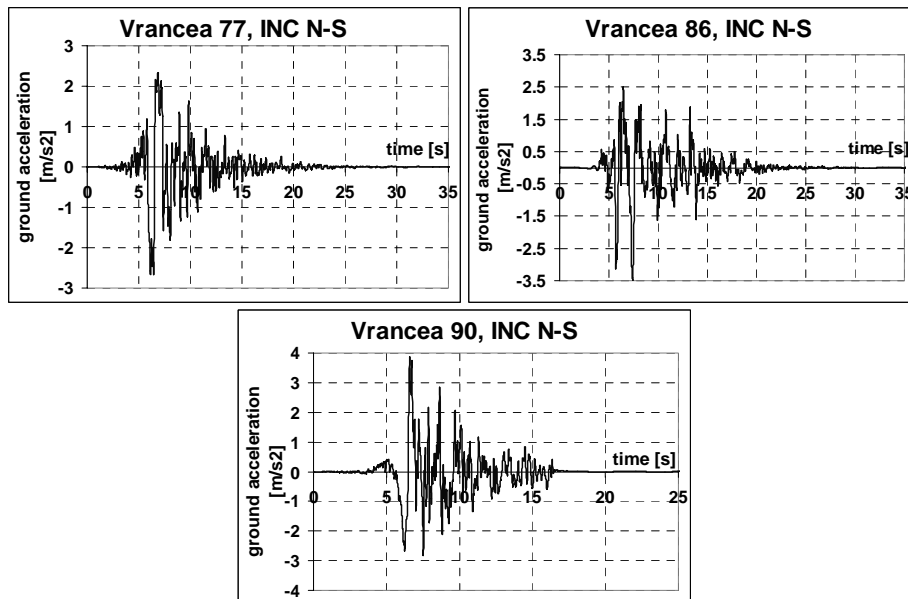
Fig. 3.7.   Recordings of earthquakes Vrancea '77, '86, '90

The incremental analysis was performed for values of the acceleration multiplier λ=0.2, 0.4, 0.6, 0.8, 1.0, 1.2, 1.4 1.6, 1.8 and 2.0 from the value of the recorded quake. All the accelerograms have been pre-scaled in order to have the ground acceleration design (0.24g) for a value of λ=1.0. The parameters recorded were the development of plastic hinges and inter-story drift. The obtained values were compared to the allowed values from SR EN-1998-1. The following tables show the values of max inter-story drift (maximum during analyses, for all stories).

The maximum inter-story drifts are compared in tables, as follows:

Max Inter-story Drift		S235/ S355	Fixed link
Limit St.	VR77 [%]	VR86 [%]	VR90 [%]
SLS	0.13	0.14	0.16
SLU	0.50	0.36	0.78
CPLS	0.63	0.48	0.94

Max Inter-story Drift		S235/ S355	Det. link
Limit St.	VR77 [%]	VR86 [%]	VR90 [%]
SLS	0.15	0.15	0.15
SLU	0.41	0.55	0.85
CPLS	0.59	0.77	1.33

Table. 3.2.Comparison of inter-story drifts for the structure with fixed and detachable link – in the solution with steel beams only

The limit states correspond to the following values of the multiplier:

SLS – λ=0.4 – a_g=0.096 (serviceability limit state)
ULS – λ=1.0 – a_g=0.24 (ultimate limit state)
CPLS – λ=1.22 – a_g=0.29 (collapse prevention limit state)

One can easily notice that the rigidity of the entire structure is affected by the rigidity of the detachable link connection, this fact leading to greater story displacement. In a similar way we can compare the values of the rotations in the plastic hinges in the link.

In the second part of this numerical simulations study, the same structure was considered, with the same geometry and characteristics, but in this case the beams were composite. The composite effect had a direct influence on the rigidity of the structure. This is confirmed by the values of inter-story drifts which are significantly smaller for composite frames with composite beams. No global or partial mechanisms were recorded. The developing of plastic hinges has been favored by considering a composite section only in the areas where no plastic hinges are expected to appear, i.e. at a distance of 2h (h-beam height) from the beam-to-column connections and outside the link.

The incremental-dynamic analysis gave similar results with those of the original structural configuration, with the general comment that the story drift and link rotations are significantly smaller than in the case of the steel structure. Regarding the inter-story drift values, these can be found in the next tables:

Max Inter-story Drift	Composite	Fixed Link
Limit St.	VR77 [%]	VR86 [%]	VR90 [%]
SLS	0.10	0.10	0.10
SLU	0.36	0.45	0.62
CPLS	0.44	0.65	1.0

Max Inter-story Drift	Composite	Det. Link
Limit St.	VR77 [%]	VR86 [%]	VR90 [%]
SLS	0.13	0.14	0.13
SLU	0.39	0.50	0.61
CPLS	0.50	0.68	0.89

Table. 3.3.Comparison of inter-story drifts for the structure with fixed and detachable link – in the solution with composite beams only

Just like the structure with steel beams, the structure with composite beams tends to be more deformable when the link has a detachable configuration. Generally the development of plastic hinges started in the links and then spread at CPLS limit state in the MRF beams, but these stopped at the first level. The maximum rotation requirements were within the admissible normative limits.

In conclusion, it could be stated that both configurations (steel and composite) have been designed properly, fact that is confirmed by the push-over and ID analyses.

On this basis the experimental program was developed on the dimensioned frame sub-assemblies, at 1:1 scale, with the declared scope of investigating the ductile elements. In this purpose, the analyzed parts were the beam-to-column joints for MRFs respectively an entire one-storey EBF.

The main parameter of the test program was the influence of the connection between the steel beam and the concrete slab. To this purpose, besides the basic steel configuration, composite configurations have been considered, as follows:

- partial connection – the dissipative zone from the steel profile was not considered to be tied with the concrete slab by means of shear connectors, according to §7.7.5 of Eurocode 8.

- full connection – a complete interaction was considered between steel and concrete, by placing shear connectors along the entire length of the beams

In order to obtain the full connection between the steel beam and slab, the criteria and specifications regarding shear connectors and composite beams in general, from SR EN1994 (6.6) and EN1998 (7.6.2, 7.6.3) were fully met.

3.3 Description of the experimental programme

The experimental tests were developed on ductile elements of the main frame which was designed and analyzed in paragraph 3.2.1.

In fact, two types of dissipative elements were investigated experimentally, i.e.:

- short links (by tests on full EBFs)
- beam-to-column joints

For both types of tests, three configurations were considered for the beams: one in which the beam is only made of steel, the second one where the beam is connected with the concrete slab by means of shear connectors (composite cross-section) on the entire span and a third one where the connectors are suppressed in the potentially plastic regions.

3.3.1 Design of the EBF specimens

The EBF which was set to be the base frame for the test series was similar to the first-story central bay structure described in paragraph 3.2.1, and adapted specifically for the conditions in the CEMSIG laboratory. The figure below shows the main structural dimensions and layout:
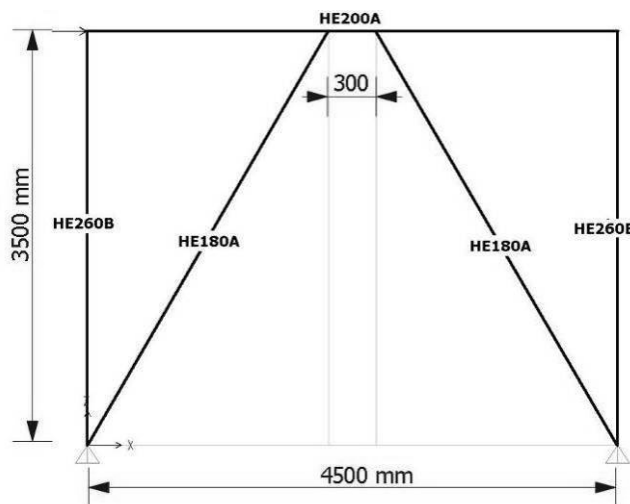
Fig. 3.8.   Dimensions and sections of the base EBF frame

According to the main objectives of the experimental study (see 3.1), the following parameters have been considered for EBF tests:
- type of loading: monotonic and cyclic
- type of link: fixed and detachable
- interaction between the steel beam and the composite slab: steel element only, connection of the non-dissipative parts and full connection (including the link).

The table below describes the 8 EBF specimens which were tested and their configurations, depending on the parameters listed before:

Test nr.	Frame	Beam type	Link	Type of loading	Connectors on the link	Name of the specimen
1	EBF	steel	fixed	monotonic	No	EBF_M_LF-M*
2	EBF	steel	fixed	cyclic	No	EBF_M_LF-C
3	EBF	steel	detachable	monotonic	No	EBF_M_LD-M
4	EBF	steel	detachable	cyclic	No	EBF_M_LD-C
5	EBF	composite	fixed	cyclic	No	EBF_Comp_LF1
6	EBF	composite	fixed	cyclic	Yes	EBF_Comp_LF2
7	EBF	composite	detachable	cyclic	No	EBF_Comp_LD1
8	EBF	composite	detachable	cyclic	Yes	EBF_Comp_LD2

* The EBF_M_LF_M specimen was considered the reference specimen in comparisons throughout the test series. All the cyclic tests were loaded on the basis of yield characteristics derived from this test (see 3.6.1). In this way all the cyclic specimens were loaded in similar conditions.

Table. 3.4.Description of the tested EBF specimens

The experimental EBFs were adapted to fit the CEMSIG laboratory set-up, with the lateral load applied at one end of the top beam (see Fig. 3.9). Unlike the real structure the tested specimens were pinned at the column base, in order to reduce the force necessary for the complete development of the plastic hinge, mainly for the case of composite beams. However, the behaviour of the link is not affected by the column-base connection type. (see Fig. 3.10)
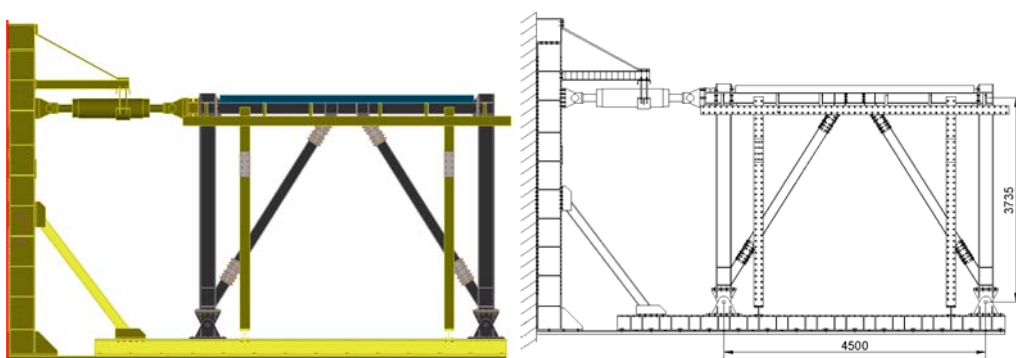
Fig. 3.9.   Experimental setup of the EBF frame
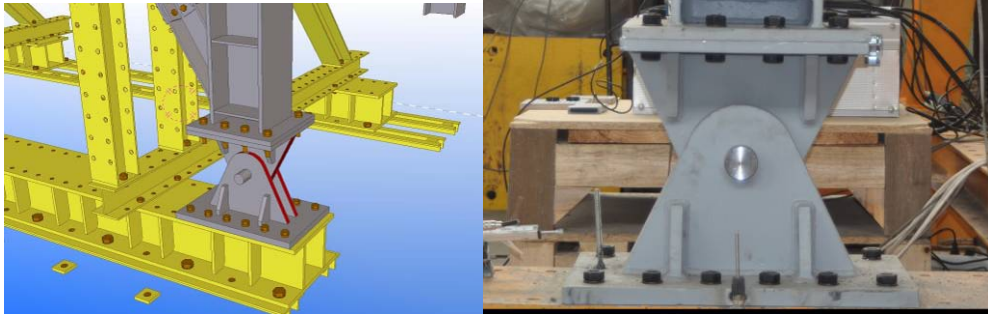
Fig. 3.10. Pinned column base

The beam-to-column connections were designed as fully resistant connections to axial load. It resulted an extended end-plate beam-to-column connection, bolted with 8xM20 HR.10.9. Details of this connection are given in Fig. 3.11:
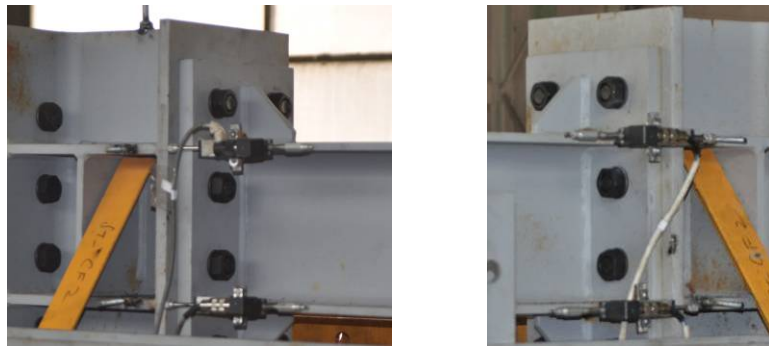
Fig. 3.11. Beam-to-column connections of the EBF frame

The brace-to-column connection was conceived as a splice connection on flanges and web in order to carry the plastic axial load of the brace (design according to EC8-1, paragraph 6.8.3 for non-dissipative elements). It resulted a 36xM16 HR.10.9 connection with splices on web and flange, as shown in Fig. 3.12:
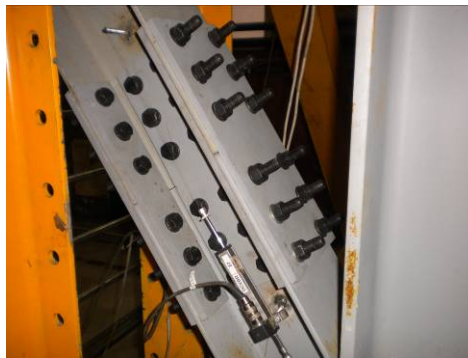
Fig. 3.12. Splice connection of the braces

In order to determine the maximum necessary force needed in the experimental tests (the maximum actuator capacity in traction is 850 kN), the experimental frame was modelled through a push-over FE Analysis by elastic-plastic analysis. For this it was considered the most force-demanding situation in which the beam was composite, over its full length.

The material was considered with its real characteristics, as determined by tensile tests for steel and compression tests for concrete. The model allows plastic hinge development at both ends of the beam and columns, in braces (axial hinges) and in link (shear hinge).

The results shown in Fig. 3.13, prove the fact that the expected failure load (approximately 750 kN) is acceptable for the testing setup.
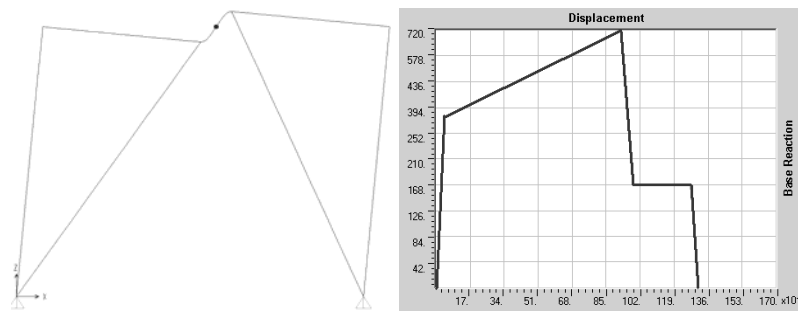
Fig. 3.13. Initial push-over analysis performed on the base steel frame

3.3.2 Instrumentation of the experimental frame

The force was applied at the column top by a hydraulic servo-actuator (Quiri HiFi J ST240/125-400) with a nominal capacity of 1000 kN in compression and 850 kN in traction, in static loading, through a MTS Flextest60 control station, with force or displacement control. The load cell integrated in the actuator was used to record the applied force.

Displacement transducers were used to monitor different absolute or relative deformations or displacements between different components. They have been located in key positions according to the type of specimen.

The displacement transducers were positioned in order to record deformations that can be divided globally into three main categories:

A. Global displacement measures of the frame, through the points located at the top of the left and right columns - by the transducers: DHTL, DHTRF, DHTRB.

B. Deformations of the dissipative elements i.e. web panel of the link, link's endplate – by the transducers: DDT1, DDT2, DSHTL, DSHTR, DSHBL, DSHBR, DSVL, DSVR.

C. Transducers used to check the slip and the displacements of the non-dissipative elements:

- at the base of the pin connections: DHBL, DVBL, DHBR, DVBR.

- the slip and elongation of the braces and their connections: DBLL, DBLR, DCVTL, DCVBL, DCVTR, DCVBR.

- the rotation of the beam-to-column joints by: DBCTL, DBCBL, DBCTR, DBCBR transducers.

The following schema shows the global monitored displacements on the frame:
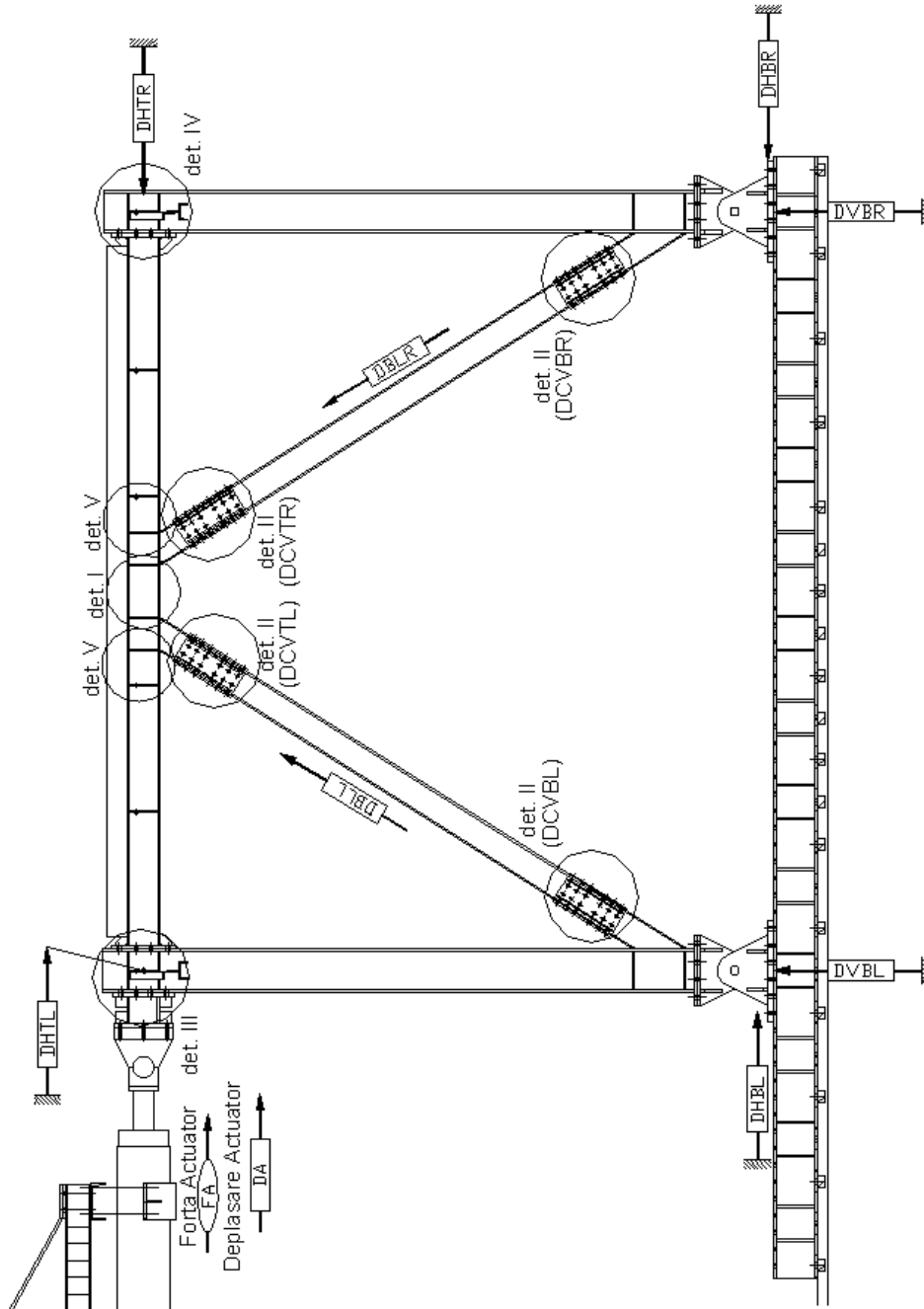
Fig. 3.14. Instrumentation of the EBF frame

The figures below show the detailed location of the transducers positioned on link and connections:

- Fig. 3.15 (detail Ia) shows the diagonal displacement transducers for monitoring link rotation
- Fig. 3.15 (detail Ib) shows the diagonal displacement transducers for monitoring link rotation, in the case when the link is detachable
- Fig. 3.17 (detail II) shows the transducers measuring the slip in the brace connection
- Fig. 3.18 (details III & IV) shows the transducers measuring the rotation in the beam-to-column connection
- Fig. 3.19 (detail V) shows the transducers positioned so that they could measure the slip and/or lifting of the slab in the dissipative zone of the beam

det.Ia   det.Ib
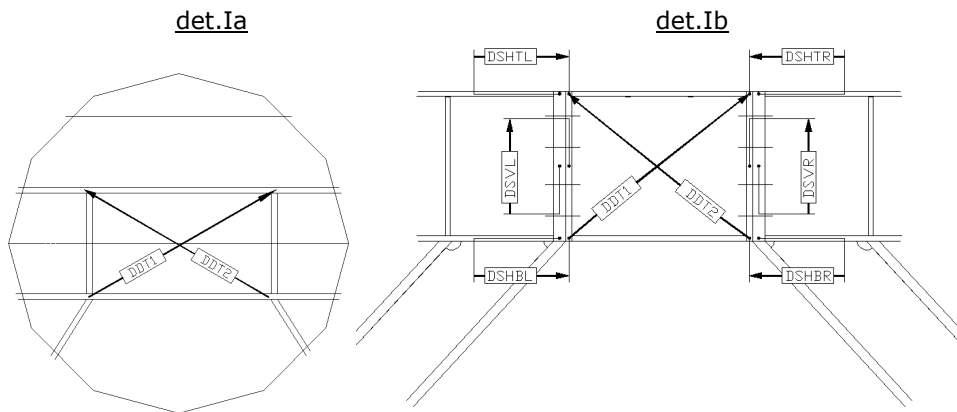
Fig. 3.15. Instrumentation of the fixed and detachable link

The link's rotation was computed with a relation proposed and certified by Stratan [28], as follows:
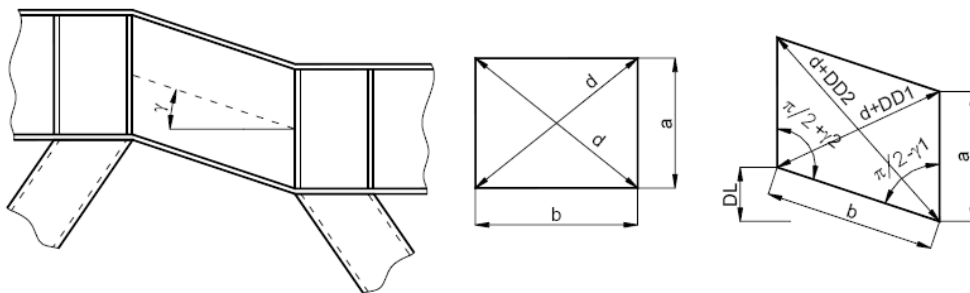
Fig. 3.16. Deformation of the link element and dimensions of the web panel

Where γ is calculated by:

$$\gamma = \frac{\sqrt{a^2 + b^2} \cdot (DD2 - DD1)}{2 \cdot a \cdot b}$$

[28]   (1a)

in which DD1 and DD2 are the recordings of the two transducers measuring the diagonals of the link, throughout the experimental test. In a more synthetic approach, the previous formula can be written as:

$$\gamma = \frac{\sqrt{190^2 + 300^2} \cdot (DDT2 - DDT1)}{2 \cdot 190 \cdot 300} \tag{1b}$$
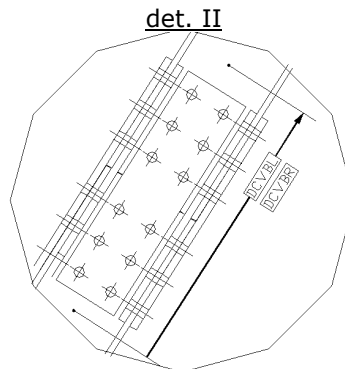
Fig. 3.17. Instrumentation on the brace connection
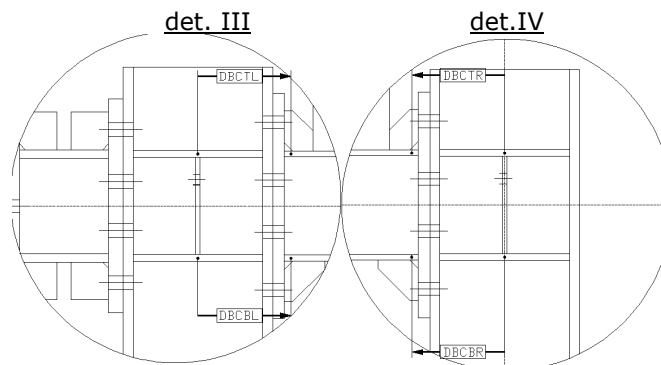
Fig. 3.18. Instrumentation of the beam-to-column connection
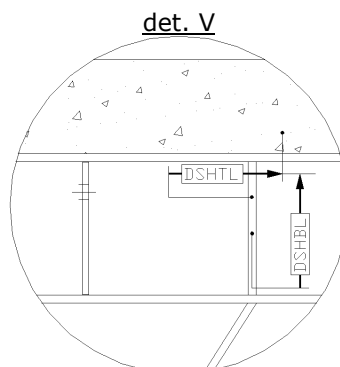
Fig. 3.19. Transducers measuring the slab's relative movement

All the displacements and force were recorded simultaneously through a HP3852A data acquisition unit, connected to a computer:

Fig. 3.20. The data acquisition system

3.4 Tests performed on material samples

Before performing the full-scale tests, material samples were retrieved from profiles and concrete slab and tested in order to find their real mechanical characteristics. From the steel profiles, test samples were extracted from both the web and flanges, and cut according to the specifications of norm SR EN10002. The steel material tests were performed on an universal testing machine INSTRON (in the CEMSIG laboratory), capable of static loads up to 1200 kN and dynamic loads of 1000 kN. The elastic-plastic deformations of the flat specimens were measured via an optical extensometer, and also confirmed by hand measurements. For each batch 3 specimens were tested.

The material testing setup and an example of processed results can be seen in the following picture:
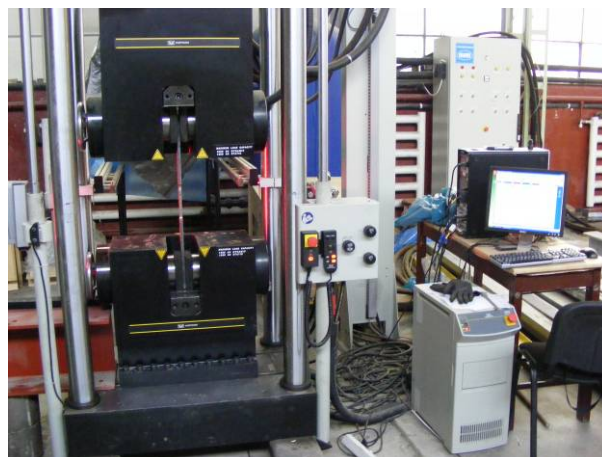
Fig. 3.21. Tension testing of the flat specimens

During the pouring of the concrete for the composite beams, the concrete was vibrated. After the maturing period of 27 days, the test cubes which were taken at the moment of the pouring were tested in the lab in order to determine the concrete's ultimate strength, and to check if the concrete's class suits the desired values of C20/25.

Fig. 3.22. Reinforcement of the composite beam

The concrete compressive tests were performed on cubic specimens. Tests were performed on a standard machine of 600 kN, following the standard compression procedure:

Fig. 3.23. Testing of the concrete cubes

The table below shows the main mechanical characteristics of the materials:

Element	Profile	Part of the profile	Supposed Material Class	Yield strength [N/mm²]	Ultimate strength [N/mm²]	Tensile Strain at Break [%]
EBF Beam	HE200A	web	S235	323	475	32.24
		flange		304	434	35.01
EBF Brace	HE180A	web	S355	326	511	29.46
		flange		398	533	36.81
EBF Column	HE260B	flange	S355	283	440	48.06
Node Beam	HE260A	web	S235	263	396	43.82
		flange		265	390	52.15
Node Column	HE260B	flange	S355	283	440	48.06
EBF's Slab Concrete	12 cm	-	C20/25	-	23	-

Table. 3.5.Nominal values for the tested materials

On the values resulted from tests the following conclusions could be drawn:
- columns are made from a lower class of steel then the design value;
- the beams are rather S275 than S235;
- the concrete fits its prescribed values (C20/25), with a mean compressive stress of 24.5 N/mm^2.

The M16 bolts were also tested in tension. Two failure modes of the bolts (from the link-beam connection) were noticed during the tests, namely by tearing of the threaded section and by bolts braking in tension. Otherwise, the bolts' resistance was compliant with the one given in the norms (SR EN1993-1-8, table 3.4).

Fig. 3.24. Failure of the bolts at the link-beam connection

3.5 Loading protocols for the tested specimens

The general ECCS procedure was used for monotonic and cyclic tests (1986). From the monotonic base test (EBF_M_LF-M) were computed the yield characteristics (yield displacement and corresponding force). These values resulted by a graphic method at an intersection point of the lines defining the elastic rigidity of the F-Δ curve and the one tangent to the graph, having 1/10 of this elastic rigidity (see Fig. 3.25). The yielding characteristics have been further used for applying the ECCS standard cyclic procedure, as follows:

- one cycle at 0.25*Dy, 0.5*Dy, 0.75*Dy and at Dy
- groups of 3 cycles at each even Dy increment: 2Dy, 4Dy, 6Dy, 8Dy and so on. The graphical illustration of this loading pattern is shown in Fig. 3.26.
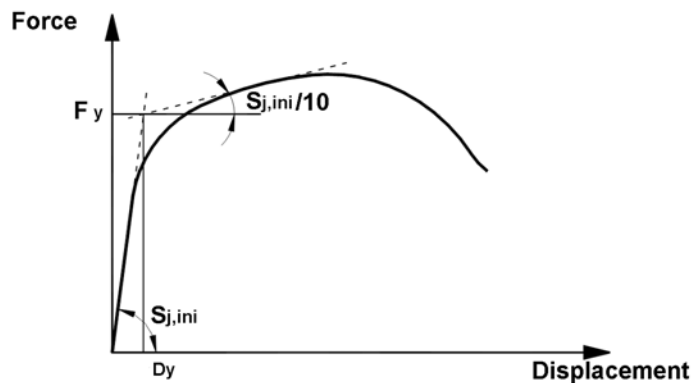
Fig. 3.25. Determining the yield displacement from the monotonic test – graphic method
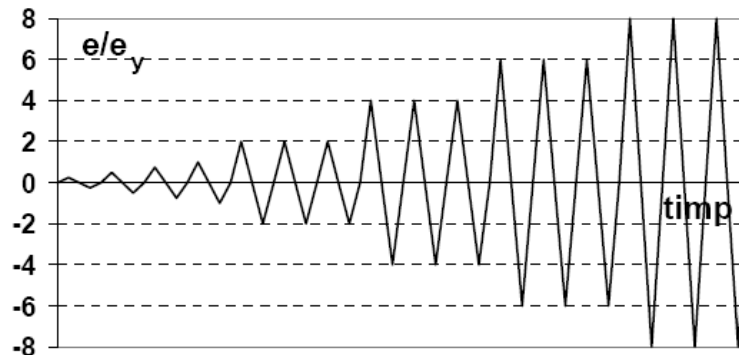
Fig. 3.26. Cyclic loading procedure applied according to ECCS specifications

The termination of each test was considered at a drop of 50% in the maximum load, also in accordance to the ECCS procedure.

3.6 Experimental results for the EBFs

3.6.1 EBF_M_LF-M specimen (steel, under monotonic loading)

This specimen served as basis of comparison for all the other EBFs which were tested. The specimen was loaded monotonically, until failure. The next chart describes the force-displacement curve for the specimen, where force represents the load induced by the actuator, and the top displacement is the average displacement given by several transducers (see Fig. 3.18), found as:

$$D_{tot} = (DHTL + \frac{DHTRF + DHTRB}{2})/2 - (DHBL + DHBR)/2$$
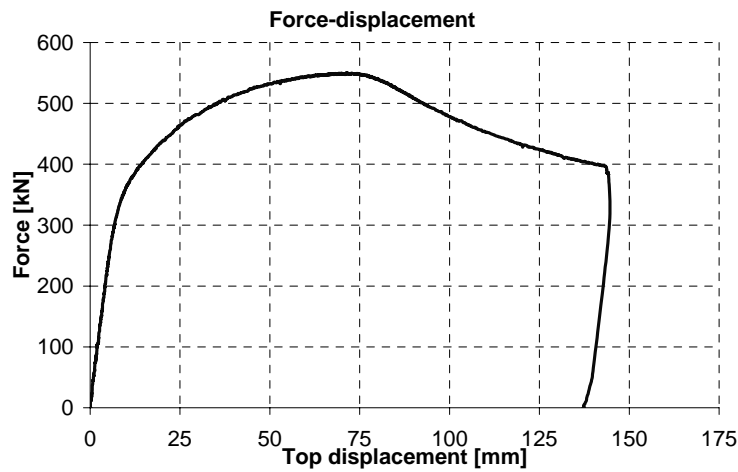
Fig. 3.27. Load-displacement curve of the specimen EBF_M_LF-M

Based on the curve above, the following values were determined in order to be used in the following cyclic tests:

S_{ini}=48.20117 kN/mm
F_y=343 kN
D_y=7.9 mm
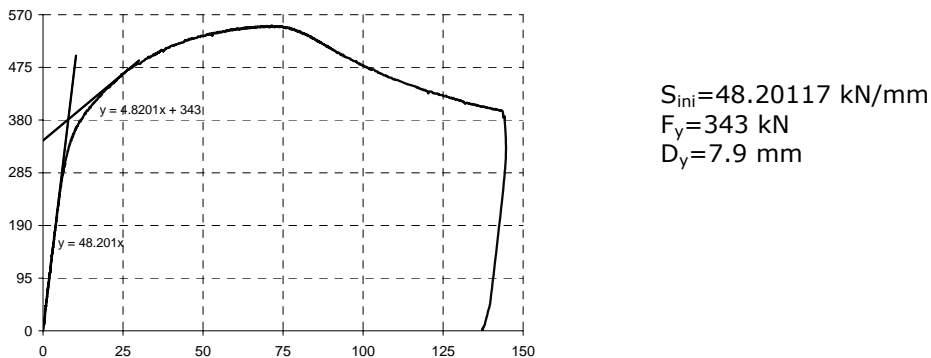
Fig. 3.28. Determination of the yield displacement and force

As expected, the link exhibited the most of the dissipated energy, as it can be seen in Fig. 3.30. In the chart below, the rotation is computed by the formula (1b). The other components such as connections and braces exhibited only elastic behaviour.
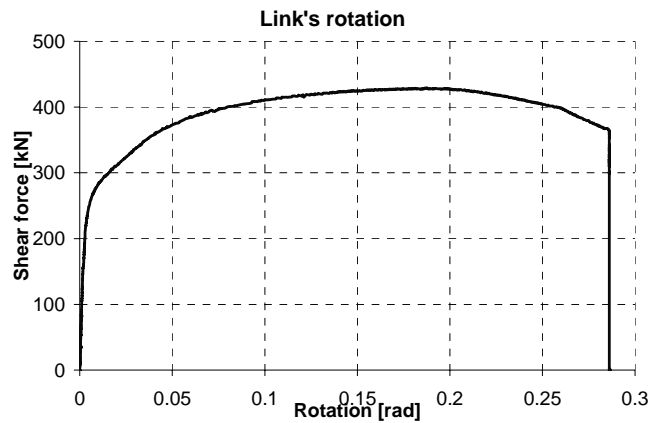
Fig. 3.29. Shear force-rotation curve of the short fixed link, with the beam in the steel

solution

The specimen proved a very ductile behaviour, reaching almost 280 mrad, a value which is much higher than the required limit of P100-1/2006, SR EN1998 (80 mrad) and FEMA356 (110 mrad). In fact the specimen did not fail but it had only a significant shear distortion of the link's panel as it could be seen in Fig. 3.30. The termination of the loading was due to reaching the stroke limit of the actuator.

In the following pictures one can see the deformed shape at the maximum displacement:
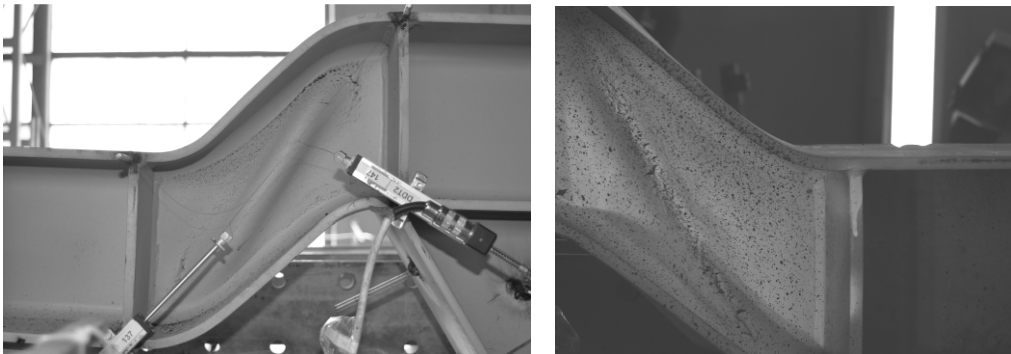
Fig. 3.30. Dissipative link failure by shear of the web (front and back)

The deformations of the connections are measured by transducers DCVBL, DCVBR (bottom left and right connections) and DCVTL, DCVTR (top left and right connections), while the global braces' deformation was given by transducers DBLL and DBLR (see also Fig. 3.15 - Fig. 3.19).

The non-dissipative elements such as the braces and the columns did not suffer any plastic deformation, nor did their connections. These elements remained in the elastic domain as shown by the recorded deformations (e.g. for the braces). Note that the remnant displacement of about 4 mm in the braces (see Fig. 3.31) is due to the connections' slip (2mm for each side – tolerances). No slips were recorded in the columns' bases.
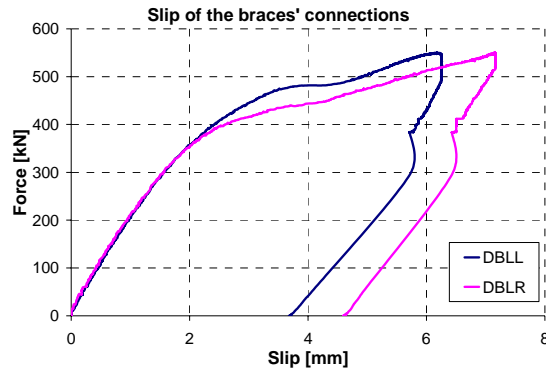
Fig. 3.31. Slip of the braces' connections

3.6.2 EBF_M_LD-M specimen (steel, monotonic with detachable link)

The characteristic of this specimen is the detachable link. The connection between beam and link was designed as a flush endplate solution (see Fig. 3.32). This was designed using the component method, with the bolts loaded in combined shear and bending.

The endplate was thicker on the beam (20 cm) and thinner on the detachable link (15 cm) in order to have deformations only in the latter element. It resulted a flush endplate connection with 4 rows of bolts M16 HR.12.9:
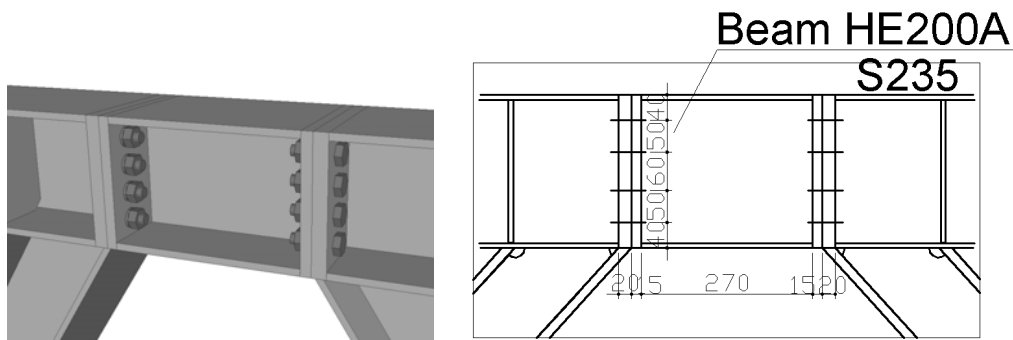
Fig. 3.32. The link-to-beam connection

The global behaviour of the specimen could be characterized as stable up to the maximum load. However, the link-to-beam connections induced a supplementary deformation, fact which is demonstrated by the initial rigidity: S_{ini}=17.43 kN/mm, which is by 63.8% smaller than the one of the base specimen

(EBF_M_LF-M). The maximum force is smaller by 10% to that of the base specimen (F_{FL}=550>F_{DL}=511).

Force-displacement
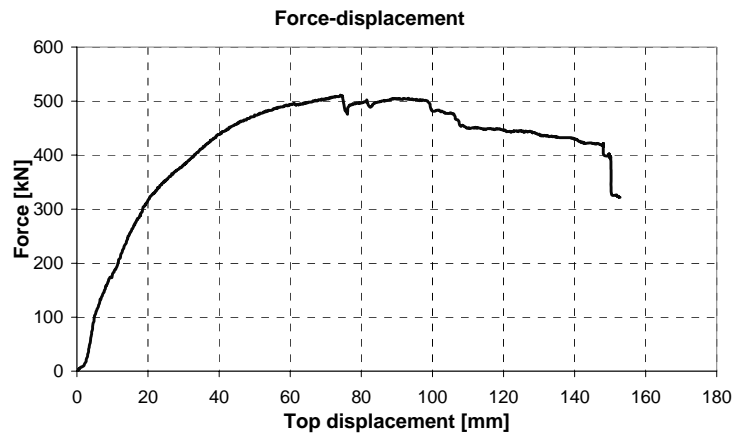
Fig. 3.33. Load-displacement global curve of the specimen EBF_M_LD-M
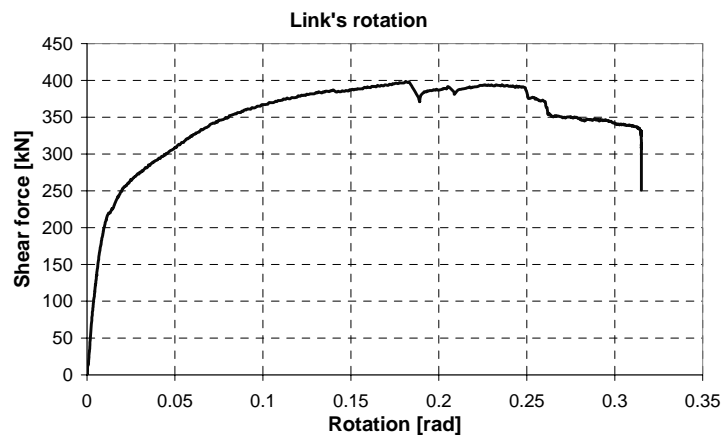
Link's rotation

Fig. 3.34. Shear force-rotation curve of the short detachable link, with the beam in the

steel solution (includes link's distortion and connections' rotations)

However, the detachable link's failure mode was greatly influenced by the connection with the beam (see Fig. 3.36). Only the endplate of the link behaved in the plastic domain, affecting the link's rotation beyond the point of maximum force. The maximum distortion observed in this case reached more than 300 mrad, greater by far than the limits stipulated in European (80 mrad) and American seismic standards (140 mrad for CPLS).

One can notice that the link's endplate distortion influenced the total rotation of the link only after the failure of the first row of bolts in tension, as seen in Fig. 3.35.
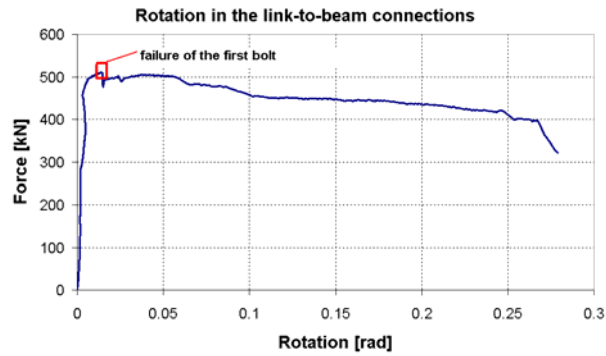
Fig. 3.35. Cumulated rotation in the link-to-beam connections

It should be said that the final failure was a combined one between link and endplate deformations. The bolts failure conducted to the descending branch of the characteristic F-γ curve.

Fig. 3.36. Dissipative detachable link failure by shear of the web

Similar to the fixed link specimen, the non-dissipative elements suffered only elastic deformations. The main member connections behaved accordingly, without slips or inelastic behaviour.

3.6.3 EBF_M_LF-C specimen (steel, cyclic test with fixed link)

The hysteretic curve had stable cycles which show very good dissipation capability.

Force-displacement
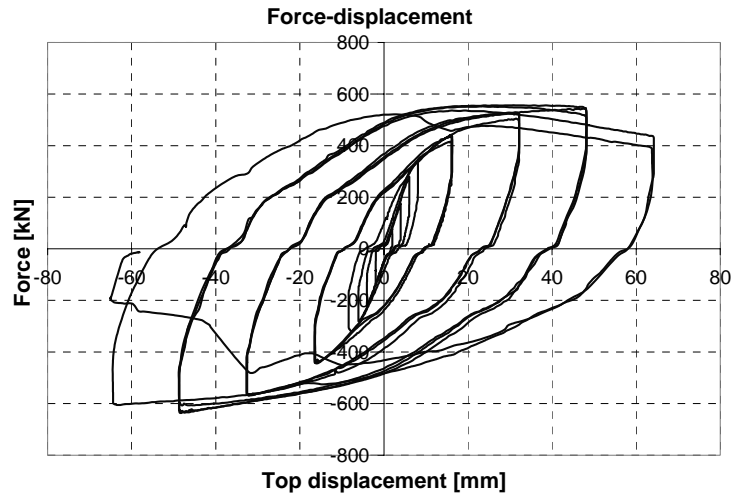
Fig. 3.37. Load-displacement curve of the specimen EBF_M_LF-C
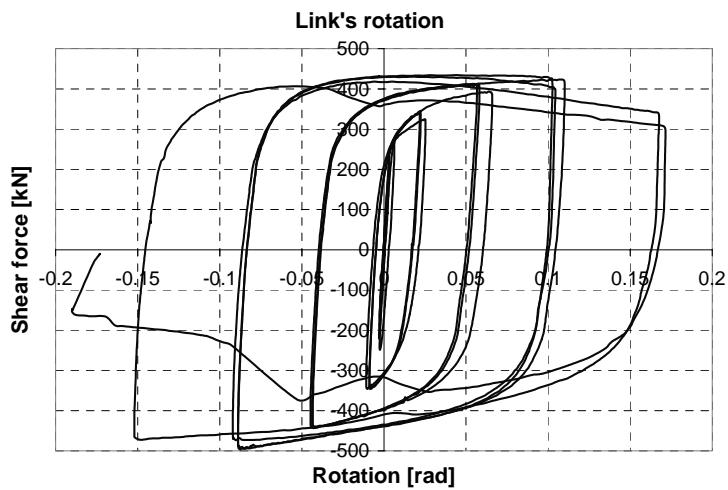
Link's rotation

Fig. 3.38. Shear force-rotation curve of the short fixed link under the cyclic load

Remarks and conclusions of the cyclic test with fixed link:
- The losses in strength and stiffness at cycles of the same amplitude are relatively small;
- Failure of the specimen occurred by complete shear of the link's web panel (see Fig. 3.39)
- The capacity of the link is the same with the one of the base specimen in terms of capable force and stiffness
- The link has reached rotation values higher than 150 mrad.

Fig. 3.39. Behaviour of the link, failure of the web in shear

3.6.4 Cyclic testing of the specimens with composite beam and fixed link EBF_Comp_LF1 and EBF_Comp_LF2

Both specimens had a composite beam, with a 12 cm concrete slab, and steel reinforcement of 12 mm diameter disposed at 15 cm apart, on both directions at the inferior and superior part of the slab. The reinforcing details can be seen below. No increase in the reinforcement area was used above the link.
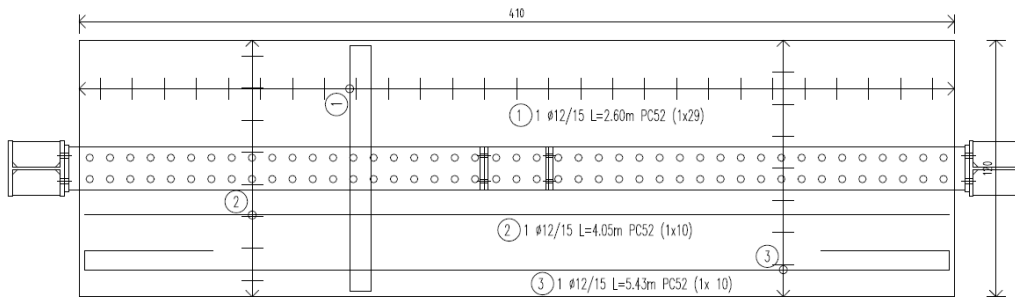
Fig. 3.40. Reinforcement of the composite beam from the EBF

Due to the need to achieve full interaction between the steel flange and the concrete slab, and because the bending moment suffers changes in sign during a cyclic test, the shear stud connectors were placed as seen in Fig. 3.40.

The main difference between the two composite specimens is the presence of connectors over the link:
- In case of EBF_Comp_LF1 the connectors have been disposed only above the beams, up to link limits
- For EBF_Comp_LF2 the connectors are disposed continuously over the top flange of the beam, including the link zone.
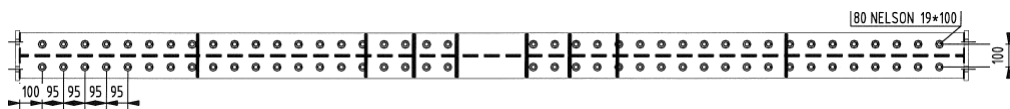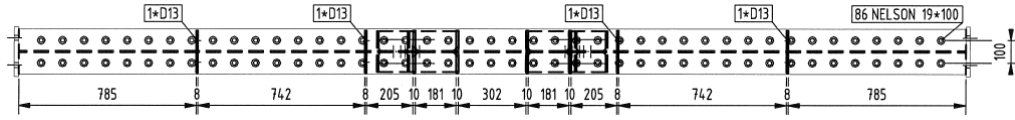
Fig. 3.41. Connectors' distribution in case of specimens EBF_Comp_LF1/2

The behaviour curves of the two composite specimens are similar:
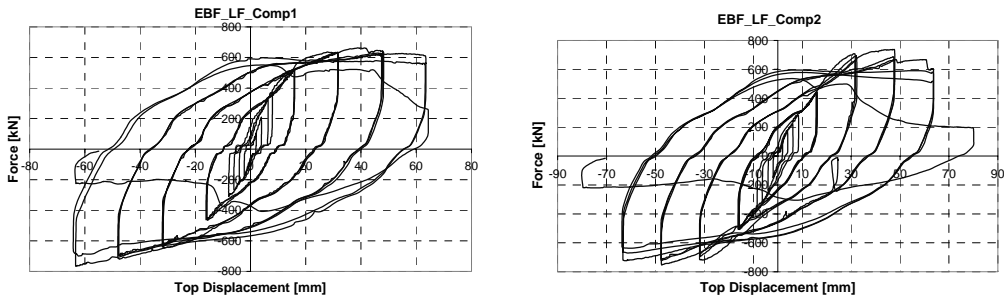
Fig. 3.42. Hysteretic curves of the two composite specimens with fixed link

The specimen with connectors on the dissipative element has proven to have a slightly higher ultimate force and rigidity and a slightly better dissipation capacity. Now, if we compare the link's rotation in these two cases, the above mentioned conclusions remain valid, as we can notice from the following diagrams:
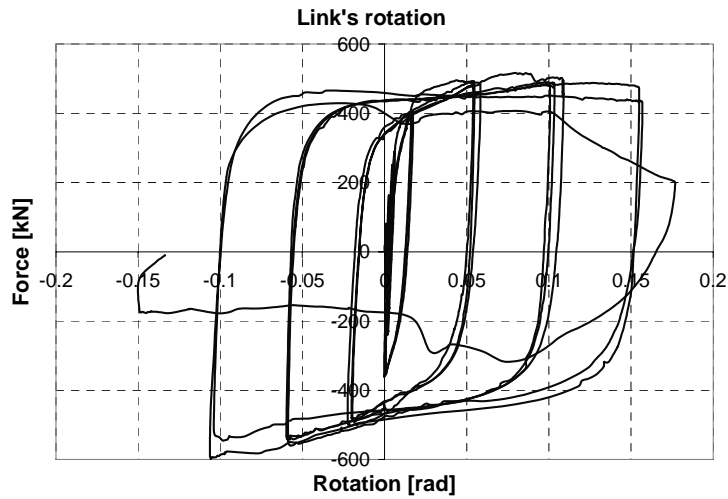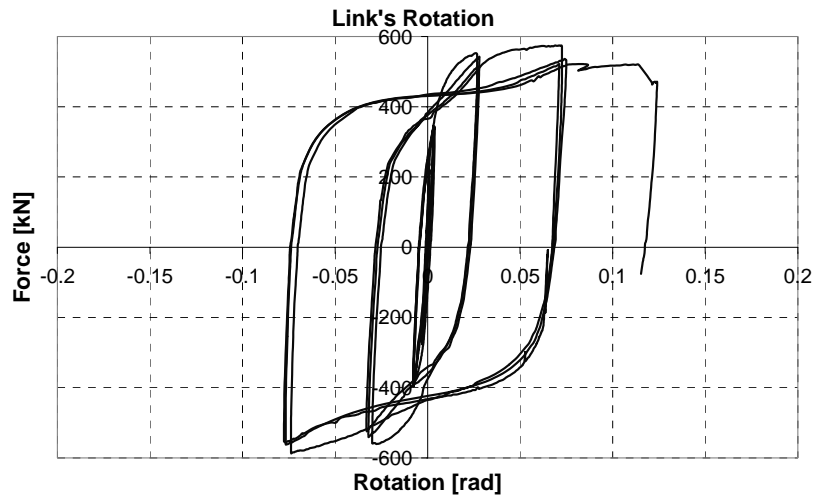
Fig. 3.43. Shear force-rotation curves of the short fixed composite link under the cyclic load, specimens EBF_LF_Comp1 and EBF_LF_Comp2

The link rotation curve in the case of EBF_LF_Comp2 is in fact incomplete on the discharging branch, due to the deterioration of the displacement transducer's readings, affected by the highly-damaged concrete slab above the link. Fig. 3.44 and Fig. 3.45 present the failure conditions for links and concrete slab.
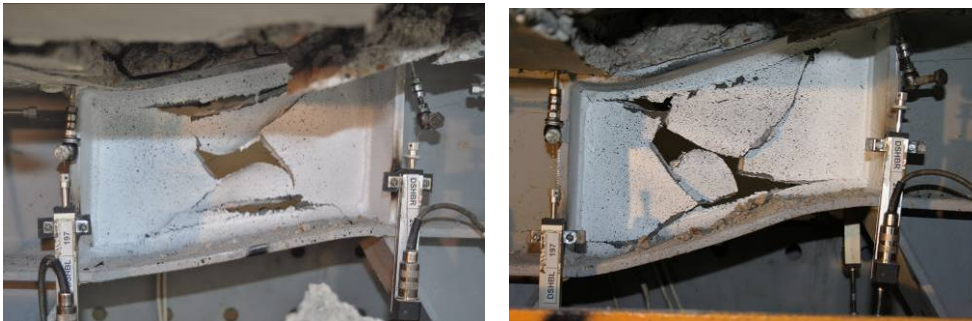
Fig. 3.44. Damage of the fixed link during the tests of EBF_LF_Comp1 and Comp2

Fig. 3.45. Damage of the concrete slab during the tests of EBF_LF_Comp1 and Comp2

However, in the ultimate state, in the second case, when shear connectors were placed on the link, the damage to the concrete slab has a bigger extent. Generally, the damage of the slab was local, with crack patterns developing at angles of 45 degrees from the position of the link. No relative deformations (horizontal or vertical) occurred between the concrete slab and the steel flange.

3.6.5 Cyclic testing of the specimens with composite beam and detachable link EBF_Comp_LD1 and EBF_Comp_LD2

The specimens had both a detachable link with bolted endplate connection to the beam, following similar detailing of the steel links. The difference between the links was (just as in the previous two cases) given by the interaction with the concrete slab:
-    the first tested frame EBF_Comp_LD1 was without shear stud connectors on the link;
-    the second specimen, EBF_Comp_LD2, had shear connectors placed on the beam's and link's flange.

Thus, the results where greatly influenced in this case by the presence of the concrete slab. The first observation is that the detachable link suffered considerable less slip in the connection to the beam. Because of the fact that the neutral axis changed its position and that the reinforcement had a tying effect towards the beam-to-link connection, this connection suffered no damage at all (quite different from the case when the beam was made only of steel). Overall, the frame with composite beam and detachable link had a behaviour comparable to the case of the frame with composite beam and fixed (continuous link). The hysteretic curves for the two tests can be seen below:
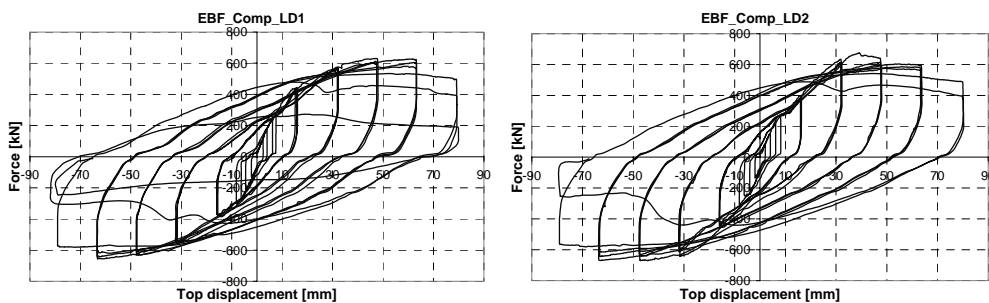
Fig. 3.46. Hysteretic curves of the two composite specimens with detachable link

The slab was damaged only above the link region, the concrete being completely crushed. The detachable link was the only element to suffer plastic deformations, besides the slab, which lead to the classical failure mode - shear of the web. The link reached levels of rotation of about 110-140 mrad up until its failure. Overall, the behaviour of these specimens was very similar to that of the specimens with fixed link and composite beam.

Link's Rotation
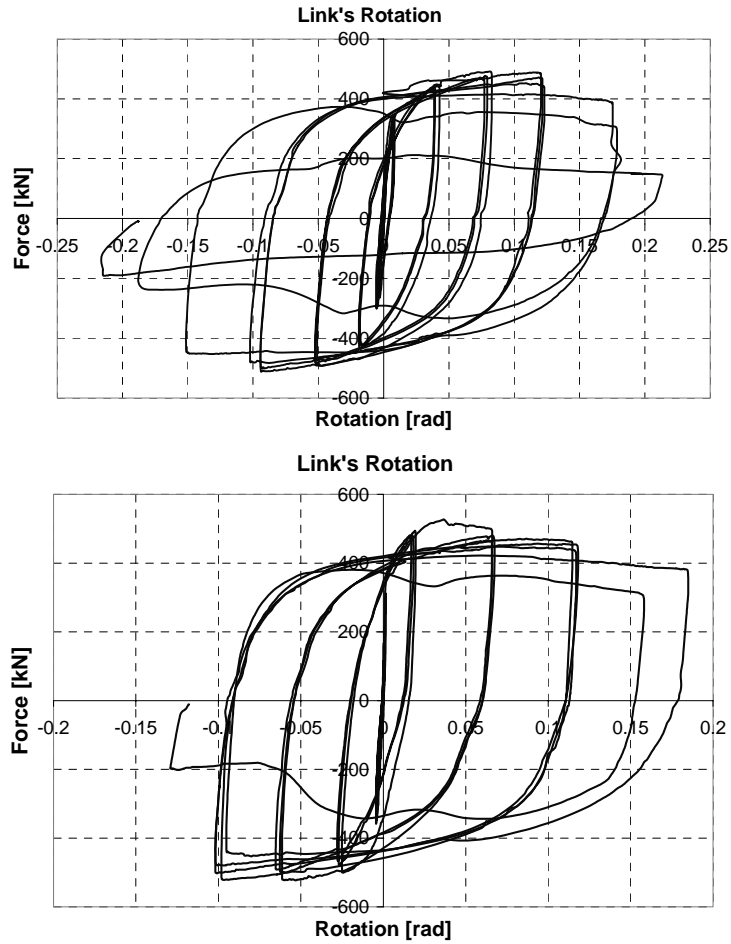
Link's Rotation

Fig. 3.47. Shear force-rotation curves of the short detachable composite link under the cyclic load, specimens EBF_Comp_LD1 and EBF_Comp_LD2

Fig. 3.48. Damage of the detachable link during the tests of EBF_Comp_LD1 and LD2

Fig. 3.49. Damage of the concrete slab during the tests of EBF_Comp_LD1 and LD2

3.6.6 Cumulative results and comparisons between all tested EBF specimens. Conclusions

The synthetic results of all EBF specimens are given in the following table:

Specimen	Sj,link	V,max [kN]	Gamma @V,max [mrad]	Gamma, max [mrad]
EBF_M_LF-M	130460	429	187	286
EBF_M_LF-C	74644	495	87	171
EBF_M_LD-M	54717	398	181	250
EBF_M_LD-C	63530	394	104	147
EBF_Comp_LF1	123414	598	105	156
EBF_Comp_LF2	152488	587	74	N/A
EBF_Comp_LD1	119714	512	94	178
EBF_Comp_LD2	147722	527	53	157

*where all the values were computed on the maximum envelope curve (cycle 1)
**$S_{j,link}$ – initial rigidity of the link
    V,max – maximum shear force developed in the link
    Gamma@V, max – rotation in the link corresponding to maximum shear force
    Gamma, max – maximum rotation attained by the link element
        Table. 3.6.Important values describing the behaviour of tested EBFs

For a better interpretation of this data, the following charts show the above results displayed following the same parameters as declared in the beginning of the study (see Table.3.4.):
        - influence of composite slab
        - influence of detachable link's connections
        - influence of loading type (cyclic/monotonic)
Envelope curves for the first and third cycle are shown below, plotted in terms of top displacement and force, for the specimens with fixed link:
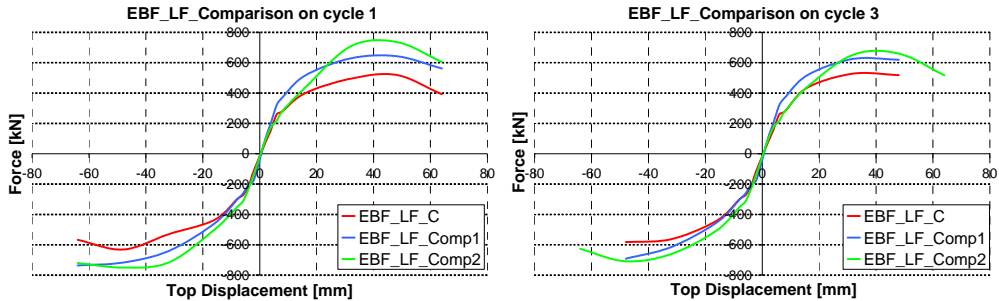
Fig. 3.50. Envelope curves compared on the 1st and 3rd cycle of the EBF with fixed link

In both cases, one can clearly notice that there is a significant increase in the ultimate resistance of the EBF, when the beam is composite. Another immediate notice is that there is little increase in rigidity and the maximum capable force with or without shear connectors in the plastic zone increases by approx. 5-10%. The composite solution did not lead to unwanted damage to the other elements of the frame, nor did it cause any premature failure. All specimens reached high levels of distortions (in link), reaching practically the requirements of modern seismic norms (80-140 mrad).

The comparison between the cyclic tests with detachable link and the two specimens with composite beam are shown below:
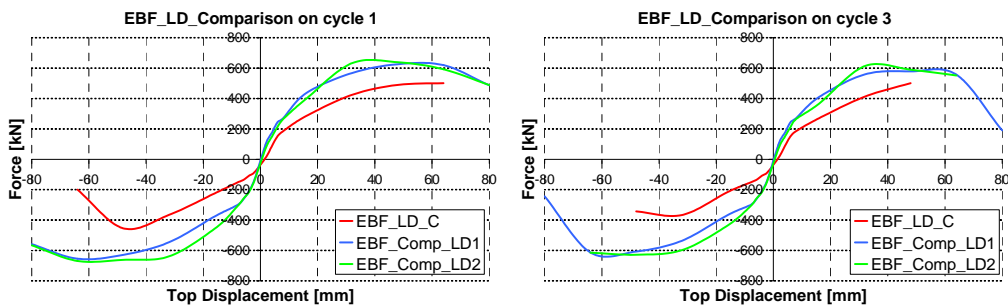
Fig. 3.51. Envelope curves compared on the 1st and 3rd cycle of the EBF with

detachable link

However, the most important conclusion is that the presence of the slab over the link element will influence noticeably the behaviour of the link, independently of the connection with the concrete slab. Similar conclusions are drawn for cycles 2 and 3, respectively.

Regarding the influence of the composite slab, the charts presented in Fig. 3.52 show the comparative results (in terms of Shear force – link distortion) for the cyclic envelope curves for all cyclic tested specimens. In order to have clear conclusions, the envelopes are drawn for the first and third cycles respectively:

-   The envelopes for the first cycle represents the „exterior" envelopes giving the maximum resistance response
-   The third cycle envelope represents the response of the element already damaged. This could be considered as a mean response in case of a strong seismic event.
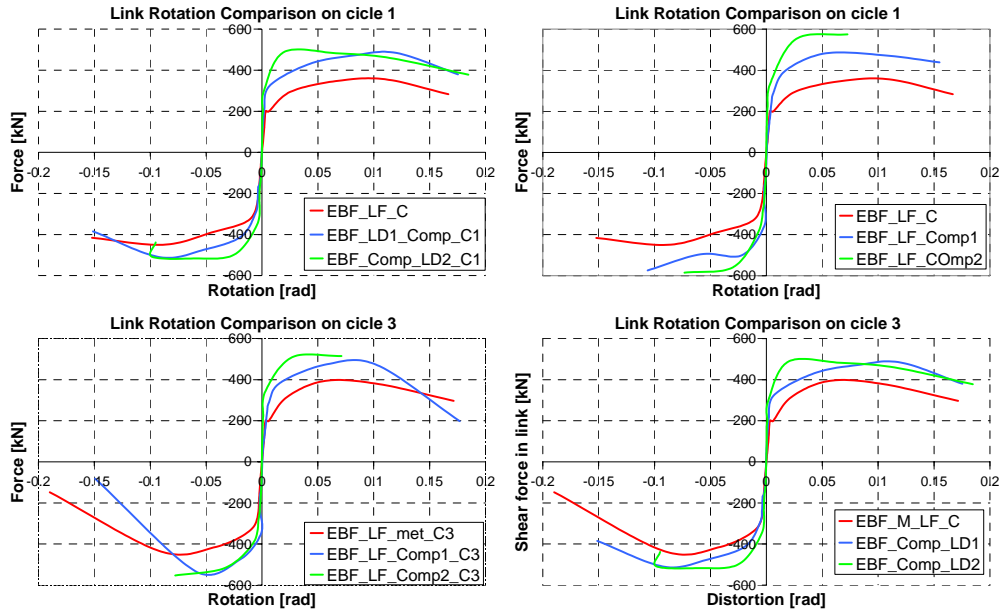
Fig. 3.52. Envelope curves compared on the link's rotation

When comparing the rotation capacities vs. shear force plots for the tested links, the following ideas can be emphasized:
-    A 20% drop in resistance for the steel specimen;
-    Higher rigidity for composite specimens (up to 30%);
-    All specimens exhibited high ductility.
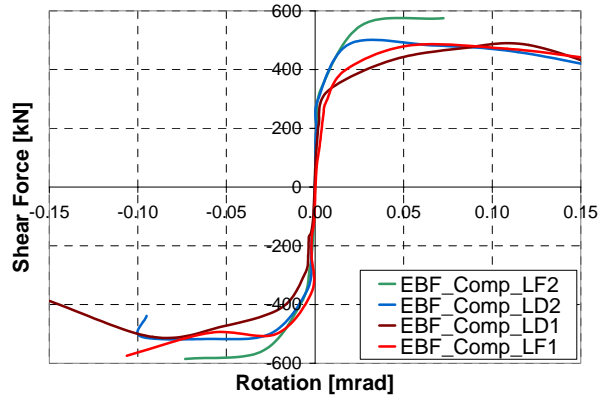
Fig. 3.53. Envelope curves comparing fixed and detachable link (composite beam)

Fig. 3.53 shows the difference between envelope responses of composite specimens for fixed and detachable links. As expected, the link-to-beam connections introduce a certain release in their response. This can be divided into two stages:
-    An initial loss of rigidity due to the pinching effect ();
-    Bending of the end plate in the higher cycles of the tests ().

Fig. 3.54. Pinching effect on the link-to-beam connection

However these limitations are rather small and the two resistances can easily be compared. The presence of concrete slab was rather beneficial for the global behaviour of composite LD specimens as compared to pure steel LD specimens (where the connection suffered some damage).

The cyclic loading influenced the global behaviour of the specimens, when compared to the monotonic ones, with respect to the following parameters:

- Up to 40% decrease in rigidity
- Up to 15% increase in resistance
- The cyclic specimen reached smaller ultimate rotations, up to 171 mrad, compared to 286 mrad (see Fig. 3.55)
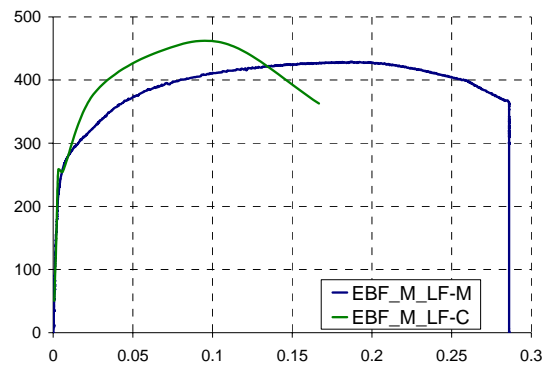
Fig. 3.55. Behaviour of the steel specimens, tested monotonic and cyclic

3.7 Design of the beam-to-column joints with RBS

The beam-to-column joints' design characteristics were retrieved from the real base structure (see §3.2.1):

- Column: HEB260 (S355) used for the first set of tests; HEB300 (S460) used for the second set of tests;
- Beam: HEA260 (S235), used for both sets.

The typology of the specimens is by direct welding of the beam onto the column flange, with reduced beam section (RBS) near the connection (see Fig. 3.56).

   The experimental investigation was performed on two sets with small differences in specimen's dimensions as shown in Fig. 3.56. The reason for the two sets of tests was due to the unsuitable shop welds which failed in the first set.

   As a result a second series of tests was designed, based on the improved welding execution, leading finally to appropriate results. The structural dimensions and layout of the specimens can be observed below:
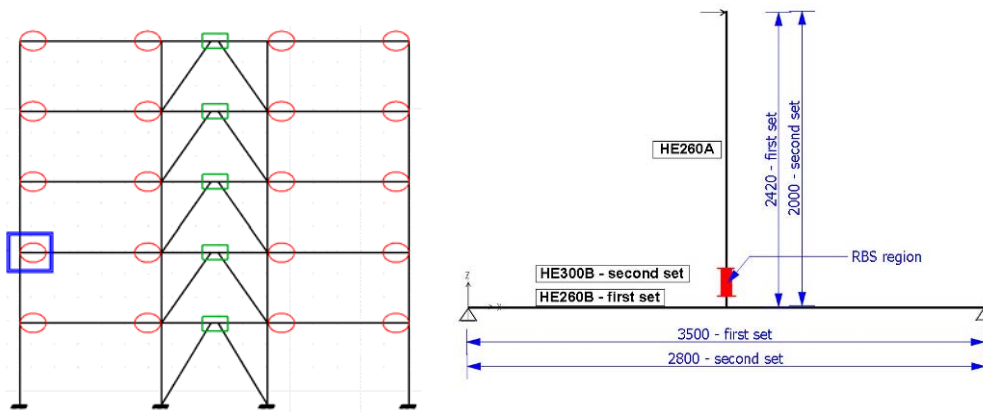
Fig. 3.56. Dimensions and sections of the tested RBS nodes

3.8 Experimental setup of the RBS joints and instrumentation

   The easiest way to test these specimens in the CEMSIG laboratory was by rotating the node by 90 degrees, so as the beam becomes vertical and the actuator loading horizontal. The specimens were prevented from out-of-plane displacements by a guiding frame. These conditions lead to the experimental setup shown in Fig. 3.57:
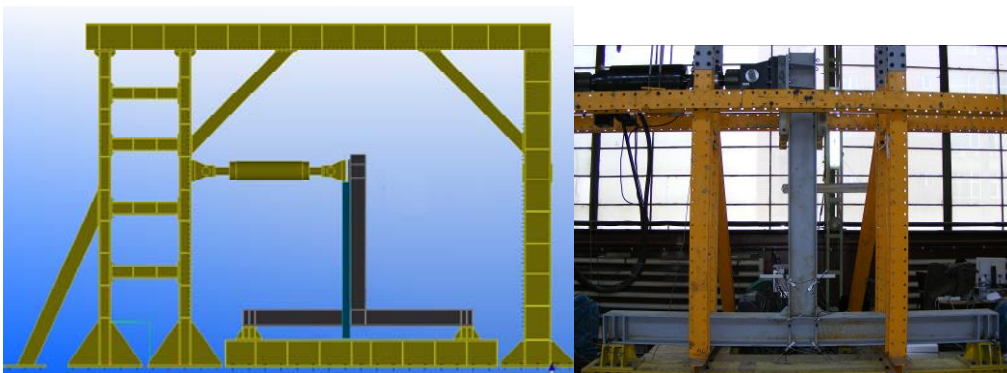
Fig. 3.57. Experimental setup of the RBS nodes

In the table below are described the RBS specimens which were tested, including the parameters which were changed in each test depending on:
- steel only or composite beam;
- the interaction between the two materials (with or without connectors over the RBS);
- the type of loading (monotonic or cyclic).

Test nr.	Beam type	RBS	Type of loading	Connectors on the flange in RBS	Name of the specimen
1	steel	Yes	monotonic	No	DB-M
2	steel	Yes	cyclic	No	DB-C
3	composite	Yes	cyclic	No	DB-Comp1
4	composite	Yes	cyclic	Yes	DB-Comp2
5	steel	Yes	cyclic	No	DB-C RLD
6	composite	Yes	cyclic	Yes	DB-Comp RLD

Table. 3.7.Beam-to-column joints tested in the CEMSIG laboratory

The force was applied at the end of the beam via the same Quiri hydraulic actuator with the capacity of 1000 kN. All monitored displacements were recorded by electronic transducers with capacities of 50 mm and 100 mm, by a HP data acquisition unit.

Material samples were also tested in order to check the steel quality for both the beam and column (see §3.4). The design of the RBS was performed according to EN1998-3:2005, Anex B, section 5.3.4, resulting the following geometric properties:
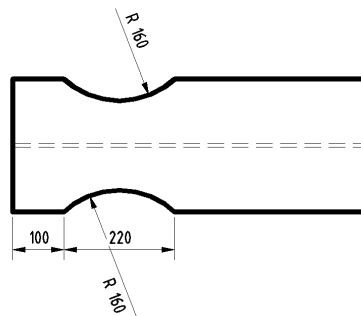
Fig. 3.58. Reduction of the beam section

The specimens with composite beams had a 12 cm slab with a width of 1m, which was considered to interact with the steel profile by means of shear stud connectors. The slab's reinforcement was designed according to SR EN1998-1: Annex C.
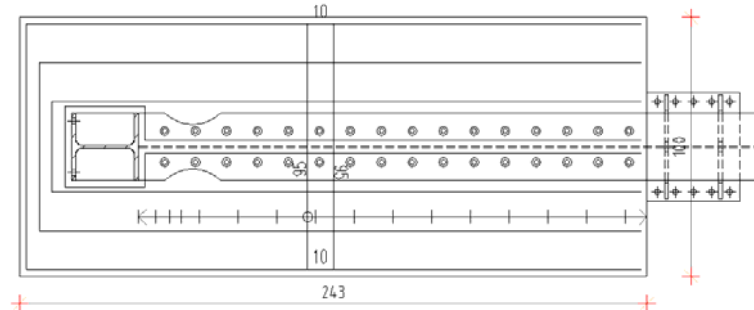
Fig. 3.59. Reinforcing of the concrete slab around the RBS joint

Measuring devices (force cell and displacement transducers) were placed in order to be able to measure the following main data:

- Beam's displacement (top – by means of DTF and DTB transducers, see Fig. 3.60);

- Local rotations, deformations and distortions in the dissipative elements: RBS, web panel of the column, welds (through DBLL, DBLR, DDT1, DDT2, DWL, DWR transducers, see Fig. 3.61);

 - Slip at the column's end (transducers DHBL, DVBL, DHBR, DVBR, see Fig. 3.60);

- Force at the loading point, from which one could deduce the moment in different locations.

The position of each transducer can be identified in the following drawings:
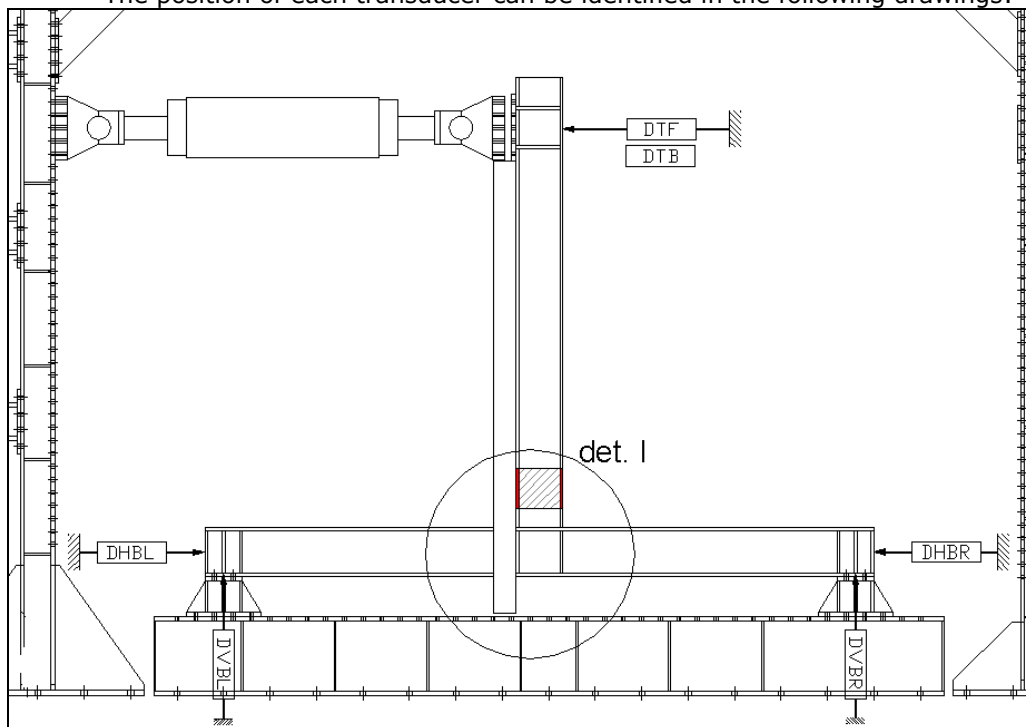
Fig. 3.60. Instrumentation of the RBS nodes
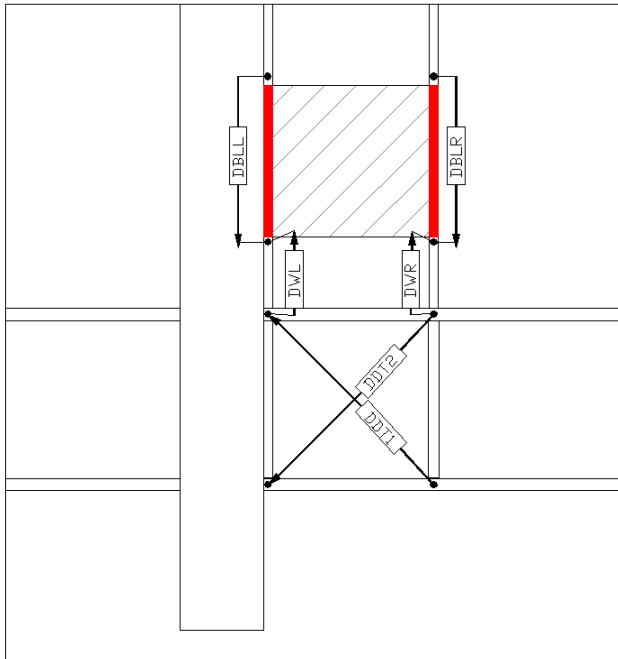
$$\gamma_{RBS} = \frac{(DBLL - DBLR)}{h_b - t_{fb}}$$

$$\gamma_{weld} = \frac{(DWL - DWR)}{h_b - t_{fb}}$$

$$\gamma_{col.web} = \frac{\sqrt{a^2 + b^2} \cdot (DDT2 - DDT1)}{2ab}$$

$$where \quad a = h_c$$
$$b = h_b - t_{fb}$$

Fig. 3.61. Instrumentation of the dissipative zone of the node

3.9 RBS experimental results

3.9.1 Steel base specimen – DB-M

The test was carried out until degradation of the specimen occurred. Based on the force-top displacement curve was determined the yield displacement D_y, yield force F_y and the initial rigidity.
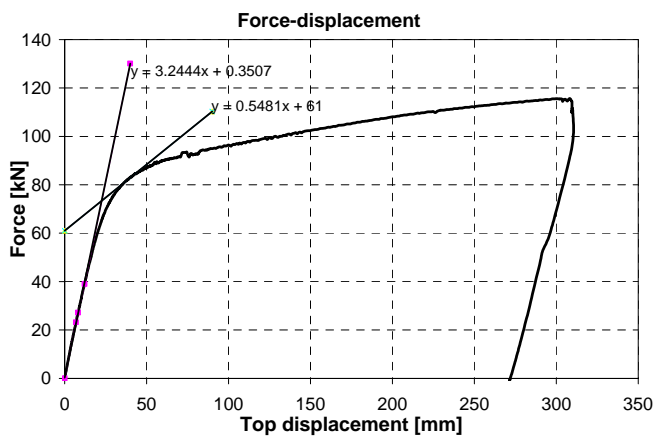
$S_{j,ini}$=3.33 kN/mm
D_y=20 mm
F_y=60 kN

Fig. 3.62. Load-displacement curve of the specimen DB-M

Although in this case the dissipative element is the beam, due to a smaller resistance of the column's material, the plasticization is divided into two components:
-   RBS zone;
-   Column web panel (CWP) in shear.

The following chart shows the force-rotation curve (recorded by DTF, DTB transducers, see Fig. 3.60):

Rotation of the node
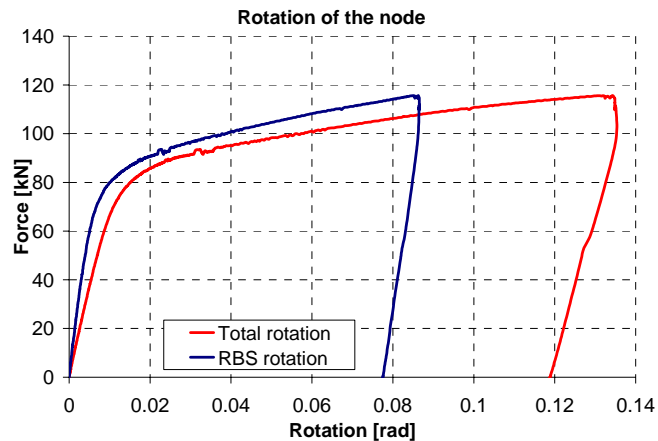
Fig. 3.63. Force-rotation curve of the steel node with reduced beam section

As it could be noticed, a large amount of final rotation is assigned to other components than RBS, principally to CWP in shear. However, the total RBS rotation could be judged as high, exceeding 80mrad for RBS solely.

For Fig. 3.63 was chosen a force representation instead of moment (usually met in such representations) for a unitary representation: the level arms which will multiply the force are significantly different in RBS centre (1.96m) and CWP centre (2.28m) respectively.

The following images show the behaviour of the plasticized zones in the specimen during the test and the failure pattern, by local buckling of the beam's flange in the RBS:

Fig. 3.64. Failure of the node with RBS at maximum displacement

The test's end was due to the actuator's displacement limit.

As a conclusion, a very important notice should be added for the first series of RBS specimens: due to the fact that the steel quality of the column was lower by the one ordered from the manufacturer (S355 – ordered, S275 – received, see table 3.5), the column's web panel became the component with the smallest resistance and in consequence highly influenced the joints' total rotation.

3.9.2 DB-C specimen

The DB-C specimen represents the cyclic specimen, having identical configuration to the base specimen DB-M. Testing was performed after determining the yield displacement and defining the load pattern according to the ECCS protocol. The D_y value was 20 mm (see Fig. 3.62).

The global joint rotation could be considered as satisfactory, reaching 80 mrad, but this is not due primarily to RBS but CWP. Moreover, due to deficient execution, the specimen failed by welds fracture, after reaching the maximum available stroke in the actuator at an increment of 8xDy - third cycle.
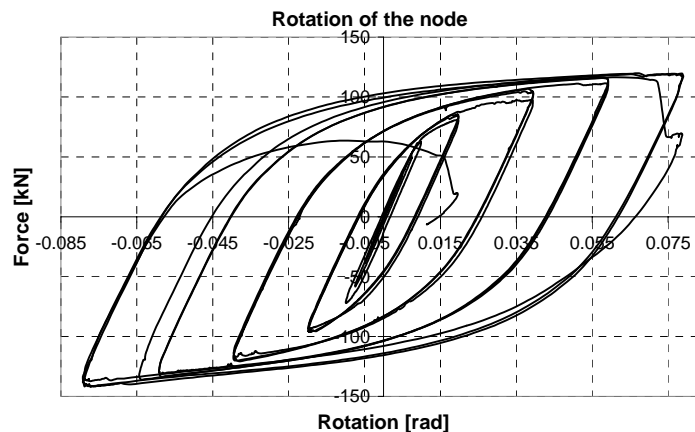
Fig. 3.65. Force-rotation curve of the steel joint with reduced beam section, under cyclic load

Fig. 3.66. Failure of the welds in the beam-column joint and CWP distortion

3.9.3 DB-Comp1 and DB-Comp2 (cyclic) specimens

The composite specimens were fabricated using similar typology as in the case of steel (DB-M and DB-C) specimens, and connecting the steel beams to a 12 cm slab as described in §3.8. The reinforcing of the joint was designed according to the provisions of Eurocode 2, Eurocode 4 and Eurocode 8, regarding the composite beams near columns. The concrete had the same class as in case of EBF specimens (C20/25). Also, following the same parameters as in the EBF study, a difference in the two tested cases is represented by the steel-concrete interaction on the flange of the beam, in the RBS zone:

- Thus, the first tested specimen had no connectors on the reduced beam section (DB-Comp1);
- The second tested specimen presented a continuous connection over the beam, including the plastic zone (DB-Comp2).

The loading of the specimens was satisfactory up to the third cycle for an increment of 8xDy, when, as in the case of cyclic steel specimen, the welds between the flange of the beam and the flange of the column have cracked.

The force-rotation hysteretic curves for the two composite joints are shown in Fig. 3.67 and Fig. 3.69:
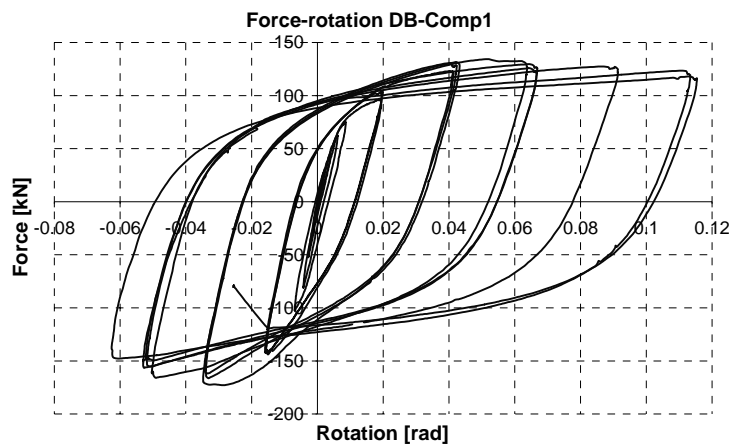
Fig. 3.67. Force-rotation curve for the DB-Comp1 specimen
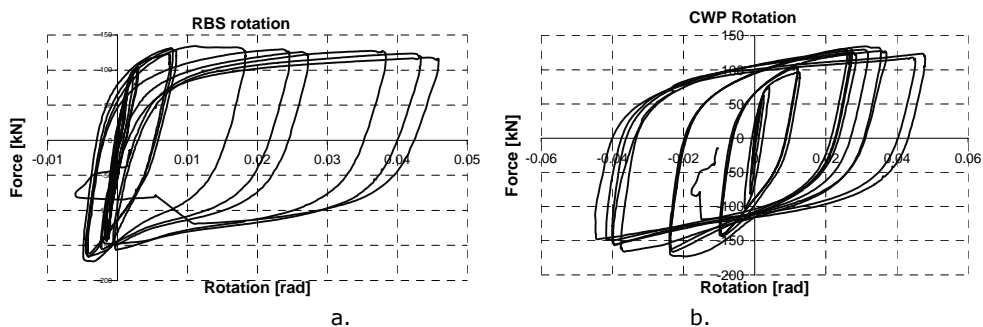
Fig. 3.68. Rotation of the RBS and CWP respectively

The total rotation of the joint (Fig. 3.67) represents practically the sum of CWP and RBS zone rotations. The asymmetry of the global curve is due to RBS zone (Fig. 3.68 a.) which developed plastic rotation only for positive bending (concrete in tension). The plasticization in negative bending was prevented by the higher composite section resistance. Contrary to this, the CWP rotation is symmetrical (see Fig. 3.68 b.) without any influence from the concrete slab. The total plastic rotation was practically equally shared between the two components (40 mrad) on positive range.

The DB-Comp2 specimen behaved similarly and confirmed the above remarks. However, the cycles are more stable in this case, although the failure was at the same amplitude and by weld failure too (see Fig. 3.66).
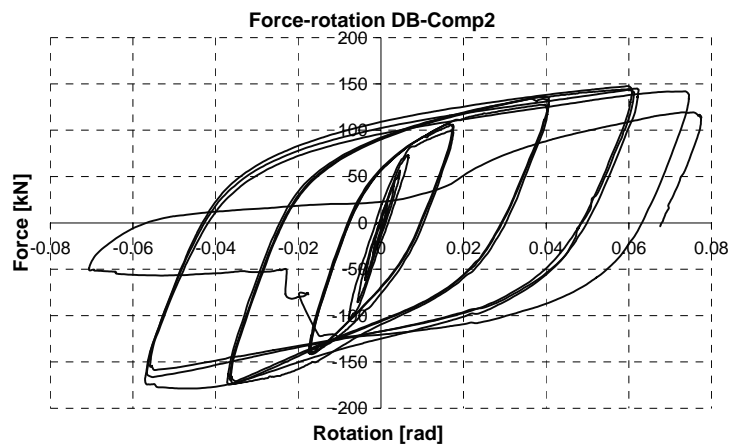
Fig. 3.69. Force-rotation curves for the DB-Comp2 specimen

Fig. 3.70. Failure of the DB-Comp1 & 2 specimens

3.9.4 Comparison of DB cyclic specimens

In conclusion, the composite specimens had a better dissipation capability than the bare steel nodes and the presence of connectors had little influence in the development of the plastic hinge, although the maximum capable force reached by

the second specimen is considerably bigger. These conclusions are proved by the comparison of the envelope diagrams for the three cyclic tests:
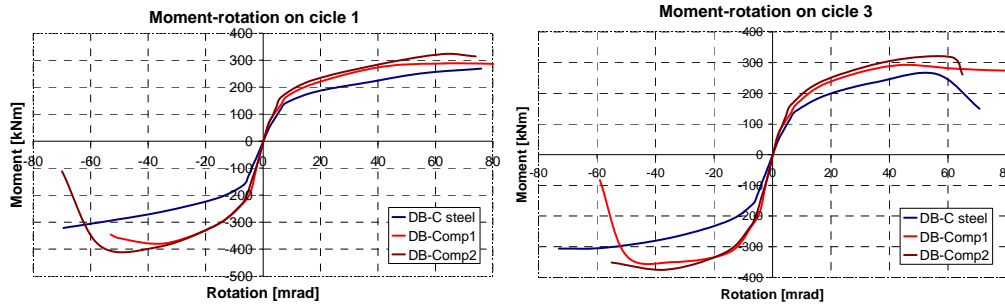
Fig. 3.71. Comparisons of the moment-rotation envelope curves for the tested nodes

Fig. 3.71 presents the moment-rotation envelopes for DB specimens. For a good understanding, the results are shown in diagrams characteristic to cycle 1 and cycle 3 respectively.

As it can be noticed, the composite specimens took advantage of composite behaviour and in consequence there are small differences in their behaviour, although DB-Comp1 has no connectors over the RBS.

In comparison with the steel specimen, the composite ones have shown higher stiffness, especially on positive behaviour (42.95 kNm/mrad for DB-Comp1 and 36.72 kNm/mrad for Db-Comp2 in regard to 25.38 kNm/mrad for DB-M). The maximum resistance is also significantly higher for composite specimens:

- 321.98 kNm for composite and 268.69 kNm for steel specimens in positive bending;
- 392.90 kNm for composite and 321.67 kNm for steel specimens in negative bending.

For all specimens the ductility was limited by premature failure of the welds.

3.9.5 Cyclic re-testing of the beam-to-column joints with RBS – DB-C_RLD & DB-Comp_RLD

Due to the fact that the final purpose of the initial RBS specimens was not achieved (dissipation only in the RBS zone), the joint test series was completed by two new specimens, namely DB-C_RLD (steel specimen) and DB-Comp_RLD (composite specimen), both tested cyclically. The welds were designed and executed properly, by full penetration welds.
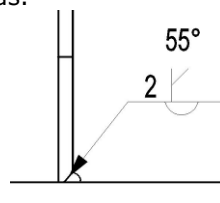
Fig. 3.72. Full-penetration welds used for the beam's flange-to-column connection

In the new configuration, the beam was the same (HEA260), while the column was replaced with a HE300B profile of S460 steel quality, as the performance of the column or connection was of no interest, the study being focused on the performance of the steel/composite beam with RBS.

In a general manner, in this series of tests the beam-to-column welds behaved in a satisfactory manner and both joints reached their maximum capable rotations. The failure type was similar for both cases, by ductile buckling of the beam's flange in the RBS and gradual reduction in joint's resistance.

In the following charts we can observe and compare the hysteretic curves in terms of applied force and total rotation, for the new specimens.
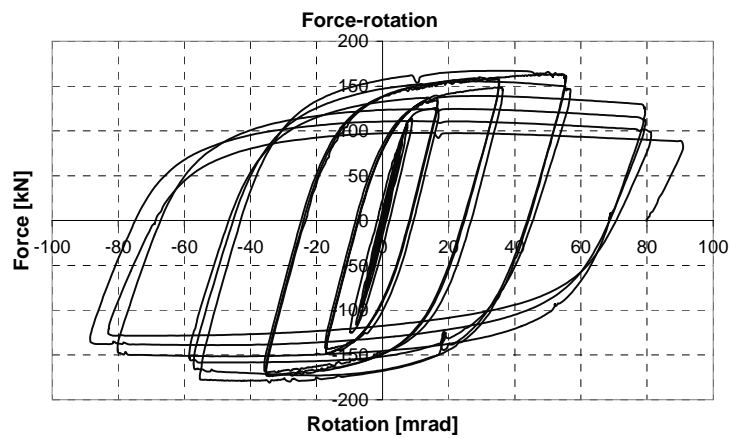
Fig. 3.73. Force-rotation curve of the steel specimen DB-C_RLD, under cyclic load
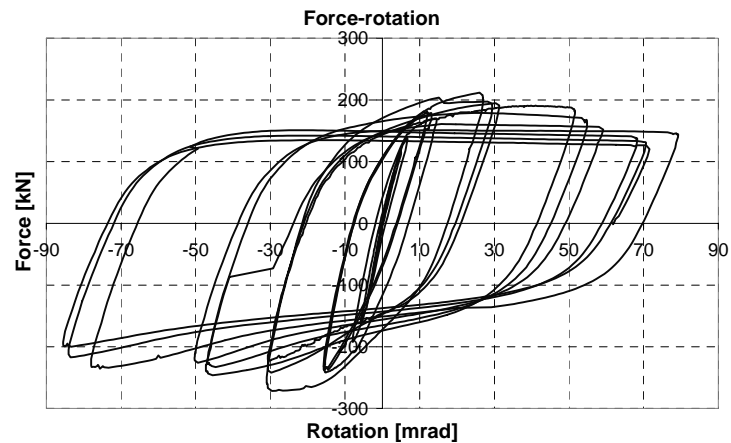
Fig. 3.74. Force-rotation curve of the composite specimen DB-Comp_RLD, under cyclic load

Fig. 3.75. Buckling of the flanges in the RBS for specimen DB-C RLD
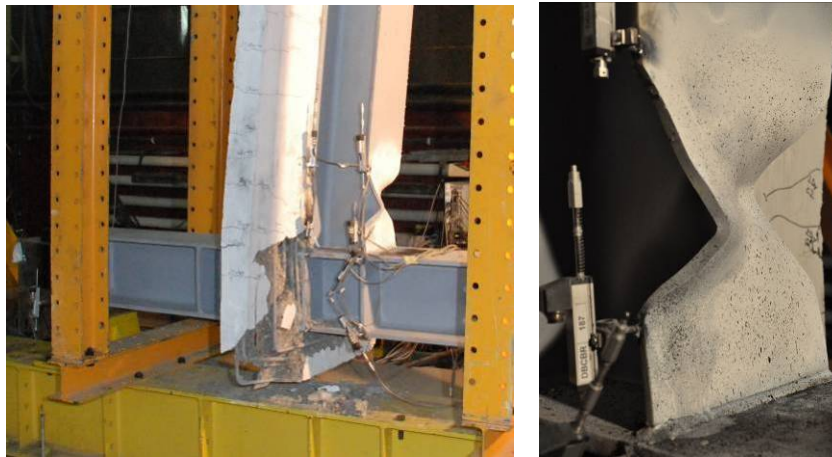
Fig. 3.76. Buckling of the compressed flange and crushing of the concrete int he RBS

for specimen DB-Comp_RLD

In these cases the total rotations (greater than 70 mrads) is due almost exclusively to RBS plasticization as it can be observed in Fig. 3.75 and Fig. 3.76. As expected, no plasticization was recorded in the CWP.

In case of the composite specimen, the upper flange was hindered to buckle due to the presence of the concrete slab, but its resistance degraded gradually during the cycles:

- By fissures parallel to column flange in negative bending
- In compression, by crushing along the fissures already formed in negative bending.

A large amount of degradation was recorded in the column zone, around which the concrete was crushed and has fallen off massively.

The new series of specimens confirmed the conclusions stressed as a result of the first test series.

Comparing the cyclic envelopes of the new specimens (see Fig. 3.77), one could notice similar rotation capacities (up to 70 mrad), higher resistances and rigidities for the composite specimen especially for negative bending (slab under compression).
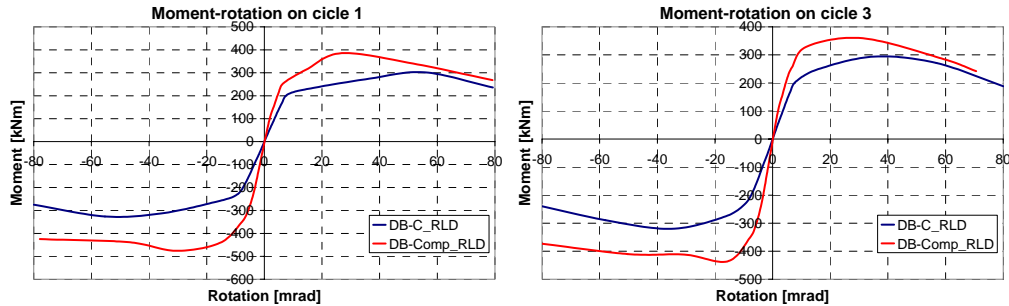
Fig. 3.77. Force-displacement envelope curves compared on cycles 1 & 3

3.9.6 Conclusions regarding the behaviour of the tested nodes with RBS

The RBS tests represent a very instructive study on the behaviour of RBS zones in composite/non-composite solutions. The following conclusions could be drawn:

- The simple disconnection of the steel beam from the concrete slab over the RBS zone is not sufficient to assure a pure steel-like behaviour. The resulted behaviour is practically very close to that of a full-composite specimen;
- The composite aspect improves the global resistance and stiffness characteristics of the joint while maintaining the ductile character of the solution. However, the composite behaviour should be considered in the design of the structure.
- A very careful detailing and execution should be applied to beam-to-column joints in order to reach the desired levels of ductility and resistance. On contrary, the steel grade mismatch could change the plasticization order, while the defective execution of welds will lead to brittle failure of joints.

3.10 Analysis of dissipation capacities

A very good tool of accounting the performances of dissipative zones is by the computation of the total dissipated energy. This is made by the integration of areas within the response curves of cyclic specimens. The figures presented below show a comparison on different series of specimens (EBF, RBS (DB) and RBS RLD respectively) on plastic cycles (3 plastic cycles are considered for each D_y multiplier – according to the ECCS procedure).
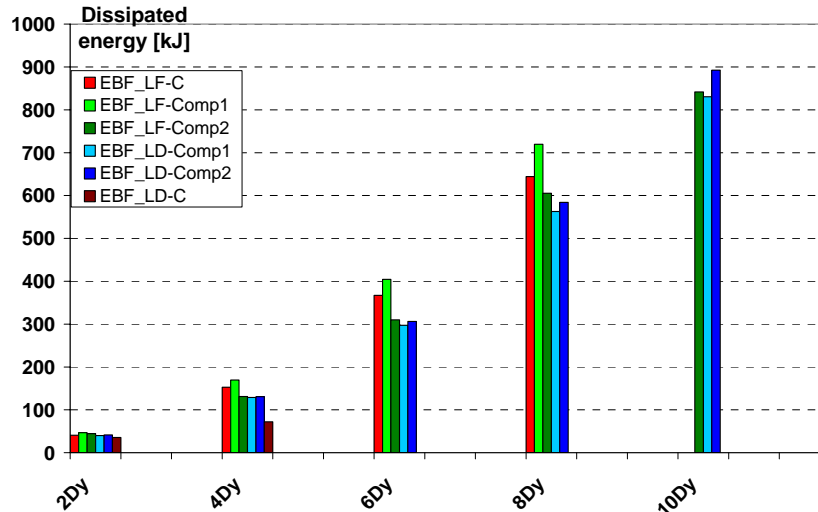
Fig. 3.78. Dissipated energies (cumulated) for the tested EBFs

In case of EBF specimens one can easily notice that generally the detachable link specimens can exhibit a smaller amount of energy in plastic cycles. However, the LD composite specimens resisted up to $10 \times D_y$ cycles, where in fact is dissipated the largest amount of energy.

The composite and metallic specimens exhibited comparable amounts of energy, per cycles. However, the total amount of energy finally depended only on the amplitude of the final cycles, which practically made the difference in total dissipated energy.

For RBS specimens there could be observed a systematic energy dissipation increase for composite specimens (about 25%) as compared to steel specimens. Here it seems that the full connection between the steel beam and the concrete slab over the full length of the beam (including RBS) is beneficial to the overall seismic dissipation capacity.
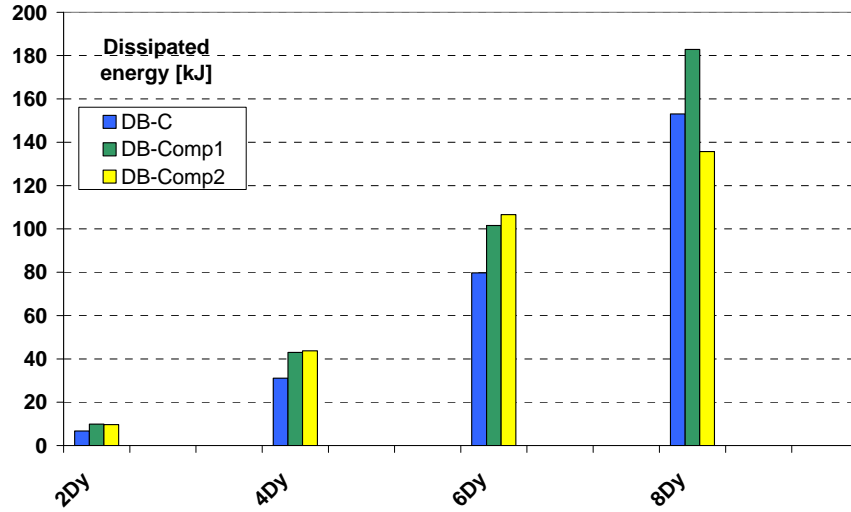
Fig. 3.79. Joints' dissipated energies (cumulated) compared
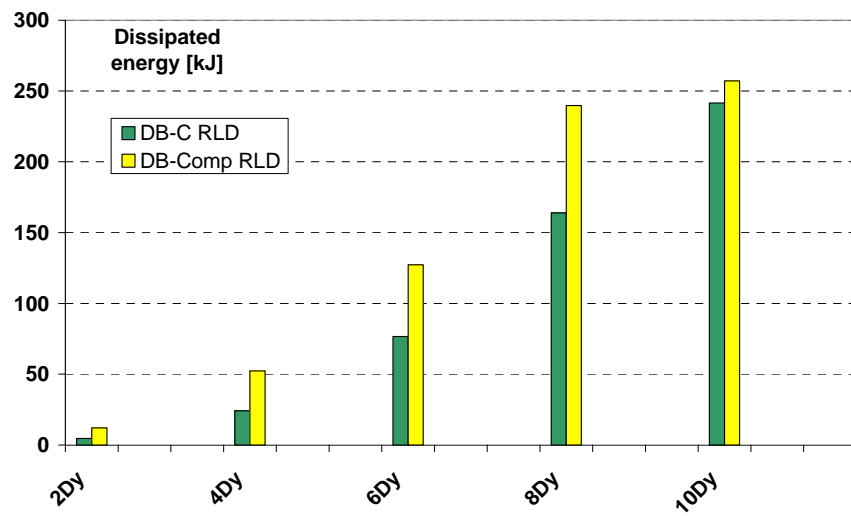
Fig. 3.80. Second series of joints' dissipated energies (cumulated)

4. NUMERICAL STUDY

4.1 Purpose of the study

The main aim of the numerical study regards the seismic response of steel and composite framed structures with plastic dissipation zones located in EBF short links (working in shear) and RBS of MR frames (working in bending). The numerical program consisted in the evaluation of seismic behaviour of a number of 8 frames. Several parameters, such as the inter-story drift, plastic rotation requirements and behaviour factors q are monitored. For this goal, adequate models of plastic hinges are proposed.

Following the above principle, all non-dissipative elements of the frames were designed to remain elastic, while the plastic zones were modelled on the basis of the results described in chapter 3.

The software used for the analyses was SAP2000 [CSI Berkeley], version 14, due to its fast modelling options of full-size structures and user-friendly interface. Also, one of the main reasons for this choice was the option to model composite beams accurately, through a newly introduced feature in the current existing software.

4.2 Calibration of numerical models

The calibration of numerical models for the analysed frames was performed in two directions, both required for an adequate model for dynamic elastic-plastic analyses:
- Realistic behaviour of plastic hinges
- Adequate model of composite beams

4.2.1 Plastic hinges definition

Plastic hinges – act as fuses in the purpose of dissipating seismic energy through elastic-plastic cycles of bending and/or shear. The specific bending (M3 type) and shear (V2 type) hinges were used in the nonlinear analyses performed on MRF, EBF and DUAL structures. The short dissipative element is usually intended to function in shear. This element is defined as a "short link" and is generally designed as a part of EBFs.

The plastic hinge that has become widely used in beams from MRF, in the vicinity of the beam-to-column joint is known as the RBS; it implies the reduction of the beam section so that the plastic behaviour is induced rather in the beam than in the column in order to prevent premature failure of the joint or column panel.

In the current practice, the model defining plastic hinges involves only the use of the steel section to develop and maintain the plastic state. Also, when considering composite cross-sections, the general tendency is to avoid having a full composite connection in the plastic zones, thus allowing the plastic hinge to fully develop in the steel profile.

The SAP2000 computer program's hinge definition module allows for the definition of various plastic hinge properties, among which the ones used in the numerical study where:
- M3 hinge – definition of a bending hinge (w/ or w/o user specifications) to be assigned to an element (e.g. beams);

- V2 hinge – assigns a shear hinge to an element (e.g. short links), again the user being able to modify the standard definition as desired ;
- P hinge – axial hinge, that can be applied for example to braces, acting in tension or compression;
- P-M2-M3 – axial and bending moment hinge, used to model the plastic behaviour of columns.

Two of the most general and comprehensive definitions for steel hinges, for both shear and bending, implemented successfully in a nonlinear calculus software, are for example, the ones in SAP2000 software:
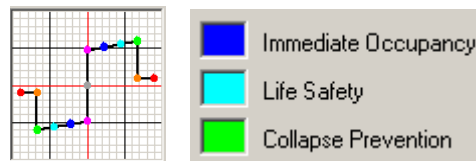
Fig. 4.1.   Example of default plastic hinge definition in SAP2000

These models are mostly used for steel sections and are symmetric in their definition (same behaviour in tension and compression). The implementation and use of a plastic hinge model for composite cross-sections, requires careful analysis and design of the structure and beams, mainly due to the differences of behaviour between tension and compression. In addition to this, the mere presence of the concrete slab (w/ or w/o connectors) influences the forming and the development of the plastic hinge, leading to higher stresses, both in the composite section in the plastic hinge region and the adjacent steel elements (i.e. braces in the EBF, column in MRF). Furthermore, the experimental tests showed that the concrete slab reduces to some extent (function of thickness, reinforcement ratio) the rotation capacity of the steel element, and tends to delay the development of the plastic hinge in such composite elements.

The experimental results obtained in the previous chapter (chapter 3) are used in order to propose and calibrate a plastic hinge which takes into account the composite effect on the plastic behaviour of the element. Furthermore, the obtained plastic hinges (shear and bending plastic hinges) are used in nonlinear analyses (time-history, pushover) on frames, by means of the structural analyses software SAP2000.

The models obtained from experimental data include only the plastic branches (rigid-plastic behaviour), while the elastic behaviour is integrated in the element's model.

The first step in creating the plastic behaviour curves for each element was the identification of the key points which lead to a behaviour which fits the experimental response envelope curve. Thus the curves were drawn based on the envelopes obtained for both bending and shear elements. In this manner, the plastic-hinges defined for the composite cross-sections are in consequence non-symmetric, and have distinct behaviours for positive and negative branches. Fig. 4.2 presents the key points definition chosen for the plastic hinges characteristic curves for RBS (moment – rotation) and short EBF links (shear force – distortion) respectively, and the FEMA recommendations for IO, LS and CP.
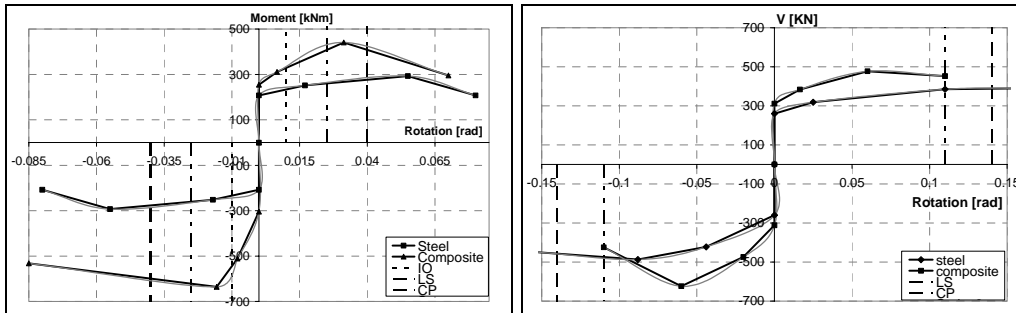
Fig. 4.2.   Plastic hinges developed in the RBS (left) and link (right) for steel and composite specimens

Based on the above envelopes, the following definitions are proposed for both the bending hinge (Fig. 4.3) and shear hinge (Fig. 4.4).
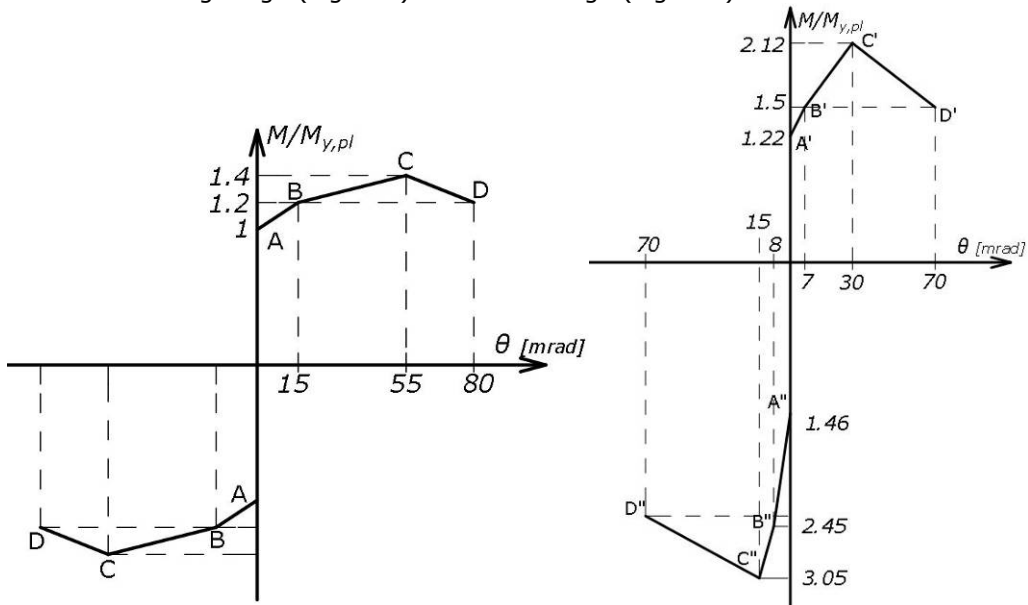
Fig. 4.3.   Theoretical definitions proposed for the steel (left) and composite (right) bending hinges from the RBS
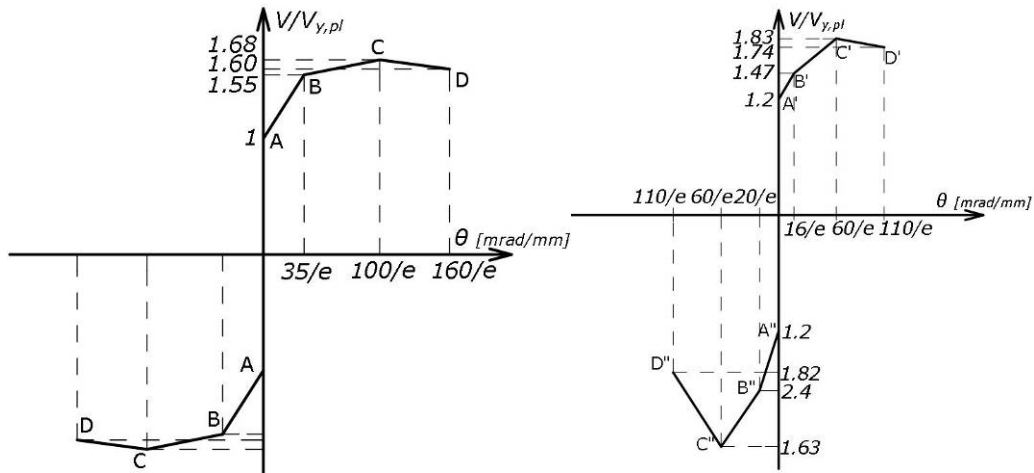
Fig. 4.4.   Theoretical definitions proposed for the steel (left) and composite (right) shear hinges from the short link*

* - Note: In the above figures, e is the length of the link, expressed in [mm], while $V_{y,pl}$ is determined with the formula: $V_{y,pl} = \dfrac{f_y}{\sqrt{3}} t_w (h - 2t_f)$.

Due to the fact that the existing hinge definitions in the design software SAP2000, are implicitly unable to predict such type of behaviours, new hinge definitions are proposed by the author, calibrated according to their real behaviour. Anyway, due to the relatively small differences between the behaviour obtained with- and without connectors, only the hinges without connectors were chosen for modelling the composite behaviour. These definitions consider the yield force function of the section, and a rotation capacity with different behaviour for positive and negative branches (compressed and tensioned concrete respectively).

Fig. 4.5 and Fig. 4.6 show the resulted behaviour for RBS and short links, based on the key points defined in Fig. 4.3 and Fig. 4.4:

Point	Moment/SF	Rotation/SF
E-	-1.75	-0.085
D-	-2.09	-0.0156
C-	-1.68	-7.900E-03
B-	-1.	0.
A	0.	0.
B	1.	0.
C	1.22	6.700E-03
D	1.73	0.0313
E	1.16	0.07

☐ Symmetric

Fig. 4.5.   Plastic hinge model proposed for the composite RBS

Point	Force/SF	Disp/SF
E	-1.36	-0.11
D-	-1.55	-0.06
C-	-1.38	-0.02
B	-1.	0.
A	0.	0.
B	1.	0.
C	1.12	0.0164
D	1.38	0.06
E	1.37	0.11

☐ Symmetric

Fig. 4.6.   Plastic hinge model proposed for the composite short link

The validation of hinge behaviour was performed by the integration of the hinges, first on the steel experimental frame curve (EBF_M_LF-M) and beam-to-column joint respectively (DB-C_RLD). In order to model the elements accurately, the real stress-strain material definitions were used as resulted from their characteristic strength tests. For the EBF it was necessary to replicate the slip in the braces' connection, by using elastic "link" elements (resembling elastic springs).

For all the materials involved in the models, multilinear elastic-plastic models were used, with the following nominal characteristics, as shown in Fig. 4.7.

Steel grade S235 - isotropic	Steel grade S355 - isotropic
$E=210000$ N/mm^2	$E=210000$ N/mm^2
$f_y=235$ N/mm^2	$f_y=355$ N/mm^2
$f_u=360$ N/mm^2	$f_u=510$ N/mm^2
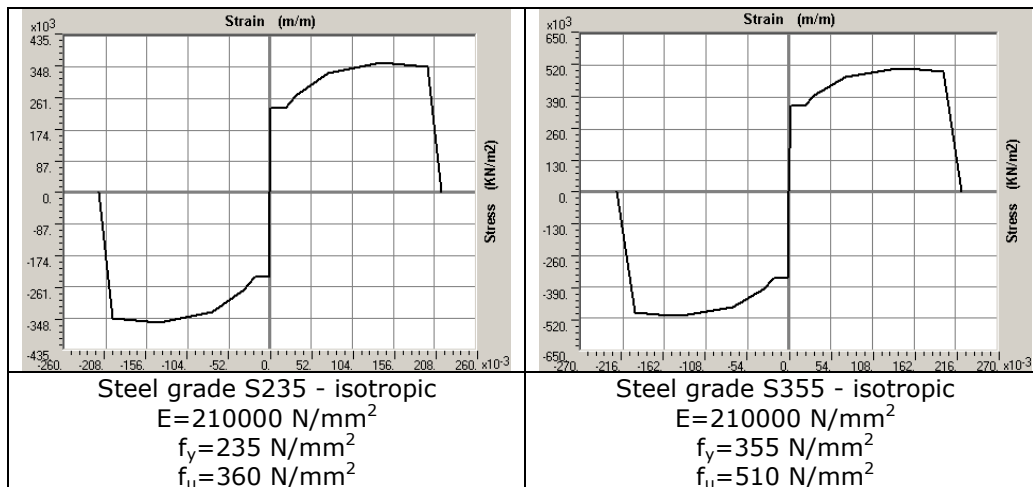
Fig. 4.7.   Material definition for steel grades S235 and S355

Due to the fact that the first attempts of frame modelling resulted in a more rigid global response, the real force-deformation curve was obtained only after integration of the global deformation of braces' connections (whose behaviour had to be matched to that obtained from the experimental tests, more precise the total slip obtained by monitoring the braces' connections; a 5mm slip corresponding to 800 kN axial force). The obtained results shown in Fig. 4.8 show a quite good agreement between the experimental and modelled curves, for both EBF with short link and joint with RBS.
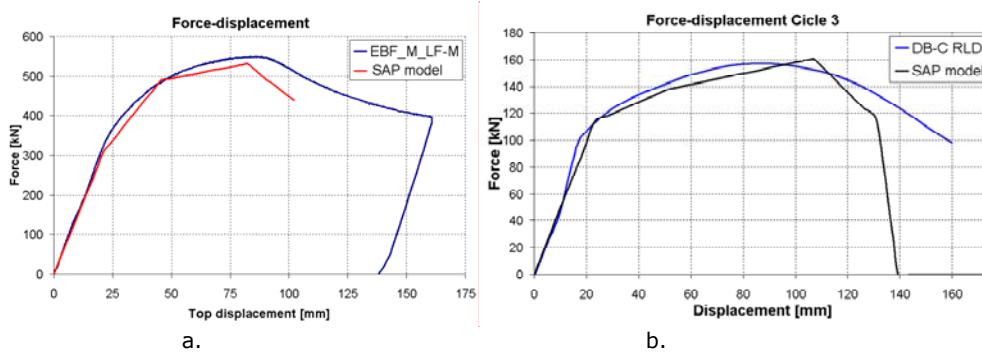
Fig. 4.8.   Steel specimens' behaviour obtained for the steel short link and RBS in SAP2000 vs. experimental test

4.3 Calibration of the composite beam response

Another very difficult problem when dealing with the advanced nonlinear analysis of composite beams is finding a numerical model which would accurately define the behaviour of the composite cross section (CS) consisting of two different materials.

Currently there are some research focused software (OpenSees, Drain 2DX) which are able to model composite CS through fibre definitions. However these programs are quite difficult to use in current design. Even SAP2000 has the option of creating fibre models, but in case of using two materials in the CS definition, the program finally selects just one global material.

The model chosen to simulate the composite beam has been adapted according to the one proposed by CSI Berkeley in April 2010, and implemented with the introduction of SAP2000, version 12.0. The model has been proven to function adequately by comparing the results obtained from modelling with the results obtained by hand calculus, for the simple cases of a simply-supported beam and a double-encased beam.

Various approaches to modelling composite behaviour are proposed in the following models:
- Model 1 – fictitious noncomposite – frame and shells are drawn at the elevation of girder centroid sharing the same joints;
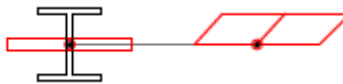
- Model 2 – composite – frame and shells are drawn at the elevation of the girder centroid sharing the same joints; shell joint offsets are used to place the deck above the girder;
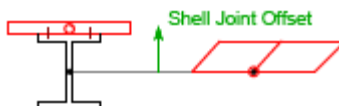
- Model 3 – composite – frames and shells are drawn at the elevations of their respective centroids and connected using body constraints; separate body constraint is used for each pair of connected joints;
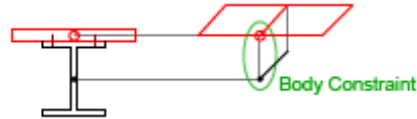
- Model 4 – composite – frames and shells are drawn at the elevation of deck centroid sharing the same joints; frame joint offsets and top centre insertion points are used to place the deck above the girder;
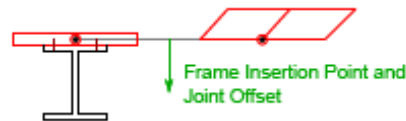
- Model 5 noncomposite – frames and shells are drawn at the elevations of their respective centroids and connected using equal constraint in Z direction; separate equal constraint is used for each pair of connected joints;
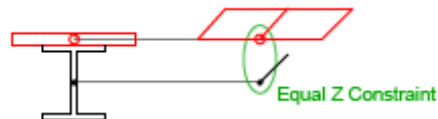
- Model 6 noncomposite – frames and shells are drawn at the elevations of their respective centroids and connected using links that are fixed in vertical direction and free for all other degrees of freedom;
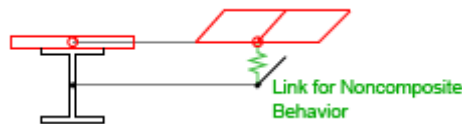
- Model 7 partially composite – frames and shells are drawn at the elevations of their respective centroids and connected using links that are fixed in vertical direction, have stiffness in girder longitudinal direction and are free for all other directions;
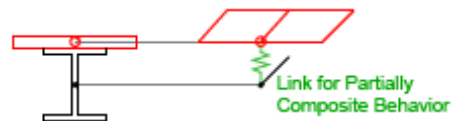
- Model 8 composite – frames and shells are drawn at the elevations of their respective centroids and connected using fixed links.
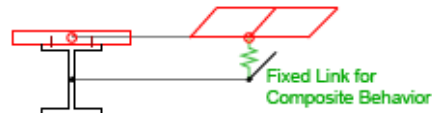
The last of the proposed models has been further used and adapted by the author in order to satisfy the requirements for longitudinal shear for modelling a complete interaction between the two materials, steel and concrete. For this purpose, the links have been placed at a maximum distance of 30 cm one from the

other (using a smaller distance between links will only increase the number of finite elements and analysis time).

The shell elements characterizing the concrete slab have been modelled as multi-layered non-linear elements in which the concrete is a shell and the reinforcements are represented by two membrane layers. Both layers have been assigned a nonlinear behaviour. At first, the slab thickness (12 cm) and reinforcement ratio (Φ12 at 15 cm) were the ones used in the experimental tests.
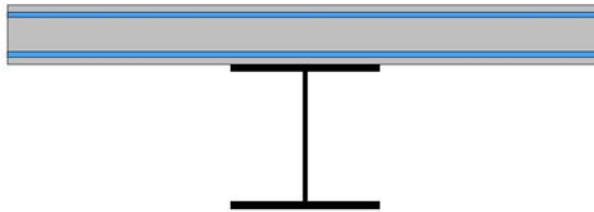
Fig. 4.9.   Composite beam modelled by finite elements

The concrete material was defined based on the compressive tests on standard cubes, using the Mander model, which was further adapted for the actual resistances:

Concrete class C20/25 – isotropic
$E = 30000$ N/mm^2
$f_{ck} = 22$ N/mm^2
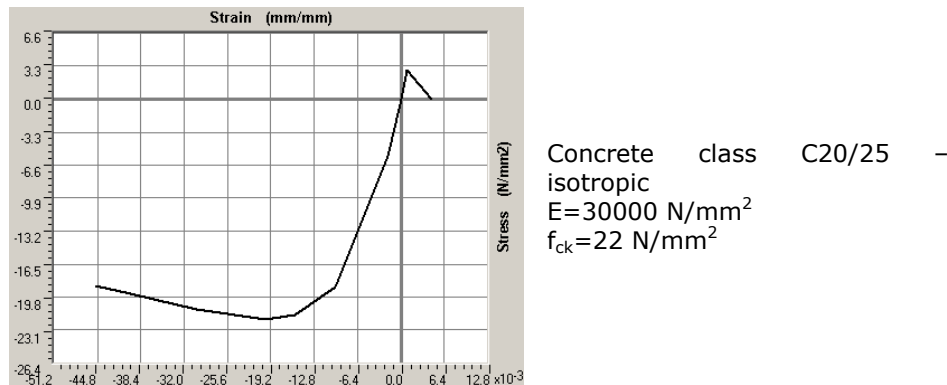
Fig. 4.10. Concrete material definition

Before using the composite beams' model in full structure analyses, a calibration was performed on a composite frame.

In the potentially plastic region a finer mesh was used to model the slab above the steel profile, due to the fact that it was noticed that the mesh quality and size highly influences the obtained results and the force required to fully develop the plastic hinge in the composite cross-section. This conclusion was valid for both shear and bending hinges. However, when modelling such a zone, one must study various configurations and choose the optimum one, function of desired run-time (highly influenced by the density of the mesh) and number of shell elements. It is to be noted here that a larger number of shell elements per section automatically generates larger files and would require a larger computing time.

In case of the slab above the short link in the EBF, an element size of 2.5 by 6 cm proved to be efficient in accurately modelling the behaviour of the slab. The behaviour of the plastic hinge was introduced according to its obtained curve – see Fig. 4.3 and Fig. 4.4. Another important aspect was that in order to obtain the accurate behaviour curve from the numerical model, the slip in the braces' connections had to be simulated via two "link" elements acting as springs. (whose behaviour had to be matched to that obtained from the experimental tests, more precise the total slip obtained by monitoring the braces' connections), which were added to both braces' ends.

Using the above mentioned conditions, the force – top displacement response follows accurately the experimental response of the EBF frame, as it could be seen in Fig. 4.12. The conclusion is valid for both the EBF and beam-to-column joint.
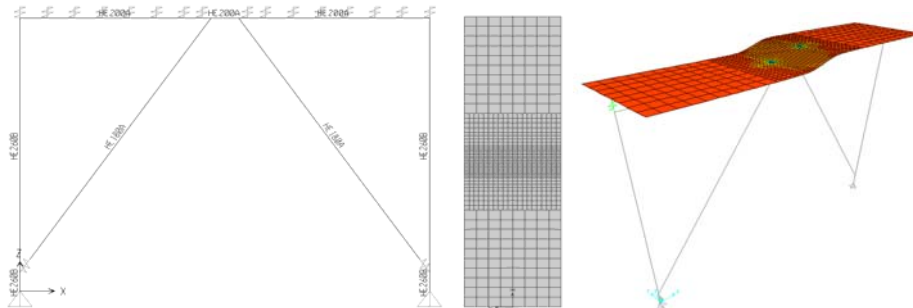
Fig. 4.11. Model of the EBF in SAP2000
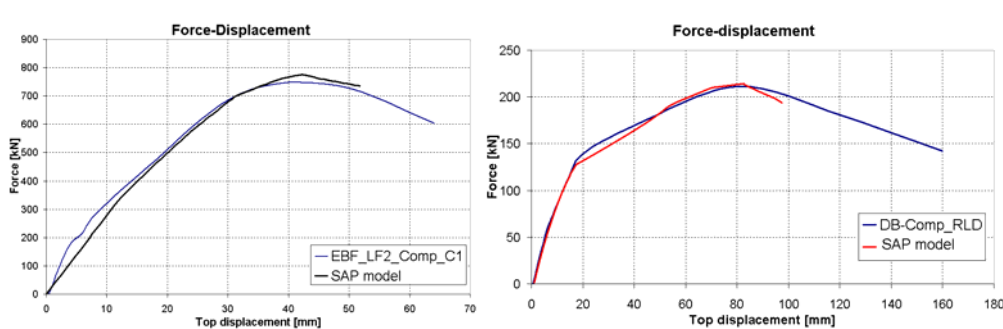
Fig. 4.12. Experimental and numerical curves obtained in case of EBF and joint pushover loading

4.4   Design of the structures for numerical analyses

In order to have a global image of the medium and high-rise moment resisting, EB or dual MR+EB frames, eight 2D frames have been designed and further analysed in elastic-plastic domain by means of time-history and pushover analyses.

The design of the analysed structures was performed according to:
-        Eurocode 3: SR EN 1993-1-1-2006

- Eurocode 4: SR EN 1994-1-1-2004
- Eurocode 8: SR EN 1998-1-2004
- Romanian Earthquake design code: P100/1-2006
- American documents: FEMA 256, FEMA 273, FEMA 356

The loads considered on all structures, uniformly distributed on floors:
- dead load: 4 kN/m^2
- live load: 3 kN/m^2, plus partition walls (according to EC1)

All floors were modelled as diaphragms. The level masses were computed according to the provisions of the Romanian seismic design code P100/1-2006. The seismic design spectra used was the one for Bucharest, with the following characteristics:
- T_c=1.6s – control period
- a_g=0.24g – peak ground acceleration
- q factor = 6 (table 6.2 from SR EN1998-1, for a high ductility class)
- value of

$$1.1\gamma_{ov}\Omega = 2.5 \; for \; EBF \; and \; DUAL \; frames$$

according to P100- $=3.0 \; for \; MRF$ 1/2006, annex F.
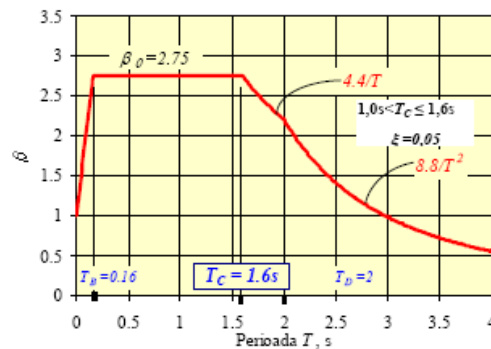
Fig. 4.13. Seismic elastic spectrum for Bucharest

The frames were modelled in the nonlinear design software SAP2000, in the following configurations:
- with steel beams;
- with composite beams.

Description of frames, their composing sections and spans are given in Table. 4.1. The structural configurations are given in Fig. 4.14Fig. 4.2.
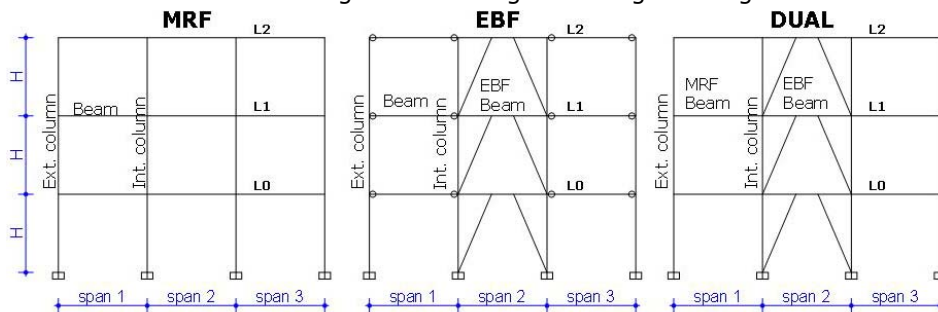
Fig. 4.14. Types of frames under study

Frame number	Frame name	Nr. of levels	Level height [m]	Spans [m]	MRF Beams	EBF Beams	Composite beams	Columns	Braces
F1S	DUAL - 4S	5	4, 4x3.5	8, 6.5, 8	IPE450	IPE360	no	HE400B	L0-L1: HE200B L2-L4: HE180B
F1C	DUAL - 4C	5	4, 4x3.5	8, 6.5, 8	IPE450	IPE360	yes	HE400B	L0-L1: HE200B L2-L4: HE180B
F2S	EBF - 4S	5	4, 4x3.5	8, 6.5, 8	IPE400	L0: HE240A L1: HE260A L2: HE240A L3: HE220A L4: HE200A	no	ext:HE300B int:HE400B	L0-L3: HE200B L4: HE180B
F2C	EBF - 4C	5	4, 4x3.5	8, 6.5, 8	IPE400	L0: HE240A L1: HE260A L2: HE240A L3: HE220A L4: HE200A	yes	ext:HE300B int:HE400B	L0-L3: HE200B L4: HE180B
F3S	DUAL - 8S	9	3.5	7, 6, 7	HE280A	L0-L2: HE300A L3-L4: HE280A L5: HE260A L6-L8: HE220A	no	ext:HE400B int:HE500B	L0-L5: HE240B L6-L8: HE200B
F3C	DUAL - 8C	9	3.5	7, 6, 7	HE280A	L0-L2: HE300A L3-L4: HE280A L5: HE260A L6-L8: HE220A	yes	ext:HE400B int:HE500B	L0-L5: HE240B L6-L8: HE200B
F4S	EBF - 8S	9	3.5	7, 6, 7	HE280A	L0-L2: HE300A L3-L4: HE280A L5: HE260A L6-L8: HE220A	no	ext:HE400B int:HE500M	L0-L5: HE240B L6-L8: HE200B
F4C	EBF - 8C	9	3.5	7, 6, 7	HE280A	L0-L2: HE300A L3-L4: HE280A L5: HE260A L6-L8: HE220A	yes	ext:HE400B int:HE500M	L0-L5: HE240B L6-L8: HE200B
F5S	EBF - 6S	7	3.5	7, 6, 7	HE280A	L0-L2: HE300A L3-L4: HE280A L5: HE260A L6: HE220A	no	ext:HE360B int:HE450M	HE200B
F5C	EBF - 6C	7	3.5	7, 6, 7	HE280A	L0-L2: HE300A L3-L4: HE280A L5: HE260A L6: HE220A	yes	ext:HE360B int:HE450M	HE200B
F6S	DUAL - 12S	13	3.5	6, 6, 6	IPE400	L0-L2: IPE400 L3-L5: IPE360 L6-L8: IPE330 L9: IPE300 L10: IPE270 L11-L12:	no	HE450M / HE450B	L0-L2: HE300A L3-L5: HE260A L6: HE240A L7-L9: HE220A L10-L11: HE200A
F6C	DUAL - 12C	13	3.5	6, 6, 6	IPE400	L0-L2: IPE400 L3-L5: IPE360 L6-L8: IPE330 L9: IPE300 L10: IPE270 L11-L12:	yes	HE450M / HE450B	L0-L2: HE300A L3-L5: HE260A L6: HE240A L7-L9: HE220A L10-L11: HE200A
F7S	MRF - 5S	6	3.5	7.5, 7.5, 7.5	IPE500	-	no	HE600B / HE600M	-
F7C	MRF - 5C	6	3.5	7.5, 7.5, 7.5	IPE500	-	yes	HE600B / HE600M	-
F8S	MRF6 - 5S	6	3.5	6, 6, 6	IPE400	-	no	HE500B / HE500M	-
F8C	MRF6 - 5C	6	3.5	6, 6, 6	IPE400	-	yes	HE500B / HE500M	-

Table. 4.1.Structures* used in numerical analyses

  * - Note: All dissipative elements such as beams and links were designed using steel grade S235, while the elastic elements such as braces and columns were made of S355 (the exception here is frame F4S/C, EBF with 8 stories, where the EBF beams were made of S355).

The analyzed frames are all façade frames isolated from hypothetical square structures. The study covers a wide range of structures, from low-rise 4 story EBF and DUAL (MRF+EBF frames) structures, MRF structures and up to 8 and 12 story EBF and DUAL configurations.

In order to fully observe and characterize the behaviour of the above mentioned frames, the time-history Incremental Dynamic Analyses (IDA) involved the use of 7 earthquake recordings, all of them recorded from the Vrancea source, but different in magnitude. Fig. 4.15 shows the accelerograms, as recorded in different years on different stations. The recordings were scaled on the design spectrum for Bucharest (Tc=1.6s).
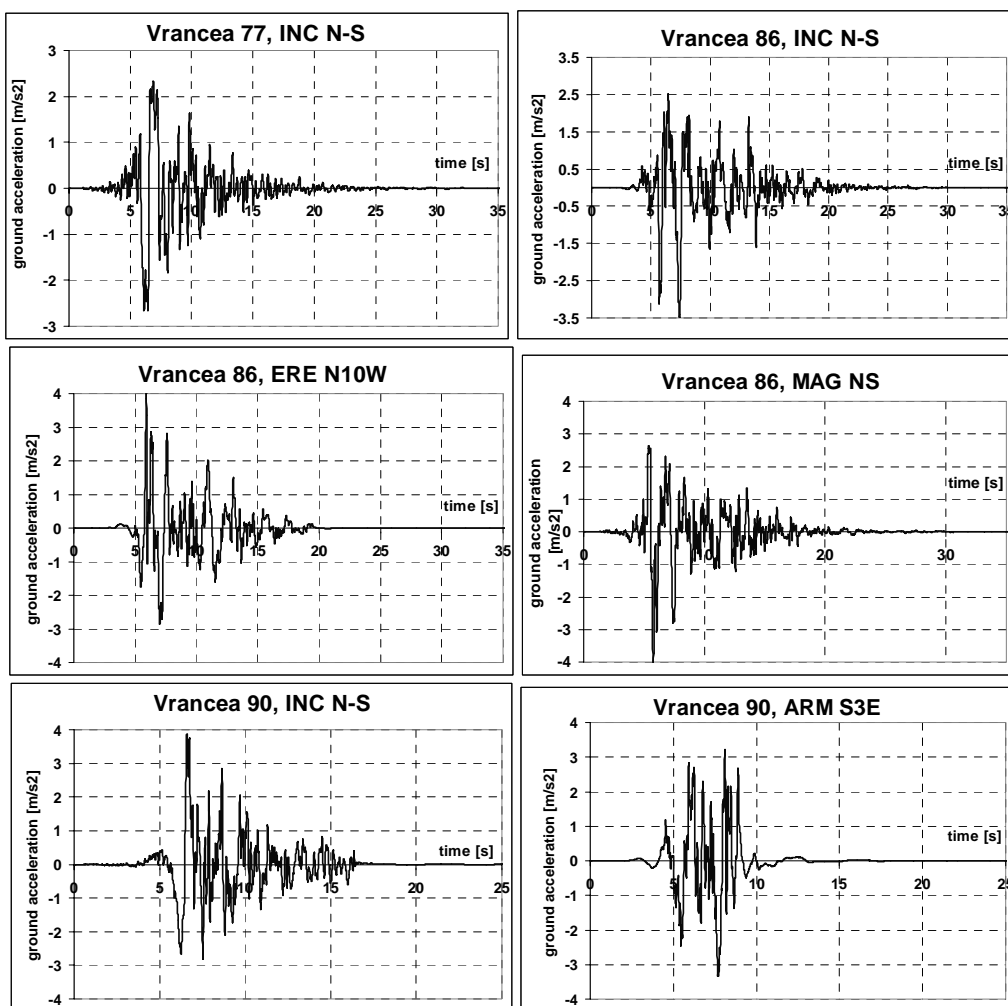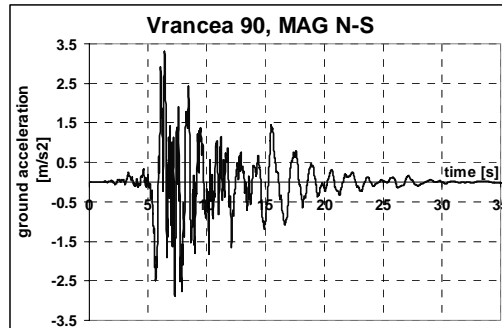
Fig. 4.15. Vrancea-type accelerograms used for time-history analyses

4.5 Monitored results

In the first stage, on each set of structures was run a push-over analysis, in order to check and determine the order in which the plastic hinges are forming and also to see whether the structure reaches the target displacements for the SLS and ULS determined by the N2 method [46].

The second stage comprises IDA analyses performed on each of the seven accelerograms until the structure reaches a failure point. Failure (ultimate) criteria for the analyzed frames were considered at the attainment of one of the following points:

- Development of a structural mechanism;
- Reaching the maximum rotation capacity in a hinge;
- Reaching the maximum allowable inter-story drift limit.

From the results retrieved from IDA, an evaluation of the structural behaviour factor was performed, in order to have an appreciation of the dissipation capacity of the structures and also a comparison to the values used in design. The behaviour factor was computed by $q=\lambda_u/\lambda_1$, where λ_1 represents the ground motion intensity factor for which the first plastic hinge is developed, while λ_u the factor for which the structure is failing (according to one of the above criteria).

On the other hand, the efficiency of the building η shows the ability of the structure to withstand a certain earthquake, computed by the formula $\eta=a_{gu}/a_g$.

4.6 Full set of numerical results for the 8 story DUAL frame

The 8 story DUAL frame is considered a typical structure that combines the advantages of MRF and EBF. First, the push-over analysis results are shown, for giving the general pattern of plastic hinges formation, then are given the results for different IDA with accelerograms.

4.6.1 Push-over results:

In the tables below are shown the rotation level marks of the plastic hinges, as defined for both the link in the EBF and RBS. They are adapted, corresponding to the ductility values obtained experimentally:
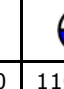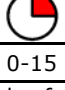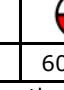
Link hinge	Rotation [mrad]				Max. Value
Pattern	◔	◑	◕	●	166
Steel	0-40	40-110	110-150	>150	
Pattern	◔	◑	◕	●	115
Composite	0-15	15-60	60-110	>110	

Table. 4.2.Levels of rotation for the plastic hinge in the short link*
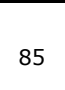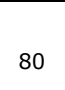
RBS hinge	Rotation [mrad]				Max. Value
Pattern	◔	◑	◕	●	85
Steel	0-15	15-55	55-80	>80	
Pattern	◔	◑	◕	●	80
Composite	0-5	5-30	30-70	>70	

Table. 4.3.Levels of rotation for the plastic hinge in the RBS*

* - Note: As a general rule in the presentation of results, the red colour will show results obtained by structures with composite beams, while blue will depict results obtained with steel beams (both for hinge definitions and graphs).

The maximum values for the rotations given in the tables above are not necessarily reached during analyses. They appear mostly for the definition of the hinges, and thus the maximum value represents the failure criterion of the hinge.

Fig. 4.16 presents the plastic hinges' development for steel and composite frames respectively. As it could be noted, first plasticization occurs in the lower-level links and later at the end of beams in RBS zones (negative bending only).

Top displ. = 0.045m   Top displ. = 0.09m (SLS)   Top displ. = 0.13m

Top displ. = 0.18m   Top displ. = 0.23m (ULS)

N/A
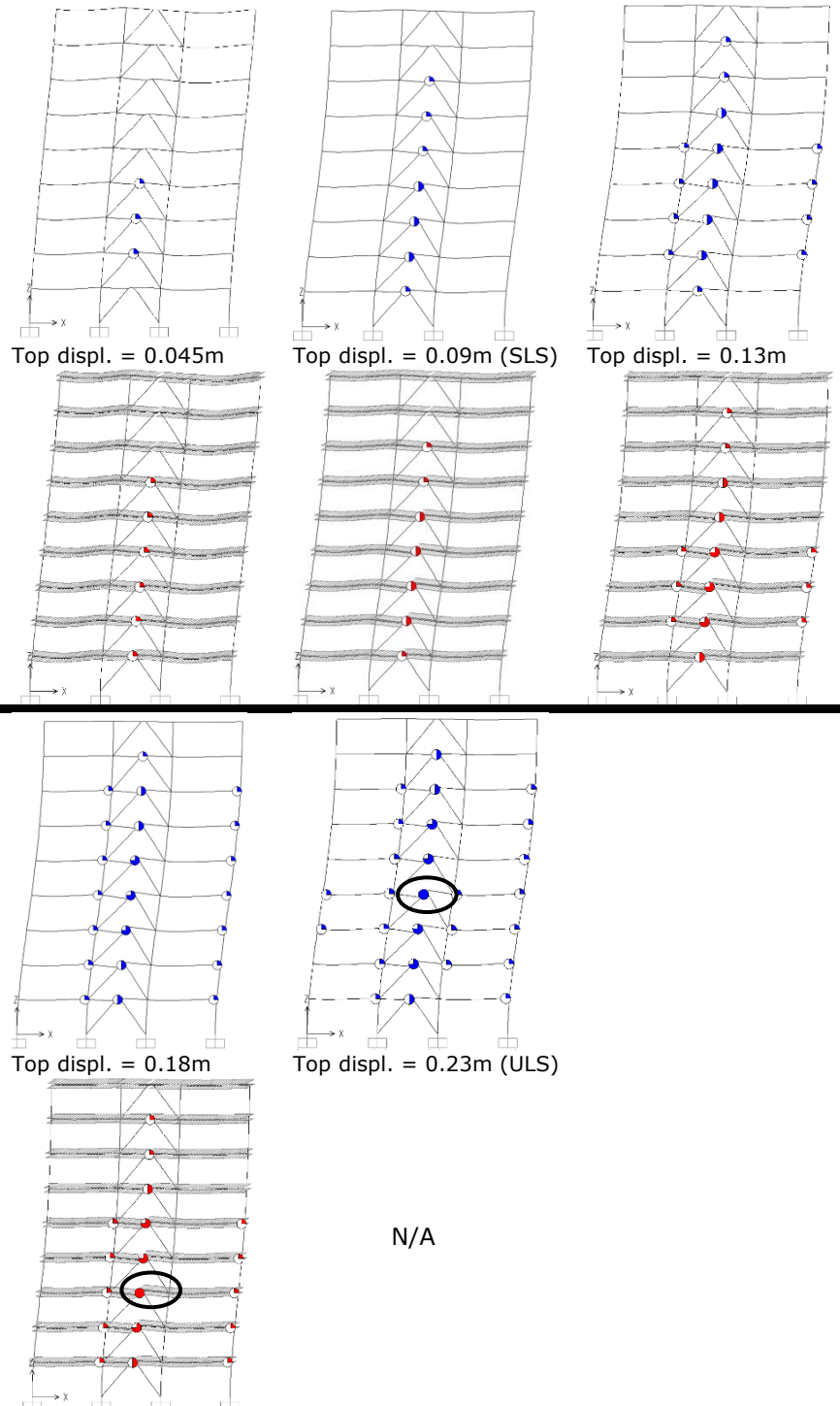
Fig. 4.16. Plastic hinge development in the 8 story DUAL frame

In both cases, the SLS deflection conditions are reached by plastic hinges only in link. The ultimate limit state corresponds to the exhaustion of rotation capacity of links, recorded in the mid-stories. It is to be noted the fact that at the ULS stage, the RBS have only initial plasticization under bending. In these conditions, a replacement of the EBF link may restore the building in a recovery state after a strong seismic motion.

Another conclusion is that for the composite beams the plastic hinges tend to develop later and have smaller rotation values. Thus the composite solution leads obviously to a stiffer structure. Due to this fact the structure with composite beams does not reach its target displacement at ULS. Even so, the overall performance of the structure with composite beams is appreciated as satisfactory, no damage occurring in the non-dissipative elements of the structure.

4.6.2 Results for Vrancea '77 (INCERC, N-S) accelerogram in ULS (design) conditions

The current paragraph presents the state of the 8 story DUAL steel and composite frames under Vrancea 1977 quake. This analysis could be considered also as a verification of equivalent elastic design by means of time-history dynamic analysis. The results involve inter-story drift, link rotation and RBS rotation, the last two being the factors which best describe the ductility of the structure. The obtained values are given for the design situation. For this the recording was scaled so as to correspond to a peak ground acceleration of 0.24g. As all the accelerograms were scaled for this value, the results are given now for an accelerogram multiplier (denoted in this work by λ) equal to 1.0.

Fig. 4.17 shows the maximum recorded values (envelopes) during the quake action for RBS rotation, link distortion as well as the inter-story drift (expressed as percentage of story height) for each story of the analysed frame.

It is noticeable here that the largest story drift is at the 2nd level, but the attained value (approx. 2%) does not exceed the value given by Eurocode 8. The link exhibits high ductility, reaching rotation values in excess of 110 mrad. In case of the steel frame, the RBS have been noticed to function according to their design prescriptions, yielding later than the links and developing hinges up to the 6th floor in the steel configuration and 5th floor with composite beams. Here the values are noticeably higher for the steel beams in comparison to the composite ones.

It could be concluded that for the particular P+8 frame analysed, the steel structure, which is more flexible, shows plastic requirements of rotation and drift greater by at least 25% than in the case of the composite structure. From this point of view, the composite structure responds better to the seismic ground motion.
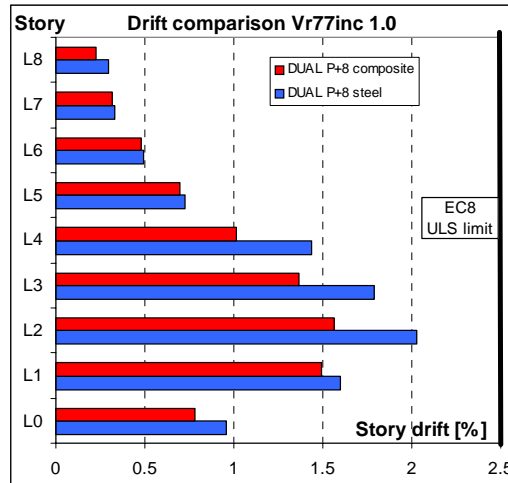
a. Design situation – drift
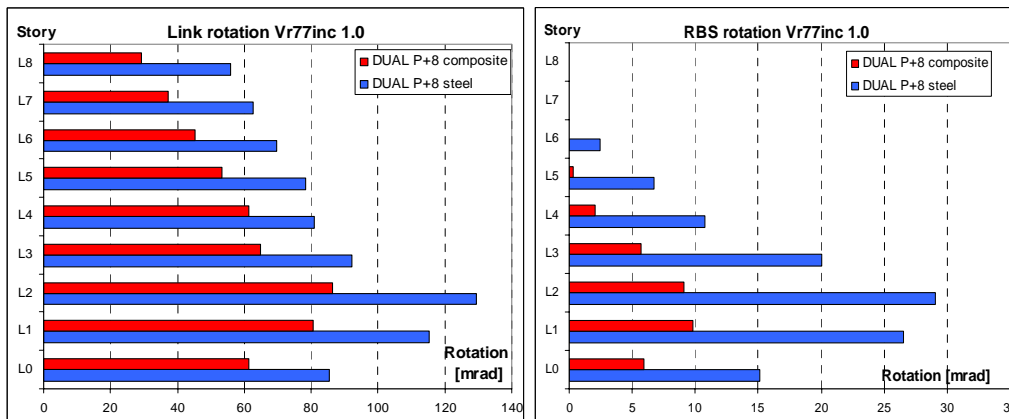
b. Design situation – link rotation

c. Design situation – RBS

Fig. 4.17. Results/levels for the 8 story DUAL structure under Vrancea `77 quake

4.6.3 Results for Vrancea '77 accelerogram, for SLS and ULS conditions

In order to illustrate the difference between the SLS and ULS conditions, the following charts show the above values at ULS but combined to those obtained for a smaller intensity (λ=0.5) corresponding to SLS conditions. While the ULS results are already known, the SLS conditions induce very small discrepancies between the steel and composite frames in what concerns the drift values and RBS zone rotation. However, for lower levels in the structure, there are significant differences in link rotations: 20 mrad for composite, up to 40 mrad for steel frame, respectively.
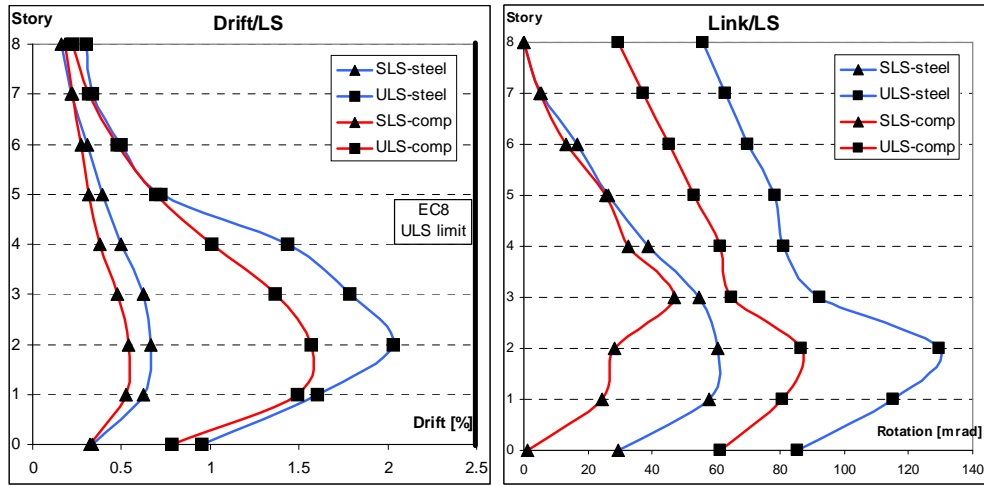
a. SLS and ULS limit states – drift comparison

b. SLS and ULS limit states – Link rotation comparison
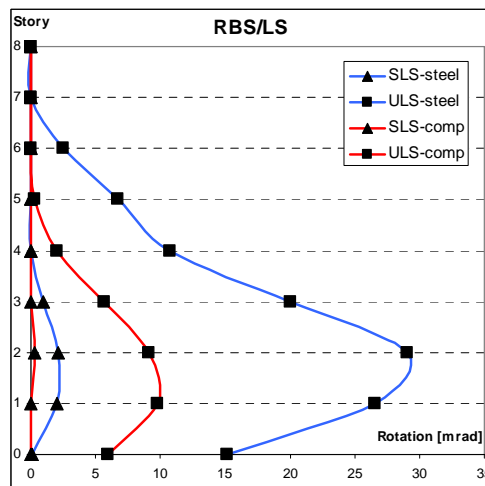
c. SLS and ULS limit states – RBS rotation comparison

Fig. 4.18. Results for the DUAL 8 story structure compared on limit states/levels

4.6.4 Results at ULS conditions for the full-set of accelerograms

Fig. 4.19, Fig. 4.20 and Fig. 4.21 present the maximum recorded values (envelopes) for drift, maximum plastic RBS zone rotation and link distortion for all the seven Vrancea-type accelerograms.

Following the same conclusion as before, when comparing the response of the two structures (steel and composite) at the design ground acceleration ($\lambda=1.0$), at each level, the difference is obvious. Moreover, the values for the rotation of the plastic hinges in the links for the composite structure appear to be more evenly distributed along the building's height. However, at ULS conditions the composite

structure could be considered safe, with all the required values for drift and rotations under the norm limiting values. The steel frame could be considered the same, with only two observations: the link distortion for Vr77 and 86 exceeds the required experimental value of 110 mrad (LS state equivalent in FEMA356 document).
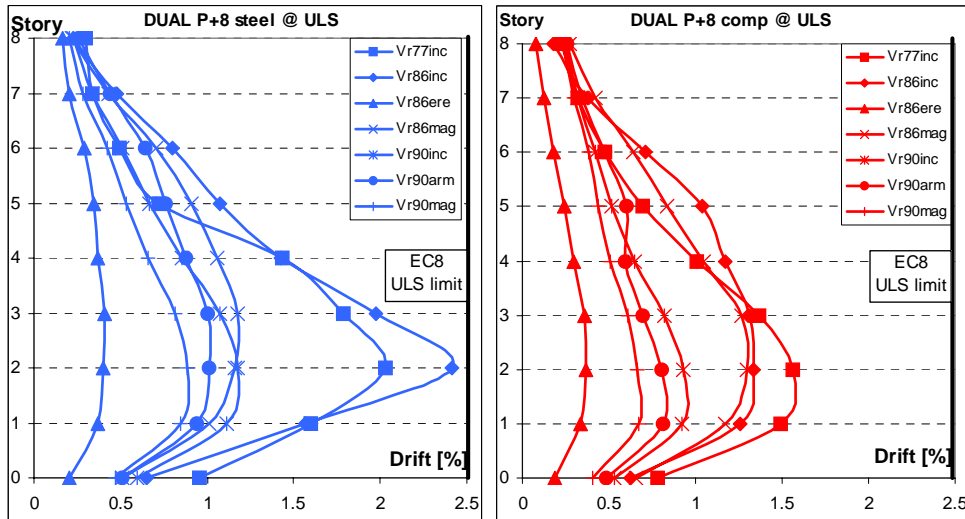
Fig. 4.19. Drift comparison/levels for the DUAL 8 story structure
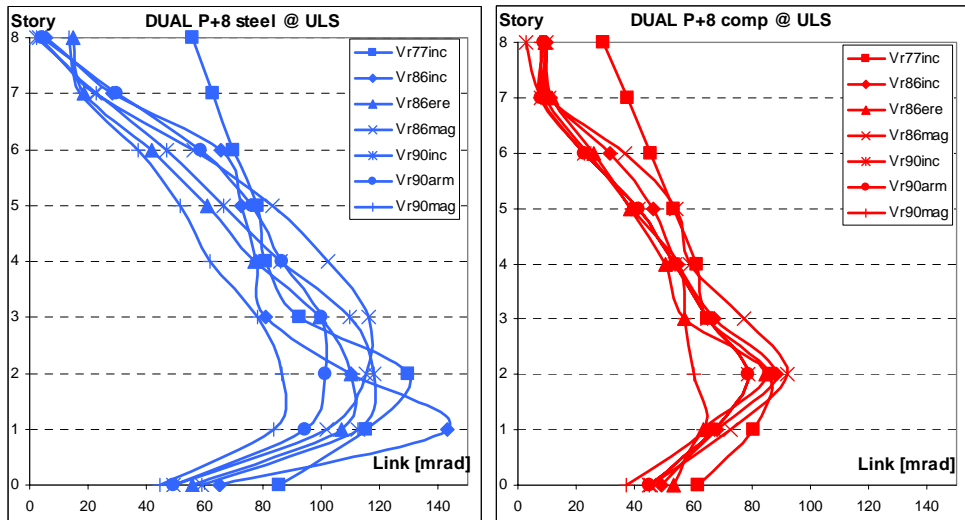
Fig. 4.20. Link rotation comparison/levels for the DUAL 8 story structure
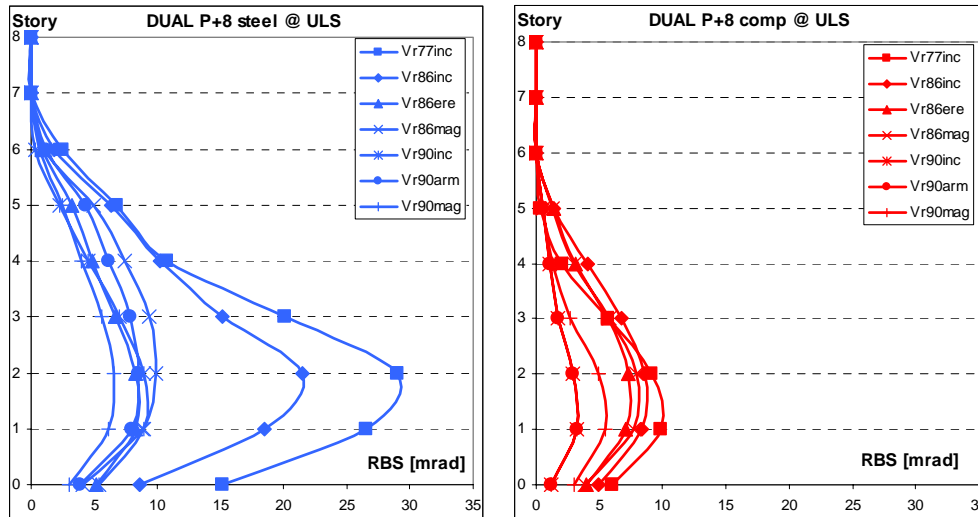
Fig. 4.21. RBS rotation comparison/levels for the DUAL 8 story structure

4.6.5 IDA results

The following set of results shows the comparison between the global responses of the 8 story structure in the steel and composite beams solution under 7 earthquake recordings from Vrancea source. The IDA were performed by step-by-step incrementation of the acceleration level and monitoring the top displacement value up to the point when a failure criterion was reached (see §4.5). Fig. 4.22 presents the obtained λ-Δ charts.

From this data the following conclusions could be drawn:
- The frame with steel beams develops plastic hinges earlier than the composite one, while the failure (either by soft story mechanism or attaining maximum rotation in one of the hinges) increment has similar values, although the steel structure exhibits higher overstrength;
- The drift values are within the code limits, but the composite structure is noticeably stiffer.
- All the frames present a safety reserve of at least 20% (λ=1.2). From this point the deformations become larger.
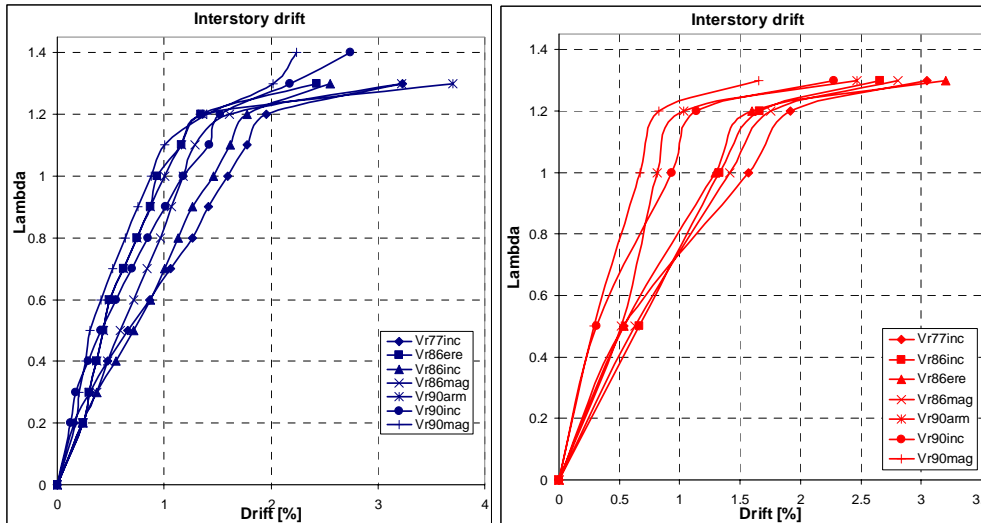
Fig. 4.22. IDA response representations for the DUAL 8 story steel and composite structure, respectively

4.6.6 Comparison between the responses of steel and composite EBF and DUAL structures

In order to check that the results obtained for the DUAL structure leads to the correct approach and conclusions, a comparison was made with a similar frame, consisting of an EBF and two hinged adjacent frames on each side, having the same spans and number of stories.

In the tables below one can compare in turn the obtained results for the two types of structure, in the design situation ($\lambda=1.0$) for each analysed earthquake recording.

In both cases, the drift, link distortion and RBS rotation have smaller values for the composite configuration, confirming in this way the conclusions drawn up to this point.

Results @ ULS - EBF - 8 stories structure					
Quake	Drift requirement [%]		Link rotation [mrad]		RBS rotation [mrad]	
	Steel	Composite	Steel	Composite	Steel	Composite
Vr77inc	1.52	1.27	146	110	---	---
Vr86inc	1.47	0.92	136	96	---	---
Vr86ere	1.36	0.85	125	61	---	---
Vr86mag	1.21	0.72	108	64	---	---
Vr90inc	1.03	0.93	92	53	---	---
Vr90arm	0.97	0.93	85	58	---	---
Vr90mag	0.83	0.53	72	59	---	---

Table. 4.4. Set of results for the 8 story EBF frame, ULS

Results @ ULS - DUAL - 8 stories structure						
Quake	Drift requirement [%]		Link rotation [mrad]		RBS rotation [mrad]	
	Steel	Composite	Steel	Composite	Steel	Composite
Vr77inc	1.59	1.56	129	86	29	9
Vr86inc	2.41	1.89	143	128	21	7
Vr86ere	1.11	1.04	110	92	8	7
Vr86mag	0.70	0.62	116	98	9	7
Vr90inc	1.17	0.93	117	110	8	4
Vr90arm	1.00	0.81	101	91	8	3
Vr90mag	0.88	0.66	86	79	6	5

Table. 4.5.Set of results for the 8 story DUAL frame, ULS

Note: all steel beams in DUAL configuration were designed using steel quality S235, while all beams in EBF configuration are steel quality S355.

4.6.7 Comparisons of IDA responses for EBF and DUAL frames for Vrancea '77, '86 and '90 accelerograms

The differences in behaviour between the two structures (see Fig. 4.23) are not so poignant when we compare the IDA obtained curves. One conclusion that can be drawn here is the fact that the EBF structure (S355 beams) has comparable drifts and rotations of dissipative zones (see Table. 4.2, Table. 4.3) with the DUAL structure (S235 beams). Generally, the DUAL frames behaved in a more rigid way. Also, the failure intensity for DUAL frames reaches in some cases values of 1.4 times greater than the design intensity.
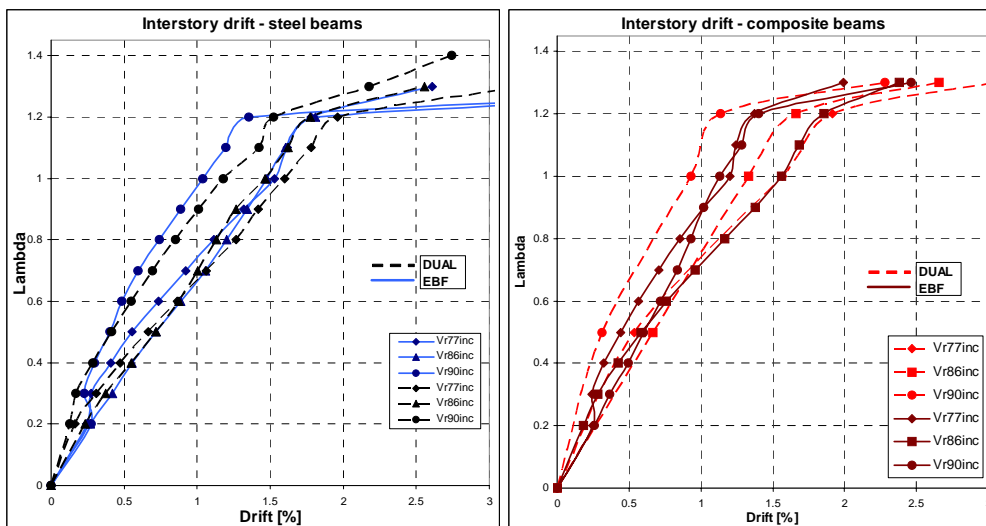
Fig. 4.23. Comparison between IDA curves for the EBF and DUAL 8 story structures

4.7 Global results obtained for structures

All structures were designed and analysed in the same manner, first in pushover nonlinear analyses, than in IDA analyses. The general conclusions remain valid for all frames, as for the 8 story DUAL configuration. Another important observation is that when composite beams are used, the first period of the structure is reduced in comparison to the steel configuration (see Appendix I).

4.7.1 Push-over results for the 4 story DUAL frame

Top displ. = 0.04 m   Top displ. = 0.08 m   Top displ. = 0.14 m
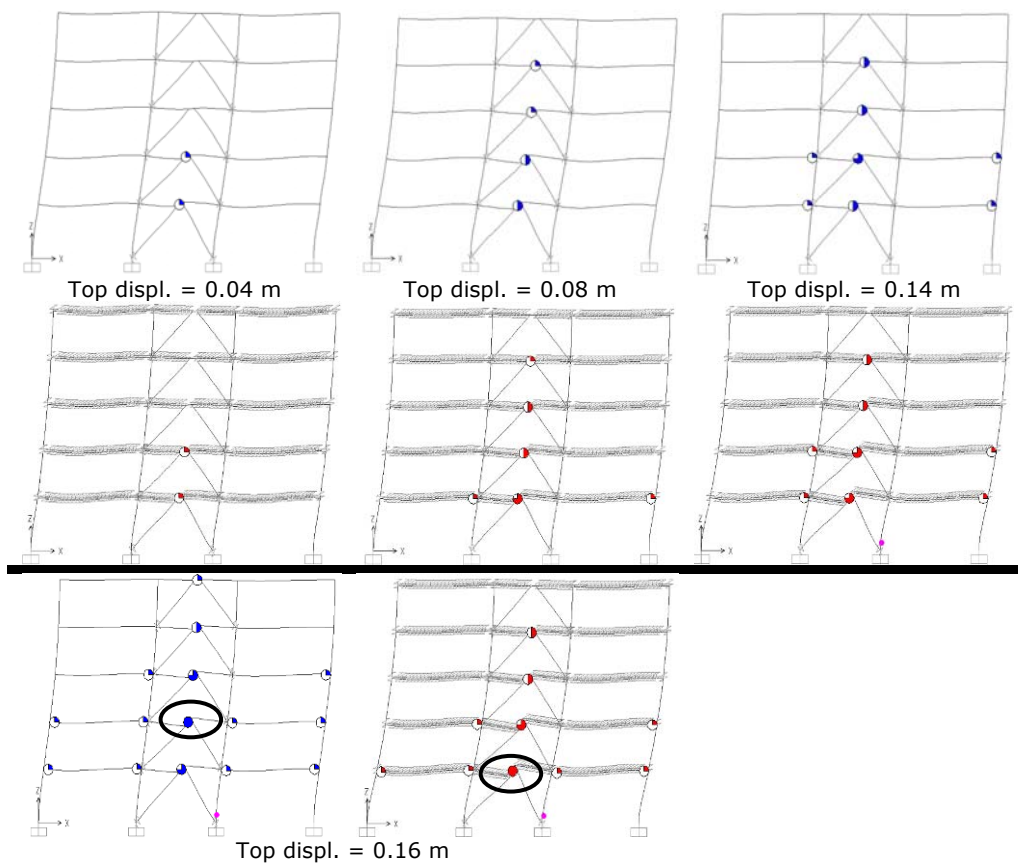
Top displ. = 0.16 m
Fig. 4.24. Pushover behaviour recorded for the 4 story DUAL frame

The link rotations for both steel and composite frame reach their maximum defined values, but their extent is different, as explained in their definitions (see Table. 4.2, Table. 4.3). The RBS plasticization for the composite solution has smaller extent reaching only the second floor, with incipient plastic values. The link hinges also develop with a delay when compared to steel. The failure mechanism is also initiated at a different level, 2nd floor in case of steel beams and 1st floor in case of composite ones.

4.7.2   Push-over results for the 4 story EB frame

Top displ. = 0.025 m   Top displ. = 0.1 m   Top displ. = 0.16 m

Fig. 4.25.   Pushover behaviour recorded for the 4 story EBF
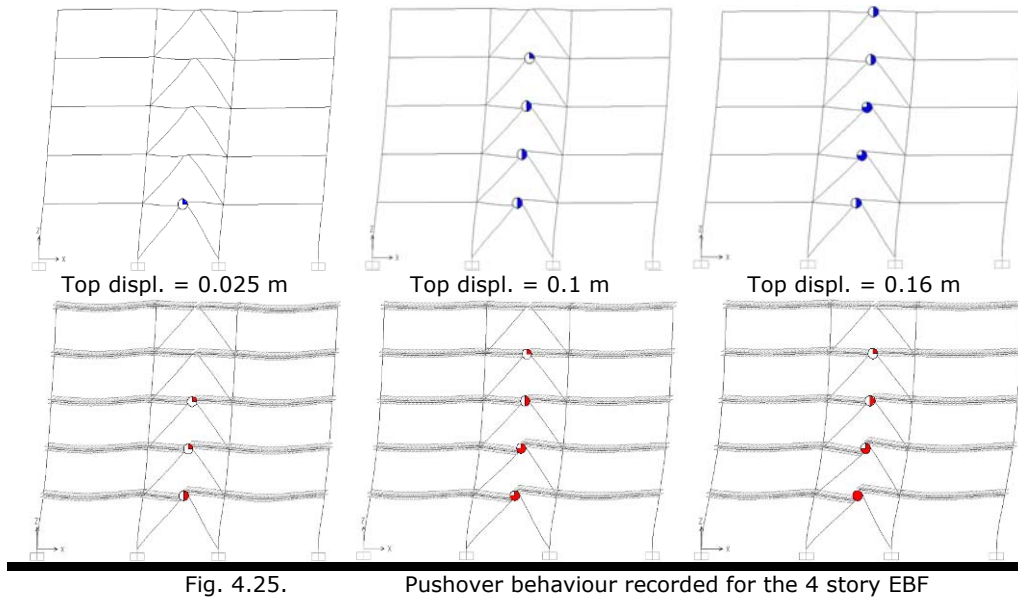
In case of the 4 story EBF structure, the behaviour is similar to that of the 4 story DUAL configuration. The plasticization of links follows the same pattern, from lower stories up to the last one, again with smaller values for the composite beams.

4.7.3   Push-over results for the 6 story EB frame

Top displ. = 0.045 m   Top displ. = 0.1 m   Top displ. = 0.16 m

Top displ. = 0.38 m
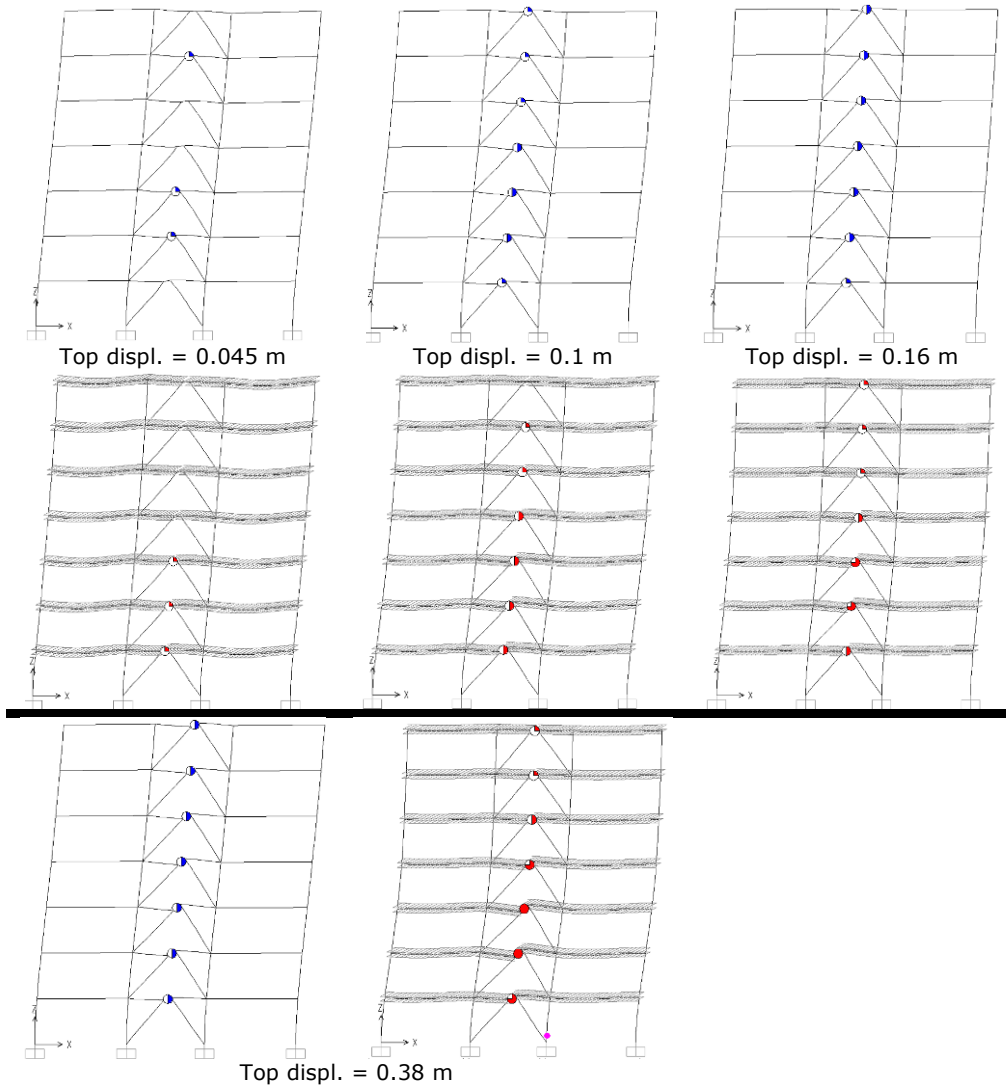
Fig. 4.26. Pushover behaviour recorded for the 6 story EBF

The maximum values defined for the composite links' hinge are attained. Here the dissipation has a different spread pattern. While for the steel structure the links tend to reach their capacity in a uniform way throughout the building's height, when composite beams are used, the higher rotations are reached at the 2nd and 3rd levels.

4.7.4 Push-over results for the 5 story MR frame

Top displ. = 0.085 m   Top displ. = 0.21 m   Top displ. = 0.46 m
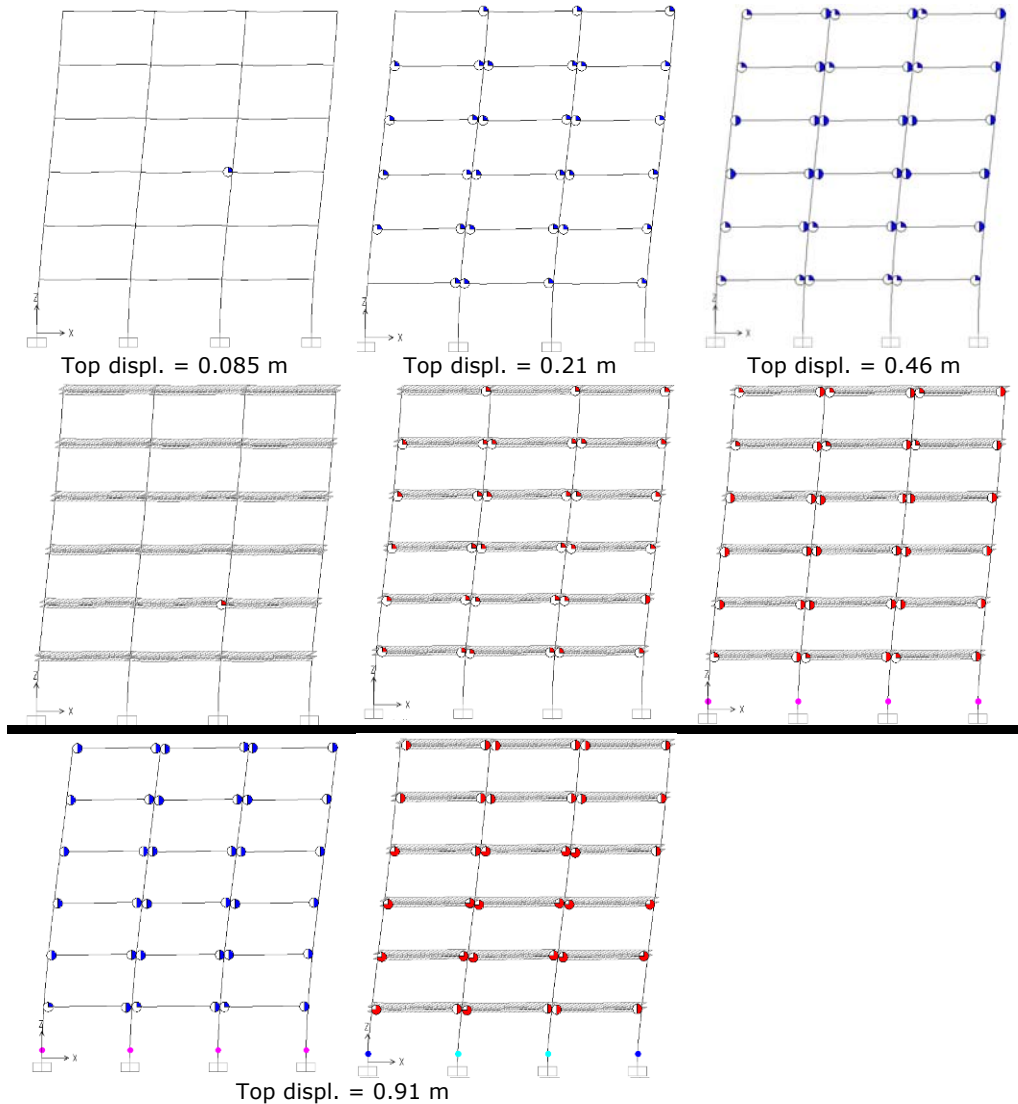
Top displ. = 0.91 m
Fig. 4.27. Pushover behaviour recorded for the 5 story MRF (spans of 6m)

The global increase in structural stiffness remains valid for the MRF systems. While the plastic mechanism is identical, the structure with composite beams tends to develop higher stresses at the column's bases. Spread of the plastic hinges is quite uniform, but higher values are attained by the hinges in composite beams at levels 2 and 3.

4.7.5 Push-over results for the 12 story DUAL frame

| Top displ. = 0.08 m | Top displ. = 0.13 m | Top displ. = 0.25 m |

Top displ. = 0.3 m   Top displ. = 0.4 m
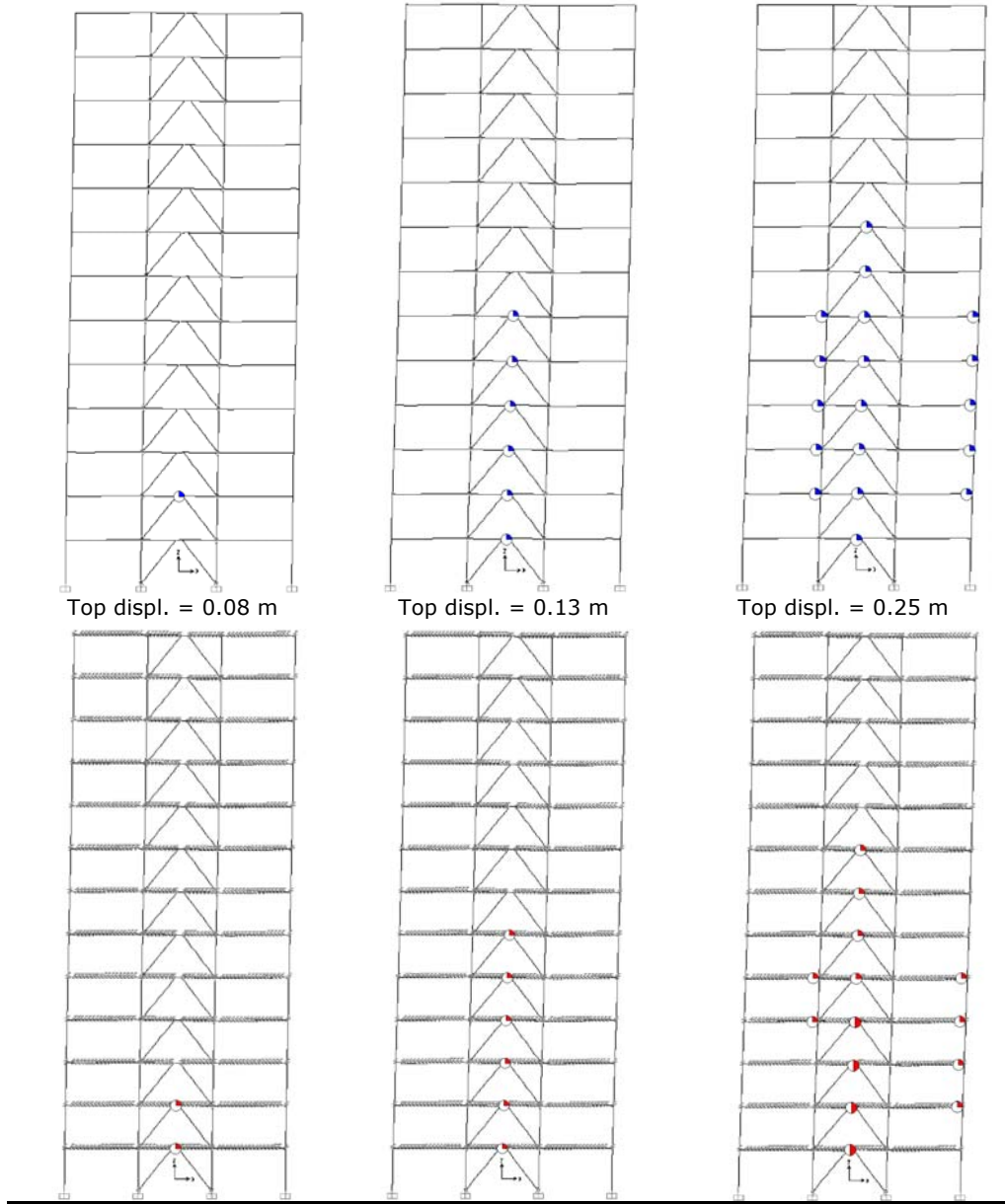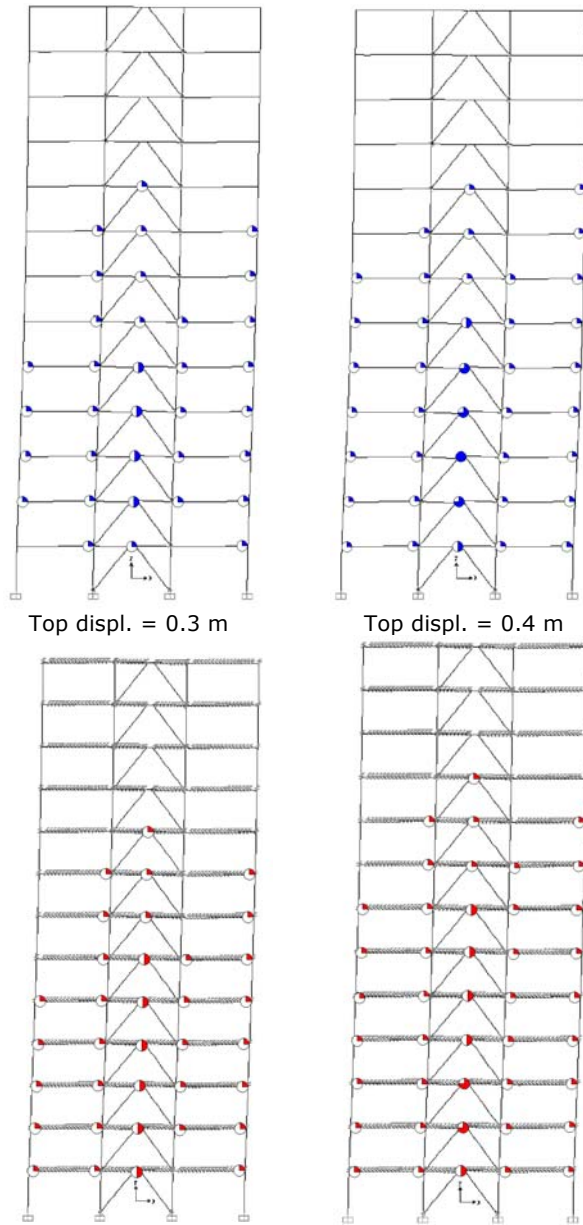
Fig. 4.28. Pushover behaviour recorded for the 12 story DUAL structure

In every aspect, the high-rise frame's behaviour is within the main ideas stated so far. As it can be seen from the numerical simulation, the order of the plasticization is respected, first the hinges appear in the links, then in the RBS, both developing at each level as the lateral displacement is increased.

4.7.6 SLS and ULS global requirements

Fig. 4.29 - Fig. 4.31 present the maximum requirements for SLS (λ=0.5) and ULS (λ=1.0) for all the structures under analysis.

One of the most important remarks when looking at all results compared on limit states is that the difference between the structures with steel and composite beams is obvious, for both limit states and for all structures.
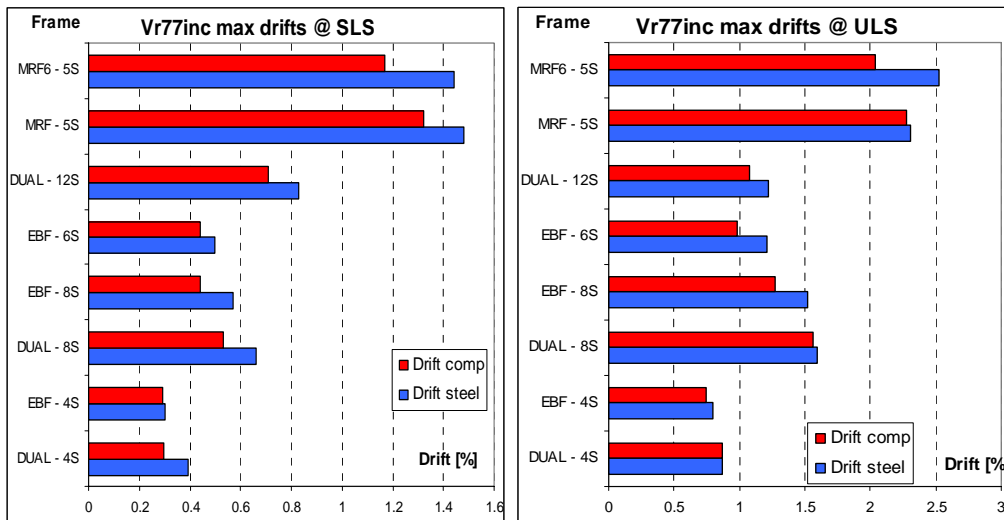
Fig. 4.29. Drift comparison/limit states for all simulated structures
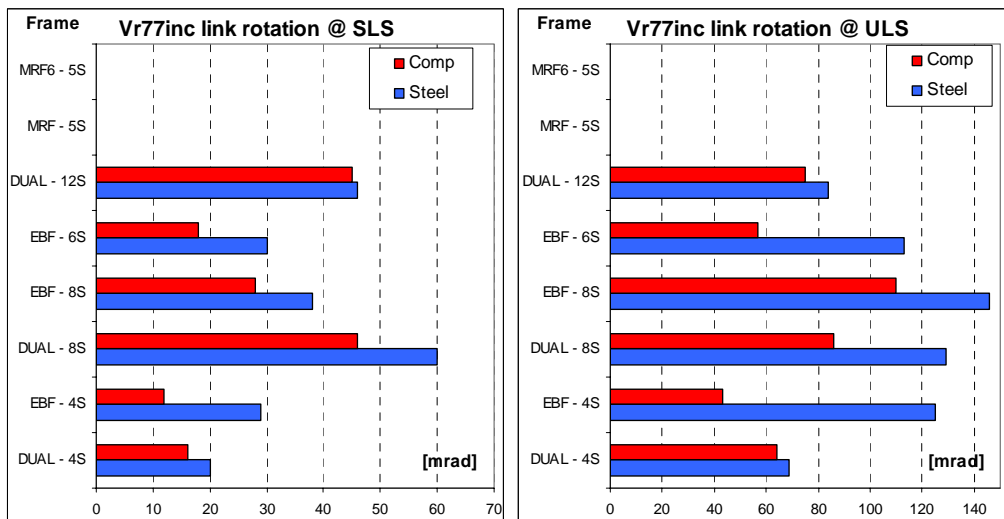
Fig. 4.30. Link rotation/limit states for all simulated structures

The most deformable structures – MRFs – present the highest drift values (Fig. 4.29) but even for these cases, the maximum recorded values remain in

acceptable limits: 1.5% for SLS and 2.5% for ULS. For all the cases, the composite beams induce a higher rigidity and in consequence smaller deformability.

The same conclusions can be drawn for link rotations (Fig. 4.30) and RBS zones (Fig. 4.31). Due to the absence of EBF links, the MRF can exhibit their plastic dissipation capacity only through RBS zones, requiring values of 20-25 mrad.
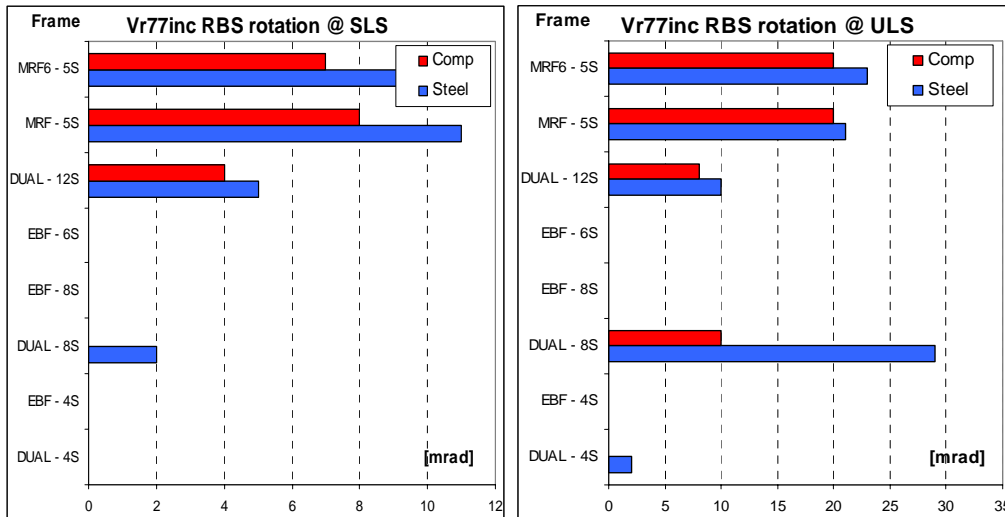
Fig. 4.31. RBS rotation/limit states for all simulated structures

4.7.7 Verification at ULS function of structural typology

Following the general remarks observed up to now, it results very clearly the fact that the inter-story drift and plastic requirements are always higher in the case of steel frames as compared to the composite ones.

The eccentric braces (DUAL and EBF structures) prove to be a very efficient way for limiting the maximum inter-story drift values at ULS, values being constant around 1%. In contrast, the MRFs may reach 2.5%, close to the failure criterion for displacement.

The inter-story drift and plastic demands in links and RBS depend on the structural typology and accelerogram. The amount of seismic input energy depends on the principal period of vibration of the structure and its projection on the acceleration response spectrum. A grafic representation of the elastic response spectra and structural periods is given in Appendix I.

This explains the particularly high demands in the case of some accelerograms. However, for each structure, analyses revealed coherent results, with small differences in monitored parameters (max 35%).

The results for high-rise structures (e.g. 12 storey DUAL structure) do not lead necessarily to higher drift or plastic rotations in hinges, when compared to low-rise buildings of the same typology. However, this could be achieved only if the design is properly accomplished.
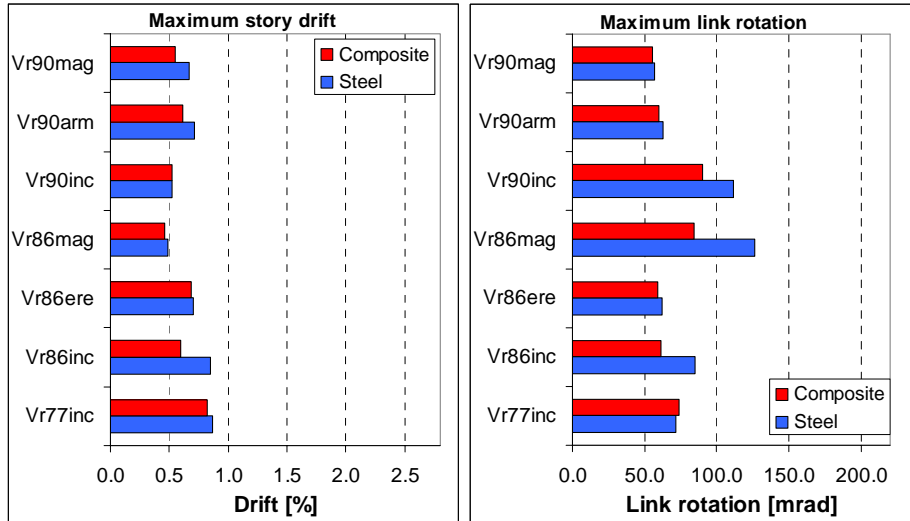
Fig. 4.32. Results obtained for the DUAL 4 story frame
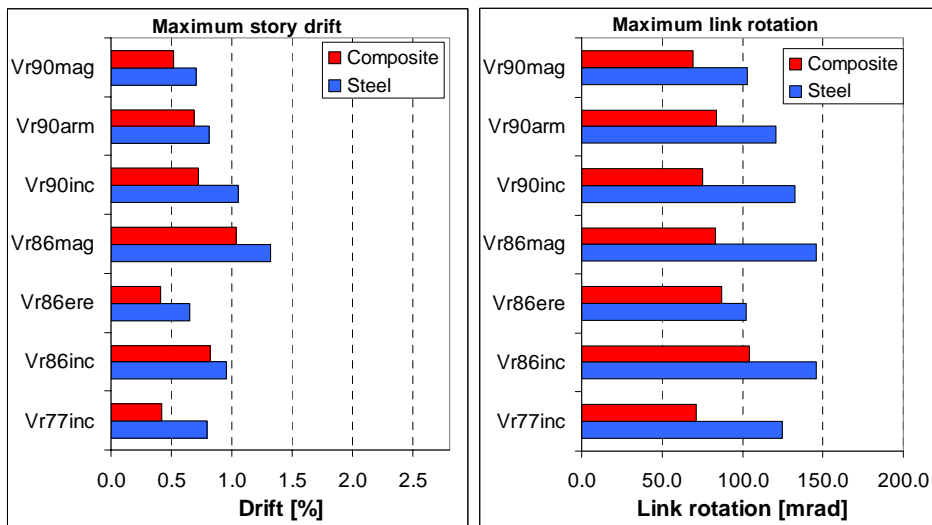
Fig. 4.33. Results obtained for the 4 story EBF
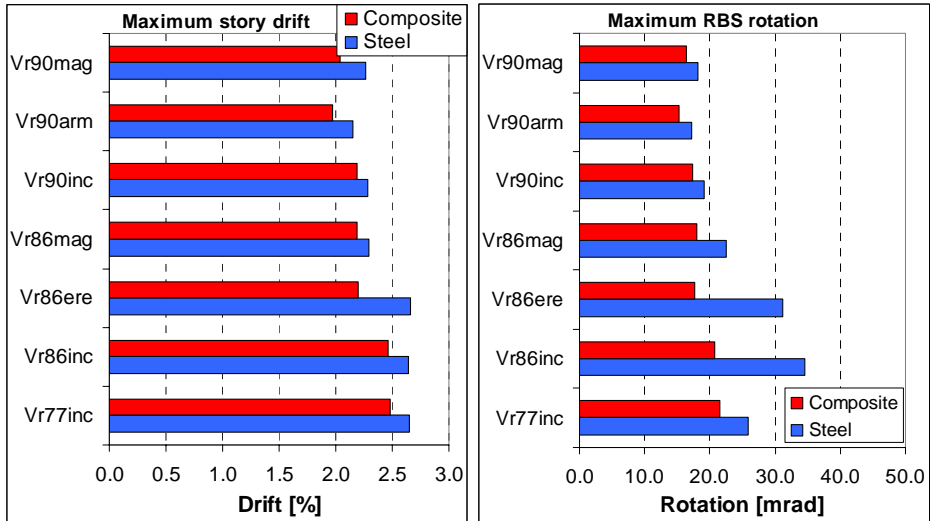
Fig. 4.34. Results obtained for the 5 story MRF
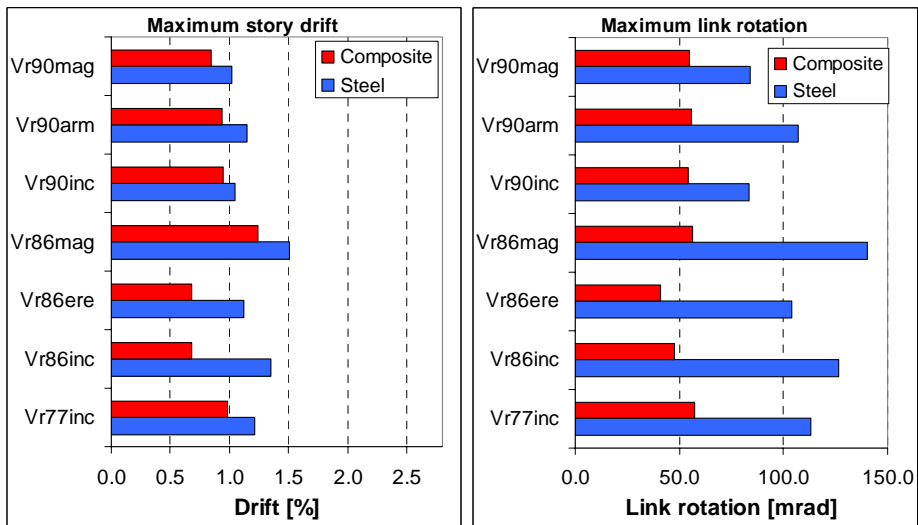
Fig. 4.35. Results obtained for the 6 story EBF
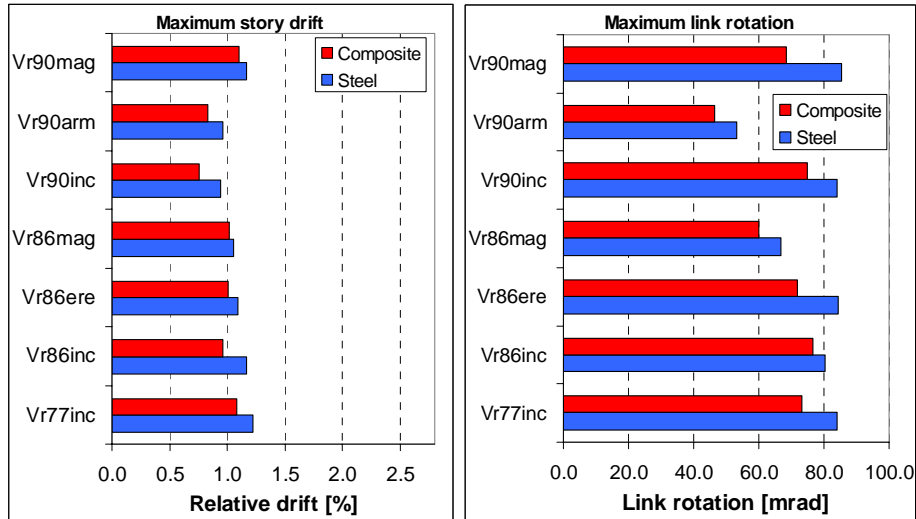
Fig. 4.36. Results obtained for the 12 story DUAL frame

4.8 Evaluation of the behaviour factor q and the structural efficiency η

Table. 4.6 gives the accelerogram multipliers for finding the q (behaviour factor) and η (seismic efficiency) for six representative frames. Due to the fact that the accelerograms used in analyses were initially pre-scaled to the design seismic intensity, the η factor is equal in this case to the ultimate value of accelerograms multiplier – λ_u.

Values listed in Table. 4.6 represent the averages computed for all the seven accelerograms considered for analyses. Exact values of the q factors for each structure and accelerogram are given in Annex II.

The computed q values show the good dissipation capacity of EBF and DUAL type frames, with numbers generally greater or equal to the design value – q=6. However, smaller values are found for composite structures. This fact could be explained by the higher rigidity induced by composite beams.

The values of the seismic efficiency proves a global minimum reserve of the structures greater than 20% which could be judged as safe for the current design. The final value of η seems not to depend on structural typology (steel/concrete, DUAL/MRF/EBF), but only on the real response to different accelerograms.

Structure	Configuration	λe, avg	λu, avg	q, avg	η, avg
F1 P+4 dual	steel	0.3	1.4	5.5	1.4
	composite	0.3	1.2	3.9	1.2
F2 P+12 dual	steel	0.2	1.4	5.8	1.4
	composite	0.2	1.2	4.9	1.2
F3 P+5 MRF	steel	0.2	1.5	5.8	1.5
	composite	0.3	1.5	5.8	1.5
F5 P+6 EBF	steel	0.2	1.2	5.9	1.2
	composite	0.3	1.2	3.6	1.2
F6 P+8 EBF	steel	0.2	1.3	6.5	1.3
	composite	0.2	1.2	5.8	1.2
F7 P+8 DUAL	steel	0.2	1.4	5.8	1.4
	composite	0.3	1.3	4	1.3

Table. 4.6. Average values obtained for q and η

4.9 Overstrength values for analysed structures

Another practical aspect in engineering design of MR and EB frames regards the values of the overstrength factors, which practically multiply the seismic loads for the combination of non-ductile elements. Here, a matter is subjected to discussion when dealing with dual frames MRF + EBF of short links:

- The overstrength product $1.1*\gamma_{ov}*\Omega$ for MRFs is relatively easy to find, by considering the values of $\gamma_{ov}=1.1$ and Ω as the minimum ratio between the plastic moments of all the beams and the stress level of each dissipative beam. The recommended value for the $1.1*\gamma_{ov}*\Omega$ product given in Annex F of P100-1/2006 (Romanian seismic norm; values derived from ASCE, table 12.2-1) for MRFs is 3 for both steel and composite frames;

- The overstrength product $1.1*\gamma_{ov}*\Omega$ for EBFs is also computed by taking the same value for γov and Ω taken as 1.5 times the minimum ratio between the plastic shear capacity of all the link elements and the stress level for the corresponding link, taken from the dissipative combination. The recommended value for the $1.1*\gamma_{ov}*\Omega$ product given in Annex F of P100-1/2006 for EBFs is 2.5 for both steel and composite frames;

- In what concerns the DUAL frames, the product is difficult to estimate, due to the fact that the frames are composed of both types of frames. The P100 code gives here the same value of 2.5 for Ω.

This paragraph presents the exact valued of the overstrength factor Ω, for the structures considered in the numerical study. Table. 4.7 presents the summary of the results for Ω and the overstrength product $1.1*\gamma_{ov}*\Omega$ for all the structures. In Annex II are given detailed results obtained on levels.

Structure	Ω EBF		Ω MRF		Ω str.		$1.1*\gamma_{ov}*\Omega$str.	
	steel	comp	steel	comp	steel	comp	steel	comp
DUAL-4	2.16	2.22	2.83	2.94	2.83	2.94	3.89	4.04
DUAL-8	1.52	1.55	1.39	1.72	1.52	1.72	2.09	2.36
DUAL-12	1.57	1.58	1.32	1.39	1.57	1.58	2.16	2.17
EBF-4	1.52	1.62	---	---	1.52	1.62	2.09	2.23
EBF-6	1.83	2.07	---	---	1.83	2.07	2.51	2.84
EBF-8	1.53	1.67	---	---	1.53	1.67	2.11	2.30
MRF-5ls	---	---	1.08	1.18	1.08	1.18	1.49	1.62
MRF-5ss	---	---	1.04	1.30	1.04	1.30	1.43	1.78

Table. 4.7.Ω factors obtained for the analysed structures

Considering the Ω values on levels, it could be seen very clearly the fact that the values are increasing from bottom to top, which means that the top dissipation elements are usually not very stressed in seismic conditions (leading to high values equal to 7 or 9). This is coherent with the order of formation of plastic hinges, shown in §4.7.1 - 4.7.5. Another conclusion drawn from these tables shows the fact that in practical application of finding Ω, the real values are always taken from the lower storeys.

For MRFs the values of Ω given in Table. 4.7 are quite close to 1 for both steel and composite structures. This proves practically the efficiency of RBS solution. The final value of overstrength product $1.1*\gamma_{ov}*\Omega$ (between 1.5 – 2) is smaller than that prescribed by norm.

However, for EBFs, the overstrength factors are greater than those of MRFs, maximum being 1.8 for steel and 2.1 for composite frames. This leads to $1.1*\gamma_{ov}*\Omega$ values of 2.5 for steel structures (identical to the ones prescribed) and 2.8 for composite. In this case the higher values obtained for Ω in comparison to MRF is tributary to 1.5 factor used for high strain-hardening effect characteristic to shear panels.

In case of DUAL frames, there have been computed Ω factors for both MR and EBFs. In this situation the MRF beams are less stressed as in pure moment resisting frames, this being proved by higher Ω values. On the other hand, smaller values are obtained for EBFs of dual frames. This leads to the conclusion that the seismic-induced efforts are redistributed as in case of pure MRF and EBF frames, namely from MRF to EBF. In the opinion of the author, and in coherence with the norm prescriptions (according to which a single Ω factor should be used for the entire structure), the highest Ω value should be considered from all the values computed for MR and EB elements. For our applications the values found could be divided in two cases:

- For low-rise buildings (e.g. 4 storey structures) the $1.1*\gamma_{ov}*\Omega$ products given in norms are smaller than the obtained values. This could lead to undersized non-ductile elements (columns and braces in this case);

- For medium-rise buildings (8 to 12 storeys) the $1.1*\gamma_{ov}*\Omega$ product is however in the limits of the norm prescriptions.

As a general comment, it could be seen that the composite frames have greater values for both Ω and total $1.1*\gamma_{ov}*\Omega$ products. This finding is however not in accordance to the existing prescriptions, which guarantees the same values for steel and composite frames.

4.10 FE modelling on assemblies – characteristics and problems

A very important aspect in the accomplishment of highly-dissipative structures (such as MRFs and EBFs) is the adequate detailing of plastic zones. This could be achieved through proper analyses with FE models followed by parametric studies on various components of the assemblies.

Present paragraph is devoted to FE calibration of some of the experimental specimens presented in Chapter 3:
- steel and composite joints with RBS for MRF;
- steel and composite EBF frames.

The FE computer program used for this modelling was Abaqus CAE v.6.7.1 [56]. For calibration of the results, the experimental curves obtained from the experimental tests were used.

All models were created using 3D solid elements, with real multilinear material models. The welds between different parts were simulated as TIE constraints. The bolted connections were modelled as the real connections, using bolt quality obtained from tensile tests. The meshes used mainly HEX and TET elements in most cases. The mesh quality has been noticed to influence only the duration of the analyses and not the results. As a general rule, it was observed that in order to obtain accurate stresses and strains, one must use a number of 3 FE per thickness of plate.
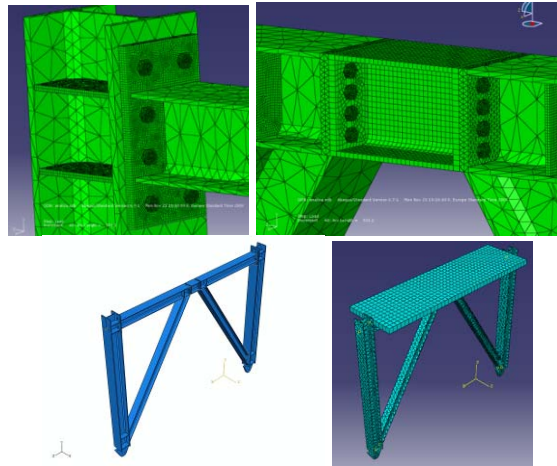
Fig. 4.37. Mesh quality and modelling of the steel and composite EBF

The steel assemblies did not present any modelling problems, with the observation that the steel and concrete materials need to be carefully defined. The loads were applied simulating experimental setup, just like in the case of the monotonic tests. Simulated models were loaded by „Static Riks" and „Standard" procedures. The „static Riks" method implies the linear increase of the load, until failure of the model is detected, while the „standard" method involves the application of a specific load value and its linear incrementation through the load step.
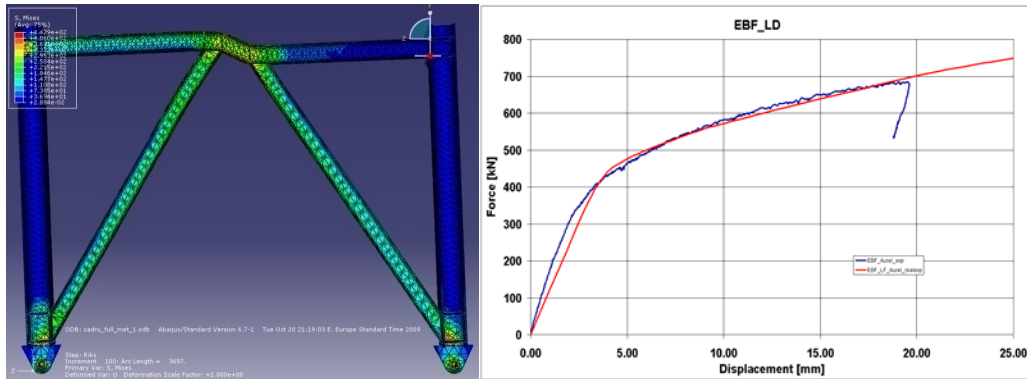
Fig. 4.38. FE model and experimental curves for the EBF frame

In case of the EBF only the testing of the steel frame was successfully simulated, while the frame with composite beam still needs some analysis tuning.

For the RBS joints, both steel and composite specimens were successfully modelled, obtaining similar results to those of the tests. The concrete model used was the „concrete damaged plasticity" from Abaqus, with different behaviour in tension and compression, each branch having its own damage parameters.
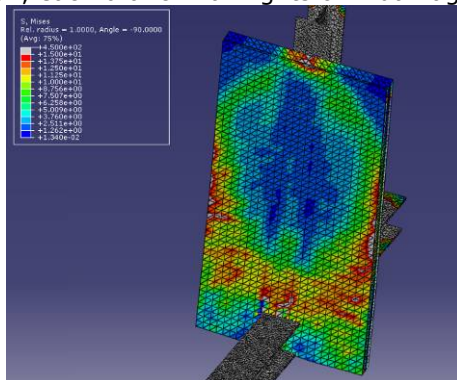
Fig. 4.39. Cracking pattern of the composite joint in tension
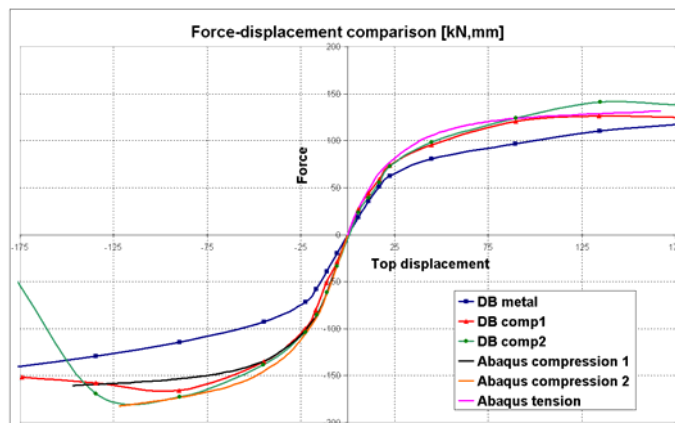
Fig. 4.40. Comparison of the experimental and FE curves for the tested joints

The obtained curves from FE models resemble quite correctly the ones obtained from the tests of the joints, both for the steel specimen and composite ones.

4.11 Conclusions and comments on the numerical study

Based on the calibration performed on the dissipative components (in SAP2000, Abaqus) one can optimize the behaviour of the short link and RBS, for both steel and composite solutions.

The Incremental Dynamic Analyses (IDA) have proven the fact that structures where the interaction between steel and concrete was modelled have had a different behaviour from the bare steel ones. The low-rise steel structures (4 stories, 5 stories) have shown higher drift and rotation requirements than the similar frames modelled with composite beams. For the high-rise structures, with a higher vibration period, the increase in strength and rigidity induced by the composite effect leads also to smaller rotations in links and RBS.

The numerical results indicate that the main plastic deformation requirements in case of DUAL (MRF+EBF) structures are to be found mainly in the links (with values around 100 mrad for the design situation) and with some contribution from the RBS (values around 20 mrad for the ULS). From this point of view, the value proposed by EC8-1, § 6.8.2. of 80 mrad for the short links in EBF becomes insufficient for the DUAL frames.

The values for the behaviour factor q, obtained for the analyzed steel structures, are close to the prescribed design values (e.g. q=6 for DUAL frames), confirming the good dissipation capacity of these systems. It is to be noted that, following the numerical analyses, for the composite structures resulted behaviour factors with smaller values than for the same structures with steel beams (e.g. for the DUAL frames, between 4 and 5, with respect to 6).

By analyzing the seismic efficiency – η, it resulted that the analyzed structures have strength and ductility reserves of about 20-40% compared to the design requirements.

5. DESIGN APPROACH AND PROPOSED PROVISIONS

5.1 Introduction

The final goal of the thesis was aimed at providing some general rules and aids that are of practical interest in the seismic design of steel frames with ductile zones located in RBS of MRF and links of EBFs. This methodology applies for bare steel beams as well as steel beams acting compositely with concrete slabs.

5.2 Design methodology

In this section, a general step-by-step design methodology and guidelines are proposed for an example structure with composite beams. The design procedure is summarized in the flowchart given in Table. 5.1 while the logical design phases are described below (in a usual design the dimensioning of elements is subjected to an iterative process):

1. Design of the structure with steel sections according to existing Eurocodes and National Anexes. A capacity design is advised, in order to control the order in which plastic hinges occur and to make sure the building reaches its target displacement. This can also be achieved through a simple Push-over analysis, while finding the target displacement may be done by N2 method. The design of non-dissipative elements is based on the overstrength factors considered in the seismic design procedure, provided that the conditions assuring the overstrength of elastic elements are fully met in the capacity design.

2. Compulsory, it is advisable to design the beams as composite from the beginning. A reduction in the beam section may occur, thus changing the beam configuration. In order to ensure a high plastic rotation capacity, the composite beams should fall in class 1 of cross sections.

3. The model of the composite beams should follow the procedures described in Chapter 4.

4. Thickness of the slab, reinforcement area and effective width should be taken into close consideration when detailing the section of the slab by the design software. In order to obtain a correct mesh of the slab, an iterative procedure is advised, in which the best ratio between mesh size / runtime should be chosen. The mesh may be more dense (smaller elements) above the plastic zones, and coarse (larger elements) where no plasticization is expected to occur.

5. If material certificates are available, real characteristics may be considered. Otherwise, the nominal material curves should be used. For the composite structure, a behaviour factor "q" of 4 is proposed. If all of the above prerequisites are met, a behaviour factor of 4.5 may be considered, for the

DUAL systems. The overstrength factor Ω may be computed as for a steel structure.

6. Hinge models for both steel and composite dissipative zones should be modelled (if possible extracted from experimental tests):
   - If tests are available, the hinges should be calibrated on appropriate response curves of dissipative zones;
   - If no such results exist (general design situation), one may consider the default definitions for the steel sections, while for the composite section the hinges should be calibrated considering the differences in rigidity, yield force and ultimate strength as stated and defined in Chapter 4.
7. The final checking of the structure should be performed by IDA on 3 earthquake recordings, of different magnitudes and terrain (preferably). The q factor should be evaluated from these analyses, in order to check the initial data.
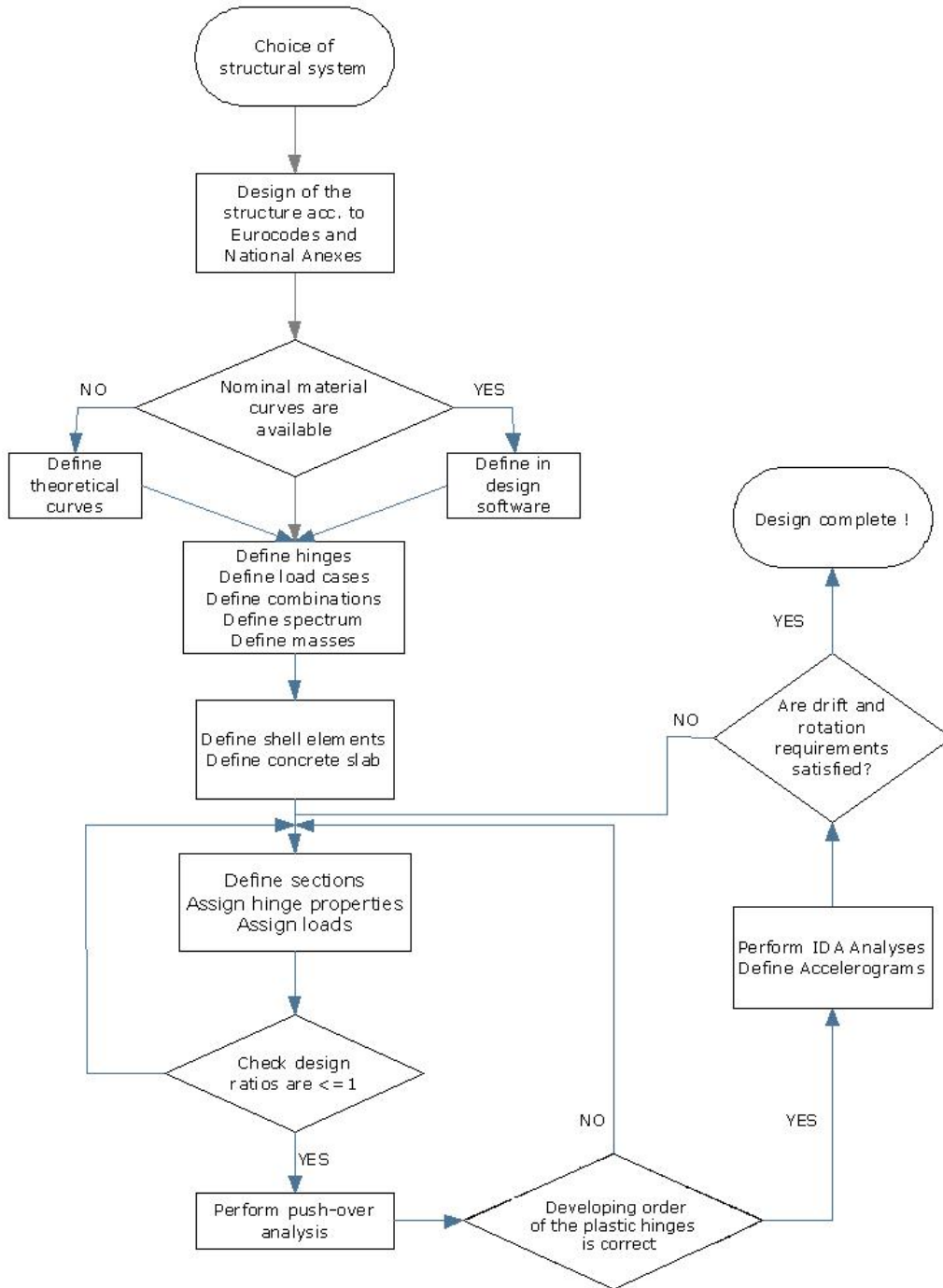
Fig. 5.1.   Flowchart of the design process

5.3   Case study – seismic design of a 6 story DUAL frame

Herein, the procedure described in the previous paragraph is exemplified through a practical design example, on a 6 story DUAL frame (MRF+EBF, see §5.2), consistent also with the experimental and numerical studies from previous chapters.
The following three structural solutions are studied:
- the design of a steel dual frame by considering the current provisions in norms with a behaviour factor q=6.
- the design of the same dual frame, but considering the composite effect of beams, without interaction over the plastic zones, as suggested by paragraphs §7.6.2, §7.7 and §7.9.3 from Eurocode 8.
- the design of the structure according to the design methodology described in paragraph 5.2, by taking the q value of 4.5 and considering the composite characteristics of beams; in this case, the composite character is preserved over the entire lengths of the beams, including the plastic hinges.

Other structural characteristics are given in the table below:

Frame type	DUAL	Notes
Span1/Span2/Span3	7m/6m/7m	
Bay	7m	
Story height	3.5m	
Columns' steel quality	S355	Nominal values
Braces' steel quality	S355	
MRF & EBF beams steel quality	S235	
Concrete slab's thickness	15 cm	For composite solution only
Reinforcement	Φ10 mm @ 10 cm, both directions	
Concrete class	C25/30	

Table. 5.1.Dual frame's global characteristics

The following steps lead to the design of the structure:
1) Computation of the applied loads:
- Dead load: 4 kN/m^2;
- Live load (office building): 3 kN/m^2 (Table 6.2, SR EN1991-1-1-2004);
- Snow load – computed according to SR EN1991-1-3-2005;
- Wind load – computed according to SR EN1991-1-4-2006;
- Seismic load – design spectrum for Bucharest (control period T_c=1.6s, a_g=0.24g); reduction factor chosen as 4.5;
- Level masses computed as for a facade frame.
2) Definition of the plastic hinges for steel and composite dissipative sections – taken as implicit for the steel frame, and adjusted to specific parameters for composite frames;
3) Modelling of the concrete slab and connection of composite beam and frame in the design software. In our case the maximum mesh size is 300 by 300 mm, while in plastic zone the mesh is 25 by 30 mm;
4) Computation of the RBS' geometry and position, according to SR EN1998-3-2005, paragraph B.5.3.4;

5) Design checks, using SR EN1993, 1998; design of non-dissipative elements with a value of the product $1.1\gamma_{ov}\Omega = 2.5$ (Acc. to P100, annex F and suggested by ASCE Standard ASCE/SEI 7-05).

6) Check of the nonlinear behaviour of the structure by means of pushover analysis (target displacements for SLS and ULS determined by the N2 method) - recommended;

7) Evaluation of the seismic performance of the structure (time-history analyses performed on 3 accelerograms characteristic for Bucharest seismic conditions from Vrancea source).

Concerning the last point, that is rather a verification of structural performance than a design criterion, there have been considered three recordings (Vrancea '77, Vrancea '86 and Vrancea '90, all recorded at INCERC centre), and scaled for seismic intensities corresponding to SLS, ULS and CPLS conditions.

The geometric and structural properties of the frame designed with composite beams, with q=4,5:
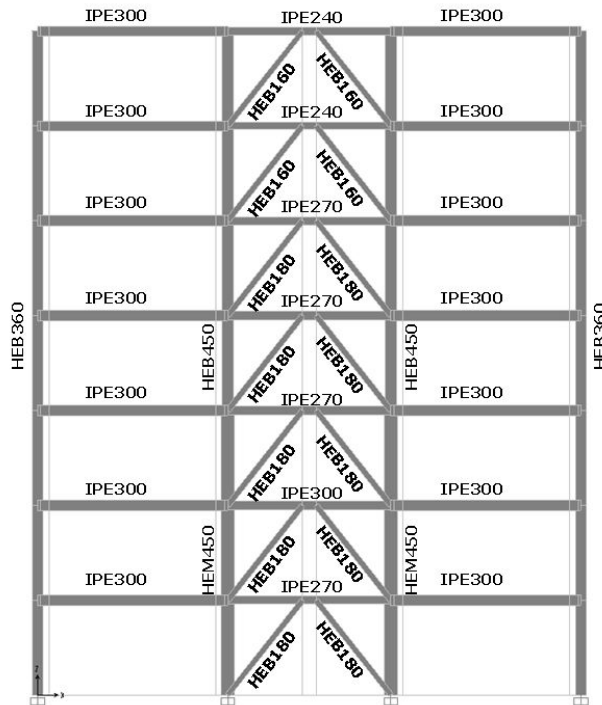
Fig. 5.2.   Frame designed for the case study

The following table gives the sections for all the three situations resulted after the detailed design procedure.

Level	MRF Beam			EBF Beam			Brace			Central Columns			Lateral Columns		
	steel	q=4	q=6	steel	q=4	q=6	steel	q=4	q=6	steel	q=4	q=6	steel	q=4	q=6
0	IPE400	IPE300	IPE360	IPE300	IPE270	IPE300	HE200B	HE180B	HE200B	HE400M	HE400M	HE400M	HE360B	HE360B	HE360B
1	IPE400	IPE300	IPE330	IPE300	IPE300	IPE330	HE200B	HE180B	HE200B	HE400M	HE400M	HE400M	HE360B	HE360B	HE360B
2	IPE400	IPE300	IPE360	IPE300	IPE270	IPE300	HE200B	HE180B	HE200B	HE400M	HE400M	HE400M	HE360B	HE360B	HE360B
3	IPE400	IPE300	IPE360	IPE300	IPE270	IPE300	HE200B	HE180B	HE200B	HE400B	HE400B	HE400B	HE360B	HE360B	HE360B
4	IPE400	IPE300	IPE360	IPE300	IPE270	IPE300	HE200B	HE180B	HE200B	HE400B	HE400B	HE400B	HE360B	HE360B	HE360B
5	IPE360	IPE300	IPE270	IPE270	IPE240	IPE270	HE180B	HE160B	HE180B	HE400B	HE400B	HE400B	HE360B	HE360B	HE360B
6	IPE360	IPE300	IPE360	IPE270	IPE240	IPE270	HE180B	HE160B	HE180B	HE400B	HE400B	HE400B	HE360B	HE360B	HE360B

Table. 5.2.Elements's sections of the analysed frames

The design shows no difference in the column sections for all three solutions. However, important differences result in the design of beams in composite solutions. The composite solution with no connection above the hinge regions has a certain advantage versus the steel, but due to the fact that it is generally designed for negative bending (where the RBS are not loaded) the sections stay close to the dimensions of the steel ones. On the other hand, the full composite solution uses significantly smaller sections.

The summary of the obtained results (Fig. 5.3 - Fig. 5.6), expressed in terms of lateral inter-story drift demands and plastic rotations in RBS zones and links show the differences between the three structural behaviours.
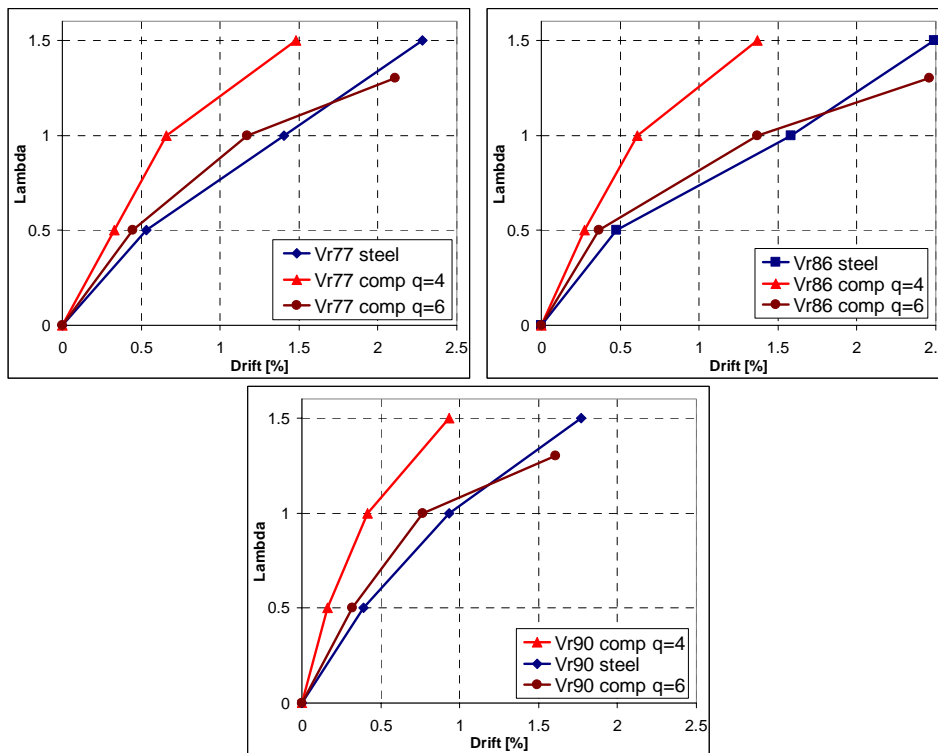
Fig. 5.3.   Drift comparison between steel and composite solutions for the studied structures

In a general manner, the steel and the derived composite structures (with q=6) are visibly more flexible than the one with full composite beams (see Fig. 5.3),

this having been proved at each levels considered in the incremental time-history analysis: ($\lambda = 0.5$ – SLS, $\lambda = 1.0$ – ULS, $\lambda = 1.5$ – CPLS). The 2.5% inter-story drift recorded for the steel structure reaches almost a physical limit of 3%, after which the second-order effects are becoming unacceptable for framed structures. In comparison, the composite frame remains at about half of this limiting value (1.5% at CPLS).

Concerning the plastic demands in hinges (Fig. 5.4 – Fig. 5.6), one could notice that in case of RBSs, the rotation requirements remain under acceptable limits (proven experimentally also) in both steel and composite conditions:

- 32 mrad for steel frame at CPLS;
- 10 mrad for full composite frame in the same conditions;
- intermediate values (although more close to steel) for composite frame with q=6.

The link remains the principal dissipative element. For all the accelograms considered in the study result high plastic requirements for both ULS and CPLS conditions (up to 160mrad for steel link, respectively 120 mrad for composite solution). Although in absolute values the composite link plastic requirement is smaller, if considering the available plastic distortions (155 mrad for steel respectively 115 mrad for composite), one could conclude that both structures reach their limitation in CPLS (see Fig. 5.4 for Vrancea 77 and Fig. 5.5 for Vrancea 86 recordings). The case of composite frame with q=6 show link distortion values close to steel solution. Another observation regards the way in which the links are working at high intensity seismic levels:

- the steel link shows high levels of rotation at ULS conditions (about 120 mrad) and consolidating up to the maximum levels at CPLS;
- the full composite solution develops most of its plastic capacity in-between the Ultimate Limit and Collapse Prevention Limit States.
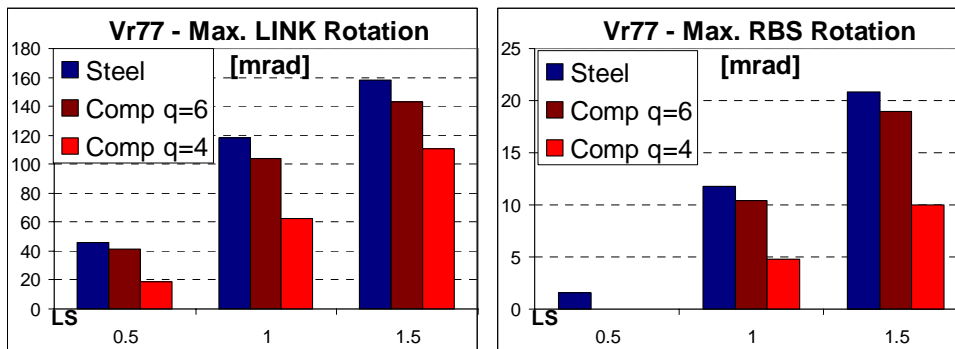
Fig. 5.4.   Maximum obtained rotations compared for the Vrancea `77 recording
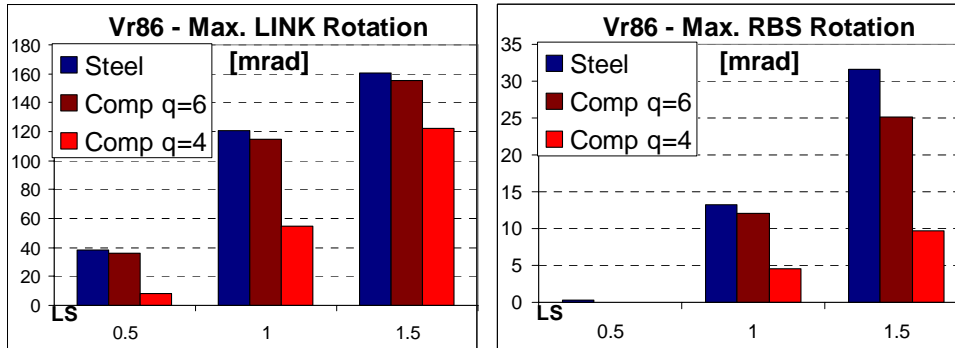
Fig. 5.5.   Maximum obtained rotations compared for the Vrancea `86 recording
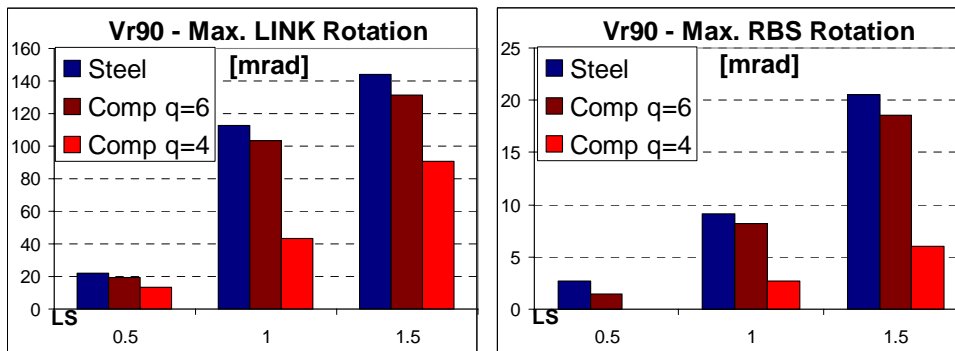
Fig. 5.6.   Maximum obtained rotations compared for the Vrancea `90 recording

The overstrength product $1.1*\gamma_{ov}*\Omega$ (see table 5.3) derived for the dual structure in a similar manner that is proposed in chapter 5 leads to values similar to those used in initial design (2.5), fact that confirms an optimum design of the structure. In consequence, no other iteration on column design is required.

EBF-6	Ω EBF			Ω MRF			Ω str.			1.1*γov*Ωstr.		
level	steel	comp q=4	comp q=6	steel	comp q=4	comp q=6	steel	comp q=4	comp q=6	steel	comp q=4	comp q=6
L0	1.39	1.88	1.54	1.94	1.33	1.22	1.94	1.88	1.54	2.66	2.58	2.12
L1	1.31	2.11	1.52	1.84	1.29	1.14	1.84	2.11	1.52	2.53	2.90	2.08
L2	1.28	1.78	1.67	1.79	1.27	1.11	1.79	1.78	1.67	2.46	2.45	2.30
L3	1.44	1.78	1.88	1.79	1.45	1.14	1.79	1.78	1.88	2.46	2.45	2.58
L4	1.77	1.82	2.13	1.81	1.29	1.13	1.81	1.82	2.13	2.49	2.50	2.93
L5	2.15	1.67	2.98	1.67	2.49	1.17	2.15	2.49	2.98	2.96	3.42	4.10
L6	3.77	3.68	10.80	1.96	4.69	1.30	3.77	4.69	10.80	5.18	6.45	14.86

Table. 5.3.Overstrength values obtained for the studied frames

Finally, an evaluation of the steel quantity used for the above compared steel and composite structures was made. By simple integration of the steel profiles it results that the steel structure requires 28.14 tons of steel (for the single frame analysed) while the full composite structure requires 24.54 tons of steel (-12.7%) – excluding the end-plates and other connection parts. In this way, the composite solution proves its economical benefit, while keeping the structural integrity in Ultimate Limit States and safety at Collapse Prevention. However, the frame

modelled with q=6 and composite beams without interaction in the plastic zones has lead to a steel consumption of 27.22 tons.

As a main conclusion, it could be stated that the full-composite frames could be a very efficient solution in design of DUAL frames subjected to strong seismic motions, even if a smaller behaviour factor is considered.

6. CONCLUSIONS AND PERSONAL CONTRIBUTIONS

6.1 Conclusions of the thesis

Chapter 1: Introduction – provides the reader the main target of the thesis, which is the study of the dissipative shear and bending zones from DUAL frames. The chapter justifies the use of composite beams, explains the interaction phenomena that occur at the steel-concrete interface and shows that these affect the behaviour of a composite beam.

Chapter 2: Hysteretic behaviour of composite beams – the purpose of the chapter is to give a brief preview of the existing similar studies and justify the necessity of the current work. The mentioned studies have proven mostly the efficiency of composite beams and their particularities when it comes to cyclic loading. None of these studies give exact measures that should be considered in the models for seismic design. Moreover, the existing norm provisions (both Eurocodes and American) are rather sceptical when it comes to defining the plastic hinges in these sections. Mostly general reinforcing guidelines and geometric characteristics are given. In the current design, the plastic hinge is considered to be efficient and safe by not ensuring the connection between steel and concrete. Still, this does not necessarily lead to a "pure steel" behaviour of the hinge, when the slab is located directly above it.

Chapter 3: Experimental program – is aimed directly at proving the previously mention assumptions by means of experimental tests. The specimens (isolated from a real structure) were chosen in such a way that they model both a bending hinge (by means of the RBS from MRF) and a shear hinge (EBF short link). The lab tests have managed to show that the initial assumptions were indeed true, by providing valuable data that ultimately lead to proposing new hinge curve definitions (with different compression and tension branches). These are able to accurately predict the behaviour of cyclically loaded composite beams.

Chapter 4: Numerical study – uses the proposed plastic hinge definitions in IDA analyses performed on 8 code designed structures. The results provided valuable conclusions and characteristics of the composite beams structural solution for seismic design. Numerical FE models were also calibrated, in order to fully comprehend the involved phenomena. Based on existing data, a new model that allows for an easier modelling of the composite beams is proposed.

Chapter 5: Design approach and proposed provisions – gives the main guidelines for the correct design (in the opinion of the author and based on the obtained results) of composite beams under cyclic loads (such as earthquakes). A new q factor is proposed for the DUAL systems with composite beams. In order to fully test and integrate the design methodology, a case study of a 6 story DUAL frame is investigated. As expected, the results underline once again the previously stated conclusions.

6.2 Contributions of the author

The main contribution of the author is represented by the design and execution of a coherent experimental program in order to investigate the dissipative behaviour of composite beams from EBF and MRF with RBS, with or without interaction with the concrete slab. The two test series studied the bending hinge from MRF beams and shear hinge from EBF links. In this direction, a number of 8 full-size EBFs and 6 beam-to-column joints with RBS were tested, both monotonic and cyclic. The results of the tests (interpreted and explained with close consideration to the current provisions) provided valuable results and emphasized the difference in behaviour between steel and composite solutions applied in the potentially plastic zones of DUAL frames.

It is worth mentioning that such experimental tests are the first ones in Romania.

The author proposes and calibrates a FE model for the design of structures with composite beams that can be easily used in structural design software SAP2000.

The obtained models for the composite beams' plastic hinges are then used in nonlinear IDA and Pushover. The extensive numerical program involved the design of 8 structures (different typologies such as MRF, EBF and DUAL), each modelled in 2 configurations, analysed under 7 earthquakes (approx. 1120 Time-history analyses). The „q" factor obtained from these analyses is discussed. The numerical program highlights the influence of the concrete slab that works together with the steel section in the dissipative elements.

A new "q" behaviour factor is proposed to be used for the DUAL frames designed with composite beams.

6.3 Published articles and dissemination of results

The main results and conclusions of the research have been presented and/or published in several conferences and national or international journals. A list of the most important papers and reports is presented below.

Conferences and Journals
- Sesiunea Nationala de Comunicari Stiintifice Studentesti, editia a VII-a, 18.04.2008, U.T. Cluj-Napoca: „Studiul Formarii Articulatiilor Plastice Intr-o Structura Duala cu Cadre MRF+EBF", author Gelu Danku.
- International Symposium: „Mineral Resources And Environmental Engineering" (B+), Universitatea de Nord, Baia Mare, 2008, ISBN 978-973-1729-74-9: "Development of Plastic Zones And Evaluation Of Rotation Capacity In Composite Members under Seismic Actions in EBF's", author Gelu Danku
- 11th WSEAS Int. Conference on Sustainability in Science Engineering (SSE '09), Timisoara, Romania, 27-29.05.2009, ISBN 978-960-474-080-2, (ISI), pg. 413-418: "Numerical Simulation of Composite Steel-Concrete Eccentrically Braced Frames (EBF) under Cyclic Actions", author Gelu Danku, Dan Dubina
- Simpozionul „Comportarea Structurilor Metalice La Actiuni Extreme", in cadrul celei de-a XI-a editii a Zilelor Academice Timisene, 29.05.2009:

"Simulare Numerica pe Cadre Contravantuite Excentric Solicitate in Regim Dinamic", authors Gelu Danku, Dan Dubina

- 6th PhD. & DLA Symposium (BDI), University of Pecs, Pollack Mihály Faculty of Engineering, September 2010: "Extensive Study of Plastic Hinges In Composite Steel-Concrete Members Subjected To Shear And/Or Bending", authors Gelu Danku, Dan Dubina.
- A 12-a Conferinţă Naţională de Construcţii Metalice, Timişoara, 26-27 Noiembrie 2010: "Formarea articulatiilor plastice in grinzi cu sectiune compusa din otel-beton in functie de gradul de interactiune", authors Gelu Danku, Adrian Ciutina, Dan Dubina.
- A 21-a Conferinţă Naţională AICPS, Bucureşti, 26 Mai 2011, titlul articolului: Modelarea articulaţiilor plastice în elementele structurale compuse din oţel-beton solicitate preponderent la forfecare sau încovoiere, autori Gelu Danku, Adrian Ciutina, Dan Dubina, published in AICPS Review, nr. 1-2/2011, ISSN 2067-4546, pg.44-52.
- EUROSTEEL 2011, Budapesta, 31 August – 2 Septembrie 2011, titlul articolului: Plastic hinges in composite steel-concrete beams of moment resisting and eccentrically braced frames, autori Gelu Danku, Adrian Ciutina, Dan Dubina, not published yet.

The results of the experimental and numerical studies were included in the framework of a national research project:

- PNCDI II „Parteneriate", contract nr. 31.042/2007 (cu titlul "Sisteme structurale şi soluţii tehnologice inovative pentru protecţia clădirilor la acţiuni extreme în contextul cerinţelor de dezvoltare durabilă PROACTEX").

The findings of tests on EBF systems of bolted links have been considered into the research project:

- SERIES TA User Agreement JRC N° 31817, "Full-scale experimental validation of dual eccentrically braced frame with removable links (DUAREM)"

Also, results of the research have been presented in the COST C26 Action "Urban Habitat Constructions Under Catastrophic Events".

REFERENCES

[1]   ESDEP course, http://www.fgg.uni-lj.si/kmk/esdep/master/toc.htm

[2]   Goel, S.C., Foutch, D.A., "Preliminary Studies and Test Results of Eccentrically Braced Full-Size Steel Structure", US-Japan Cooperative Earthquake Research Program 16th Joint Meeting, May 15-18, Washington DC, 1984.

[3]   Humar, J.L., "Composite Beams Under Cyclic Loading", Journal of The Structural Division, ASCE, Vol. 105, No. ST10, October 1979.

[4]   Moffat, K.R., "An Analytical Study of the Longitudinal Bending Behaviour of Composite Box Girder Bridges Having Incomplete Interaction", CESLIC Report CBI, Civil Engineering Structures Laboratory, Imperial College of Science and Technology, London, England, 1976.

[5]   Moffat, K.R., "Shear Lag in Steel Box Girder Bridges", The Structural Engineer, London, England, Vol.53, October 1975.

[6]   Kato, B., Aoyama, H., Okada, T., Uchida, N., "Composite Steel and Concrete Beams in the Building Structure in Japan", Regional Conference on Planning and Design of Tall Buildings, August 28-30, 1973, Tokyo, Japan.

[7]   Johnson, R.P., Willmington, R.T., "Vertical Shear in Continuous Composite Beams", Proceedings, Institution of Civil Engineers, 1972.

[8]   FEMA 350, „Recommended seismic design criteria for new steel moment-frame Buildings". Washington (DC), 2000.

[9]   Plumier A., „Reduced beam sections; a safety concept for structures in seismic Zones", Bul. Stiint. Univ. Politeh. Timisoara (Romania) 1996;41(2): pag. 46-59.

[10]   Plumier A., „New idea for safe structure in seismic zone", Proceedings of IABSE symposium on mixed structures including new materials, 1990, pag. 431-36.

[11]   Georgescu D., „Recent developments in theoretical and experimental results on steel structures. Seismic resistant braced frames", Costruzioni Metalliche 1996;1: pag. 39-52.

[12]   SAC Seismic design criteria for new moment-resisting steel frame construction. Report no. FEMA 350, SAC Joint Venture, Sacramento, CA. 2000.

[13]   Moore K, Malley OJ, Engelhardt M., „Design of reduced beam section moment frame connection", Structural Steel Educational Council: Technical Information and Product Service, California, 1999.

[14] Chen SJ, Chu JM, Chou ZL., „Dynamic behaviour of steel frames with beam flanges shaved around connection", J Construct Steel Res 1997;42(1): pag. 49-70.

[15] Popov E, Blondet M, Stepanov L., „Application of dog bones for improvement of seismic behaviour of steel connections", Report no UCB/EERC 96/05 1996, USA.

[16] Anastasiadis A, Gioncu V., „Influence of joint details on the local ductility of steel moment resisting frames", Proceedings of 3rd national Greek conference on steel structures, 1998.

[17] Anastasiadis A, Gioncu V, Mazzolani FM., „New upgrading procedures to improve the ductility of steel MR-frames", XVII C.T.A. Congress, 1999, pag. 193-204.

[18] Faggiano B, Landolfo R., „Seismic analysis of steel MR frames with dog bone connections", Proceedings of 12th European conference on earthquake engineering, 2002; paper reference 309.

[19] Engelhardt MD, Sabol TA., „Seismic-resistant steel moment connections: Developments since the 1994 Northridge earthquake", Zandonini R, Elnashai A, Dexter R, editors, Progress Struct. Eng. Mater. 1997;1(1): pag. 68-77.

[20] FEMA 351. Recommended seismic evaluation and upgrade criteria for existing welded steel moment frame buildings. Washington (DC), 2000.

[21] SR EN1998-1: 2004: Design of structures for earthquake resistance - Part 1: General rules, seismic actions and rules for buildings

[22] Ricles, James M. and Popov, Egor P., „Experiments On Eccentrically Braced Frames With Composite Floors", Earthquake Engineering Research Center, University Of California, Berkeley, California.

[23] SR EN 1994-1-1. (1992) EUROCODE 4: Design of Composite Steel and Concrete Structures. Part 1.1. General Rules and Rules for Buildings. Brussels: CEN, European Committee for Standardisation.

[24] Ciutina, A., „Comportamentul Seismic Al Îmbinărilor Cadrelor Necontravântuite Metalice Şi Compuse: Studiu Experimental Şi Simulare Numerică, teză de doctorat, INSA Rennes", 2003.

[25] M.A.Conti, V.Piluso, G. Rizzano & I.Tolone, „Seismic Reliability of Steel-concrete composite frames", STESSA 2006, Taylor & Francis Group, London.

[26] Pachoumis D.T. et al., „Reduced beam section moment connections subjected to cyclic loading: Experimental analysis and FEM simulation", www.elsevier.com/locate/engstruct

[27] Engelhardt Michael D., Winneberger Ted et al., „Experimental Investigation of Dogbone Moment Connections", Enginnering Journal (Fourth Quarter), 1998.

[28] Stratan, A., 2003, „Studiul Comportării Clădirilor Multietajate cu Cadre Metalice Duale Amplasate În Zone Seismice", teza de doctorat, UPT, 1998.

[29] P100-1-2006: Cod românesc de proiectare antiseismică

[30] European Convention for Constructional Steelwork, Technical Committee 1, TWG 1.3 – Seismic Design, No.45, 1986, Recommended Testing Procedures for Assessing the Behaviour of Structural Elements under Cyclic Loads.

[31] Plumier A., "ICONS Report 4. Composite Steel Concrete Structures". Laboratorio Nacional de Engenharia, Civil Editor, Lisbon-Portugal, 2001.

[32] Plumier, A. and Doneux, C., "European developments of seismic design guidelines for composite steel concrete structures", Proceedings of ICSCS'01 Conference, Pusan, Korea, 2001.

[33] Aribert, J.M. and Lachal, A.," Moment resistant connections of steel frames in seismic areas", pag. 299-313, Mazzolani Editor, E.F.SPON, London.

[34] Bouwkamp, J., Parung, H. and Plumier, A., "Bi-directional cyclic response study of a 3-D composite frame", Proceedings of the 11th ECEE Conference, Paris, 1998.

[35] Doneux, C. and Parung, H., "A study on composite beam-column subassemblages", Proceedings of the 11th ECEE Conference, Paris.

[36] Doneux, C. and Plumier, A., "Seismic design of the slab reinforcements of composite beams on moment frames", Internal Report for ICONS project, Université de Liège, 1999.

[37] ICONS Topic 4 Extended Group (1998), "Draft of a section Specific rules for steel concrete composite buildings", an ICONS project Report, Université de Liège.

[38] Plumier, A., Doneux, C., Bouwkamp, J.G. and Plumier, C. (1998), "Slab design in connection zones of composite frames", Proceedings of the 11th ECEE Conference, Paris.

[39] Plumier, C. and Doneux, C. (1998) "Dynamic tests on the ductility of composite steel-concrete beams", Proceedings of the 11th ECEE Conference, Paris.

[40] Sanchez, L and Plumier, A. (1999), "Particularities raised by the evaluation of load reduction factors for the seismic design of composite steel concrete structures", Proceedings of the SDSS'99 Stability and Ductility of Steel Structures Colloquium, Timisoara.

[41] Tsujii, M., Elnashai, A.S. and Broderick, B. (1999), "Experimental and analytical evaluation of behaviour factors for steel and composite frames", Internal Report for ICONS project, Imperial College London.

[42] Ioan, P., Dima, S., "Behaviour of eccentrically braced structures having active links connected or not with r.c. slab", Profesional Construct, http://www.p-c.ro/downloads.html

[43] G. Thermou, A.S. Elnashai, A. Plumier, "Seismic design and performance of composite frames"

[44] CSI Berkeley, SAP2000 v14.2.2, FAQ.

[45] Fajfar, P. (2000). "A nonlinear analysis method for performance-based seismic design". Earthquake Spectra, 16(3): 573-92, 2000.

[46] R. Simões and L. Simões da Silva, "Cyclic behaviour of end-plate beam-to-column composite joints", Steel and Composite Structures, Vol. 1, No. 3 (2001), 355-376.

[47] Dubina, D., Ciutina, A. L., Stratan, A., "Cyclic tests on bolted steel and composite double-sided beam-to-column joints", Steel and Composite Structures, Vol.2, No.2 (2002), 147-160.

[48] Bursi, O. S., Ferrario, F., Pucinotti, R., Zandonini, R., "Analysis of steel-concrete composite beam-to-column joints: bolted solutions"

[49] Kumar, P.N.N.S., "Development of a Phenomenological Model for Beam-to-Column Connections In Moment Resisting Frames Subjected to Seismic Loads, PhD Thesis, University of Cincinnati, 2006.

[50] ASCE Standard ASCE/SEI 7-05, "Minimum Design Loads for Buildings and Other Structures", American Society of Civil Engineers

[51] M. Bosco, P.P. Rossi, "Seismic behaviour of eccentrically braced frames", Engineering Structures, Vol. 31 (2009), p. 664-674.

[52] G. Vasdravellis, M. Valente, C.A. Castiglioni, "Behavior of exterior partial-strength composite beam-to-column connections: Experimental study and numerical simulations", Journal of Constructional Steel Research Vol. 65 (2009), p. 23–35.

[53] M. Malaska, "Behaviour Of A Semi-Continuous Beam-Column Connection For Composite Slim Floors", Helsinki University of Technology, Laboratory of Steel Structures Publications 20.

[54] A. Braconi, W. Salvatore, R. Tremblay, and O. S. Bursi, "Behaviour and modelling of partial-strength beam-to-column composite joints for seismic applications", Earthquake Engineering And Structural Dynamics 2007; vol. 36, p. 142–161

[55] M. A. Dabaon, M. H. El-Boghdadi, O. F. Kharoob, "Experimental and numerical model for space steel and composite semi-rigid joints", Journal of Constructional Steel Research, vol. 65 (2009), p. 1864-1875.

[56]   ABAQUS/PRE. Users manual. Hibbit, Karlsson and Sorensen Inc., 1997.

[57]   FEMA 356: Prestandard And Commentary For The Seismic Rehabilitation Of Buildings, November, 2000.

APPENDIX I

In the charts below, one can see the localisation of the structures' (from the numerical models) first period on the design spectra used:

F1 – 4 stories DUAL frame configuration

F1S P+4 dual steel		F1C P+4 dual composite	
T1	0.688	T1	0.676
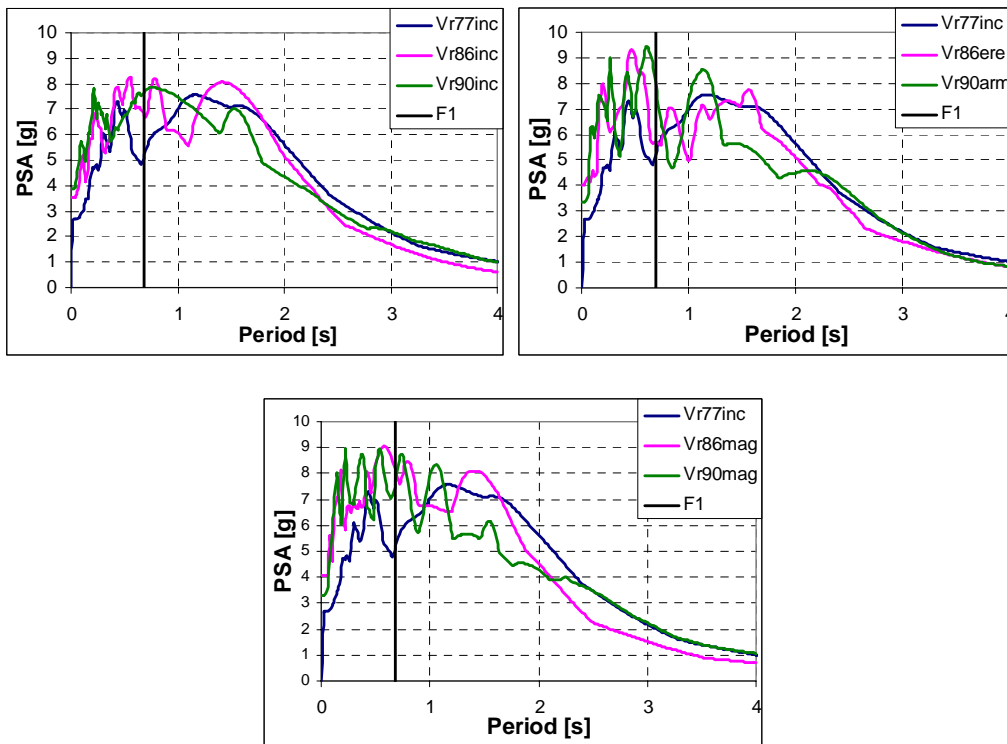
Fig. A.1.   First period for the DUAL 4 story structure

F2 – 4 stories EBF configuration

F2S P+4 EBF steel		F2C P+4 EBF composite	
T1	0.69	T1	0.6
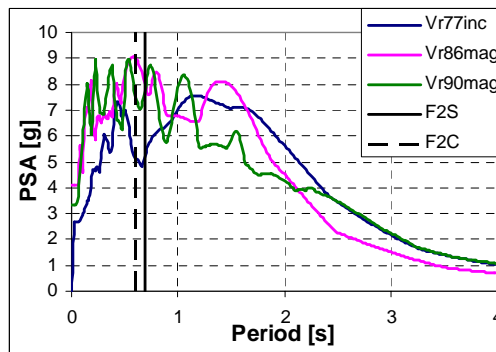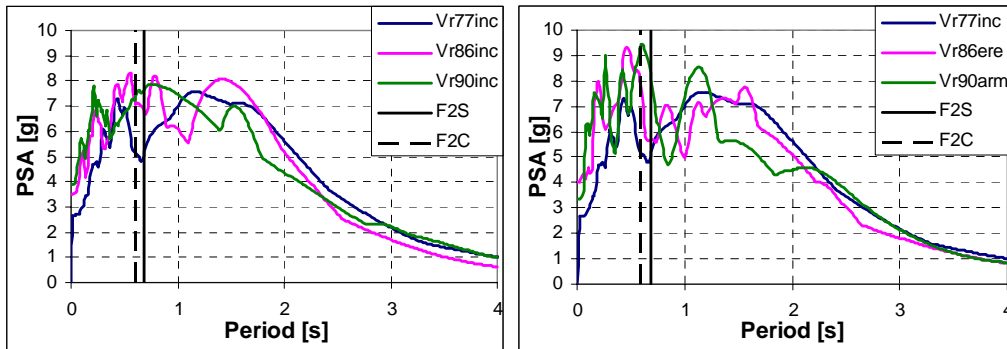
Fig. A.2.   First period for the EBF 4 story structure

F3 – 8 stories DUAL frame configuration

F3S P+8 DUAL steel		F3C P+8 DUAL composite	
T1	1.19	T1	1.14

Fig. A.3.   First period for the DUAL 8 story structure

F4 – 8 stories EBF configuration

F4S P+8 EBF steel	
T1	1.282

F4C P+8 EBF composite	
T1	1.175
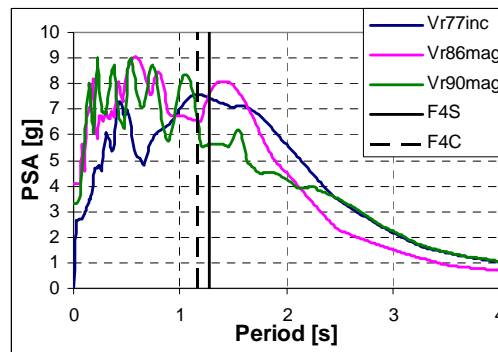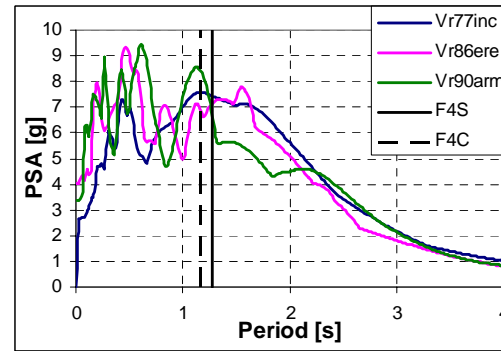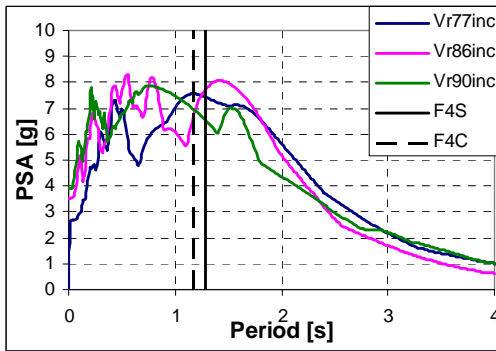
Fig. A.4.   First period for the EBF 8 story structure

F5 – 6 stories EBF configuration

F5S P+6 EBF steel	
T1	0.938

F5C P+6 EBF composite	
T1	0.878
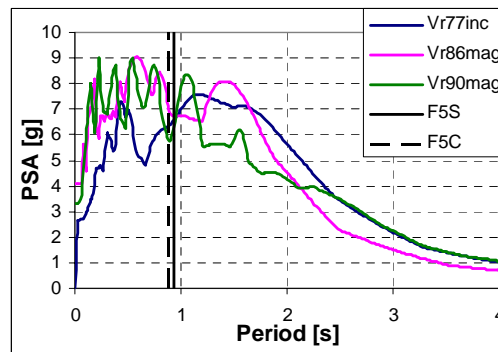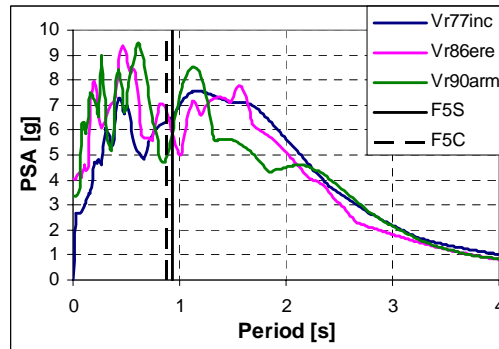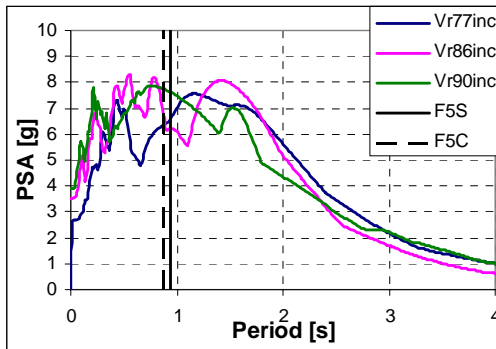
Fig. A.5.   First period of the EBF 6 story structure

F6 – 12 stories DUAL frame configuration

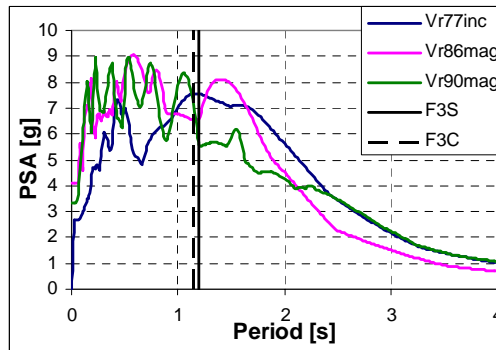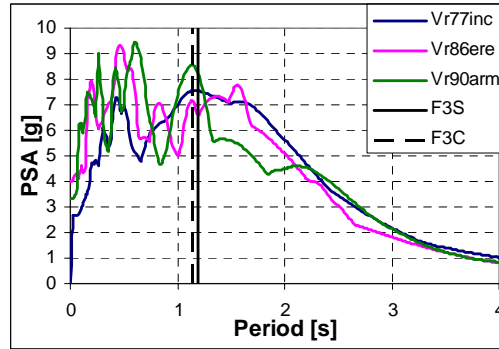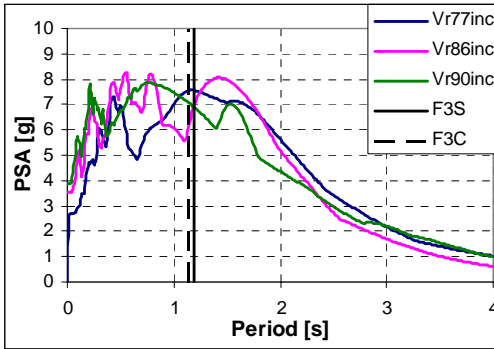| F6S P+12 DUAL steel		F6C P+12 DUAL composite	
T1	1.728	T1	1.56
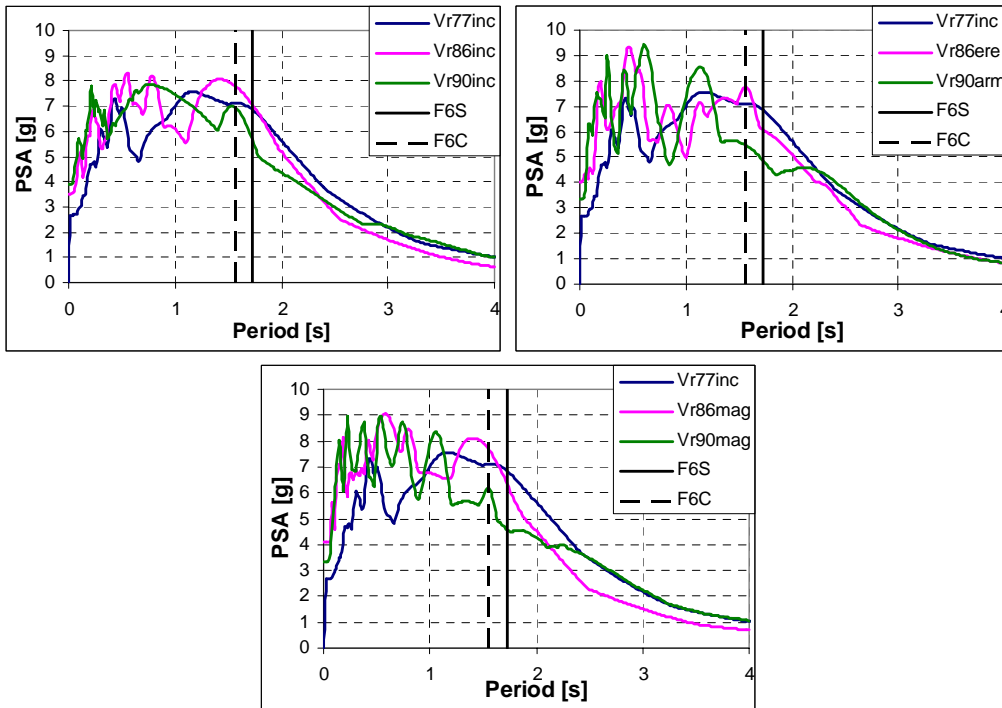
Fig. A.6.   First period of the DUAL 12 story structure

APPENDIX II

In the following table are shown the q and η factors calculated for all structures and quake recordings.

Structure	Configuration	Quake	λe	λu	Q	η	average Q
F1 P+4 dual	steel	Vr77inc	0.25	1.4	5.6	1.4	5.5
		Vr86inc	0.25	1.3	5.2	1.3	
		Vr86ere	0.25	1.4	5.6	1.4	
		Vr86mag	0.25	1.4	5.6	1.4	
		Vr90inc	0.27	1.4	5.18	1.4	
		Vr90arm	0.27	1.4	5.18	1.4	
		Vr90mag	0.22	1.3	5.9	1.3	
	composite	Vr77inc	0.3	1.2	4	1.2	3.9
		Vr86inc	0.3	1.1	3.66	1.1	
		Vr86ere	0.3	1.2	4	1.2	
		Vr86mag	0.3	1.2	4	1.2	
		Vr90inc	0.3	1.2	4	1.2	
		Vr90arm	0.3	1.2	4	1.2	
		Vr90mag	0.3	1.1	3.66	1.1	
F2 P+12 dual	steel	Vr77inc	0.2	1.3	6.5	1.3	5.8
		Vr86inc	0.2	1.3	6.5	1.3	
		Vr86ere	0.2	1.4	7	1.4	
		Vr86mag	0.3	1.4	4.66	1.4	
		Vr90inc	0.3	1.4	4.66	1.4	
		Vr90arm	0.3	1.4	4.66	1.4	
		Vr90mag	0.2	1.3	6.5	1.3	
	composite	Vr77inc	0.2	1.1	5.5	1.1	4.9
		Vr86inc	0.2	1.1	5.5	1.1	
		Vr86ere	0.2	1.2	6	1.2	
		Vr86mag	0.2	1.2	6	1.2	
		Vr90inc	0.3	1.2	4	1.2	
		Vr90arm	0.3	1.2	4	1.2	
		Vr90mag	0.3	1.1	3.6	1.1	
F3 P+5 MRF	steel	Vr77inc	0.2	1.5	6.5	1.5	5.8
		Vr86inc	0.2	1.5	6.5	1.5	
		Vr86ere	0.2	1.5	7	1.5	
		Vr86mag	0.3	1.5	4.66	1.5	
		Vr90inc	0.3	1.5	4.66	1.5	
		Vr90arm	0.3	1.5	4.66	1.5	
		Vr90mag	0.2	1.5	6.5	1.5	
	composite	Vr77inc	0.27	1.5	5.5	1.5	5.8
		Vr86inc	0.27	1.5	5.5	1.5	
		Vr86ere	0.25	1.5	6	1.5	
		Vr86mag	0.25	1.5	6	1.5	
		Vr90inc	0.25	1.5	6	1.5	
		Vr90arm	0.25	1.5	6	1.5	
		Vr90mag	0.27	1.5	5.5	1.5	

F5 P+6 EBF	steel	Vr77inc	0.2	1.1	5.5	1.1	
		Vr86inc	0.2	1.2	6	1.2	
		Vr86ere	0.2	1.2	6	1.2	
		Vr86mag	0.2	1.1	5.5	1.1	5.9
		Vr90inc	0.2	1.2	6	1.2	
		Vr90arm	0.2	1.2	6	1.2	
		Vr90mag	0.2	1.2	6	1.2	
	composite	Vr77inc	0.3	1.1	3.6	1.1	
		Vr86inc	0.3	1.2	4	1.2	
		Vr86ere	0.3	1.3	4.3	1.3	
		Vr86mag	0.3	1.1	3.6	1.1	3.6
		Vr90inc	0.3	1.2	4	1.2	
		Vr90arm	0.4	1.2	3	1.2	
		Vr90mag	0.4	1.2	3	1.2	
F6 P+8 EBF	steel	Vr77inc	0.2	1.3	6.5	1.3	
		Vr86inc	0.2	1.1	5.5	1.1	
		Vr86ere	0.2	1.2	6	1.2	
		Vr86mag	0.2	1.4	7	1.4	6.5
		Vr90inc	0.2	1.4	7	1.4	
		Vr90arm	0.2	1.3	6.5	1.3	
		Vr90mag	0.2	1.4	7	1.4	
	composite	Vr77inc	0.2	1.3	6.5	1.3	
		Vr86inc	0.2	1.1	5.5	1.1	
		Vr86ere	0.2	1.1	5.5	1.1	
		Vr86mag	0.2	1.3	6.5	1.3	5.8
		Vr90inc	0.2	1.3	6.5	1.3	
		Vr90arm	0.3	1.2	4	1.2	
		Vr90mag	0.2	1.2	6	1.2	
F7 P+8 DUAL	steel	Vr77inc	0.2	1.3	6.5	1.3	
		Vr86inc	0.2	1.3	6.5	1.3	
		Vr86ere	0.2	1.3	7	1.3	
		Vr86mag	0.2	1.3	4.66	1.3	5.8
		Vr90inc	0.2	1.5	4.66	1.5	
		Vr90arm	0.3	1.4	4.66	1.4	
		Vr90mag	0.3	1.4	6.5	1.4	
	composite	Vr77inc	0.3	1.3	4.3	1.3	
		Vr86inc	0.3	1.3	4.3	1.3	
		Vr86ere	0.3	1.3	4.3	1.3	
		Vr86mag	0.3	1.3	4.3	1.3	4.0
		Vr90inc	0.3	1.3	4.3	1.3	
		Vr90arm	0.4	1.3	3.2	1.3	
		Vr90mag	0.4	1.3	3.2	1.3	

Table. AII.1.   Factors q and η obtained from analyses

For a better understanding of the hierarchy of the beams, the Ω factors are shown in the following tables, for each structure, on levels.

DUAL-4	Ω EBF		Ω MRF		Ω str.		1.1*γov*Ωstr.	
level	steel	comp	steel	comp	steel	comp	steel	comp
L0	2.16	2.31	2.86	2.94	2.86	2.94	3.94	4.04
L1	2.29	2.22	2.83	2.94	2.83	2.94	3.89	4.04
L2	2.85	2.72	2.90	3.03	2.90	3.03	3.99	4.17
L3	3.88	3.73	3.09	3.23	3.88	3.73	5.34	5.13
L4	7.24	7.37	3.78	4.25	7.24	7.37	9.96	10.14

Table. AII.2.   Overstrength factors for the 4 stories DUAL frame

EBF-4	Ω EBF		Ω MRF		Ω str.		1.1*γov*Ωstr.	
level	steel	comp	steel	comp	steel	comp	steel	comp
L0	1.52	1.62	---	---	1.52	1.62	2.09	2.23
L1	1.75	2.04	---	---	1.75	2.04	2.40	2.81
L2	1.82	2.14	---	---	1.82	2.14	2.51	2.95
L3	2.00	2.57	---	---	2.00	2.57	2.75	3.53
L4	2.76	3.98	---	---	2.76	3.98	3.80	5.47

Table. AII.3.   Overstrength factors for the 4 stories EB frame

DUAL-8	Ω EBF		Ω MRF		Ω str.		1.1*γov*Ωstr.	
level	steel	comp	steel	comp	steel	comp	steel	comp
L0	1.63	1.63	1.81	2.29	1.81	2.29	2.49	3.14
L1	1.61	1.68	2.20	2.07	2.20	2.07	3.03	2.84
L2	1.64	1.55	1.57	1.94	1.64	1.94	2.25	2.67
L3	1.52	1.63	1.48	1.83	1.52	1.83	2.09	2.52
L4	1.58	1.76	1.43	1.77	1.58	1.77	2.17	2.44
L5	1.66	1.92	1.39	1.72	1.66	1.92	2.28	2.64
L6	2.11	2.65	1.39	1.73	2.11	2.65	2.90	3.64
L7	3.83	5.14	1.45	1.80	3.83	5.14	5.26	7.07
L8	3.19	4.64	1.62	2.13	3.19	4.64	4.38	6.39

Table. AII.4.   Overstrength factors for the 8 stories DUAL frame

EBF-8	Ω EBF		Ω MRF		Ω str.		1.1*γov*Ωstr.	
level	steel	comp	steel	comp	steel	comp	steel	comp
L0	1.81	1.91	---	---	1.81	1.91	2.48	2.63
L1	1.53	1.67	---	---	1.53	1.67	2.11	2.30
L2	1.56	1.77	---	---	1.56	1.77	2.15	2.43
L3	1.55	1.73	---	---	1.55	1.73	2.13	2.37
L4	1.60	1.93	---	---	1.60	1.93	2.20	2.65
L5	1.55	1.95	---	---	1.55	1.95	2.13	2.68
L6	1.59	2.15	---	---	1.59	2.15	2.19	2.96
L7	2.04	2.92	---	---	2.04	2.92	2.81	4.02
L8	3.22	5.90	---	---	3.22	5.90	4.43	8.11

Table. AII.5.   Overstrength factors for the 8 stories EB frame

EBF-6	Ω EBF		Ω MRF		Ω str.		1.1*γov*Ωstr.	
level	steel	comp	steel	comp	steel	comp	steel	comp
L0	2.22	2.37	---	---	2.22	2.37	3.06	3.25
L1	1.84	2.07	---	---	1.84	2.07	2.53	2.84
L2	1.98	2.26	---	---	1.98	2.26	2.72	3.11
L3	1.98	2.32	---	---	1.98	2.32	2.72	3.19
L4	2.35	2.84	---	---	2.35	2.84	3.23	3.90
L5	1.83	2.31	---	---	1.83	2.31	2.51	3.18
L6	2.36	3.61	---	---	2.36	3.61	3.25	4.96

Table. AII.6.   Overstrength factors for the 6 stories DUAL frame

DUAL-12	Ω EBF		Ω MRF		Ω str.		1.1*γov*Ωstr.	
level	steel	comp	steel	comp	steel	comp	steel	comp
L0	1.73	1.63	2.67	2.36	2.67	2.36	3.67	3.24
L1	1.60	1.59	2.07	1.94	2.07	1.94	2.84	2.66
L2	1.66	1.58	1.69	1.62	1.69	1.62	2.32	2.23
L3	1.57	1.58	1.48	1.47	1.57	1.58	2.16	2.17
L4	1.66	1.63	1.41	1.44	1.66	1.63	2.28	2.24
L5	1.76	1.74	1.36	1.41	1.76	1.74	2.42	2.40
L6	1.73	1.74	1.32	1.39	1.73	1.74	2.37	2.39
L7	2.00	2.06	1.33	1.39	2.00	2.06	2.75	2.84
L8	2.18	2.23	1.37	1.42	2.18	2.23	3.00	3.07
L9	2.37	2.42	1.38	1.49	2.37	2.42	3.26	3.33
L10	2.75	2.84	1.44	1.54	2.75	2.84	3.78	3.91
L11	3.91	3.74	1.53	1.64	3.91	3.74	5.37	5.14
L12	9.10	7.53	1.92	1.79	9.10	7.53	12.51	10.35

Table. AII.7.   Overstrength factors for the 12 stories DUAL frame

MRF-5ls	Ω EBF		Ω MRF		Ω str.		1.1*γov*Ωstr.	
level	steel	comp	steel	comp	steel	comp	steel	comp
L0	---	---	1.14	1.37	1.14	1.37	1.57	1.88
L1	---	---	1.08	1.18	1.08	1.18	1.49	1.62
L2	---	---	1.08	1.23	1.08	1.23	1.49	1.69
L3	---	---	1.02	1.40	1.02	1.40	1.40	1.93
L4	---	---	1.02	1.71	1.02	1.71	1.40	2.36

Table. AII.8.   Overstrength factors for the 5 stories MR frame (7.5 m span)

MRF-5ss	Ω EBF		Ω MRF		Ω str.		1.1*γov*Ωstr.	
level	steel	comp	steel	comp	steel	comp	steel	comp
L0	---	---	1.21	1.36	1.21	1.36	1.67	1.87
L1	---	---	1.04	1.30	1.04	1.30	1.43	1.78
L2	---	---	1.06	1.32	1.06	1.32	1.46	1.82
L3	---	---	1.07	1.48	1.07	1.48	1.46	2.04
L4	---	---	1.12	1.80	1.12	1.80	1.54	2.47

Table. AII.9.   Overstrength factors for the 5 stories MR frame (6m span)

APPENDIX III – EXPERIMENTAL TESTS

The mechanical properties of the structural steel and reinforcing steel components were determined from coupon tests in accordance with standard SFS-EN 10 002-1 "Metallic materials. Tensile testing. Part 1: Method of test (at ambient temperature)" (1990).
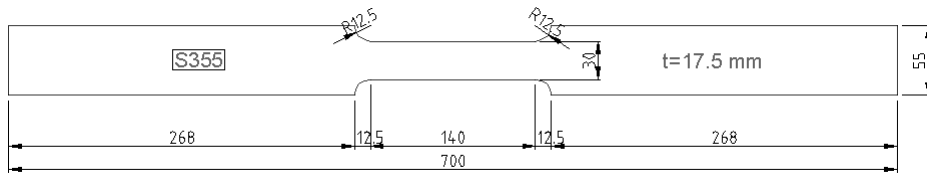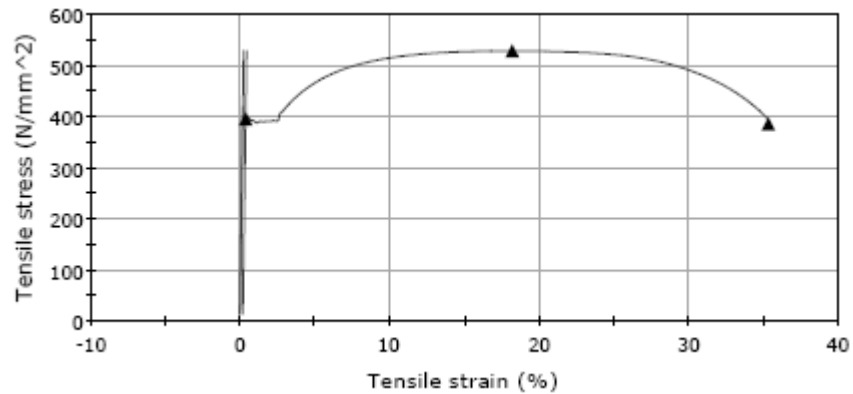

Fig. A.7.   Example of a material specimen

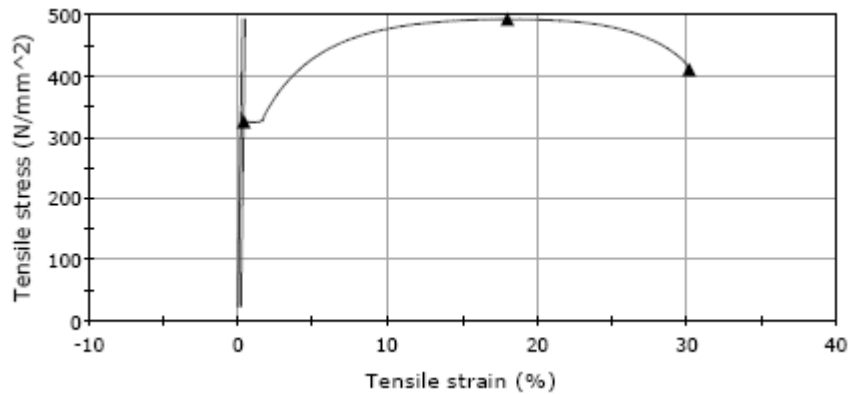Fig. A.8.   Stress-strain curve for HEA180 profile (EBF braces)

Fig. A.9.   Stress-strain curve for HEA200 profile (link's web)
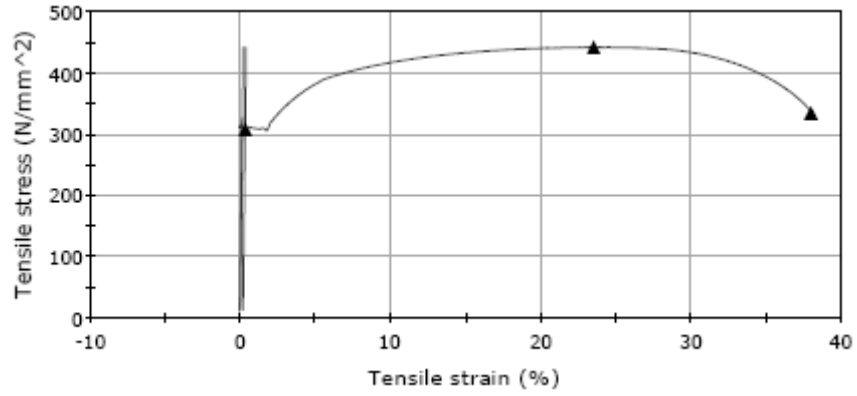
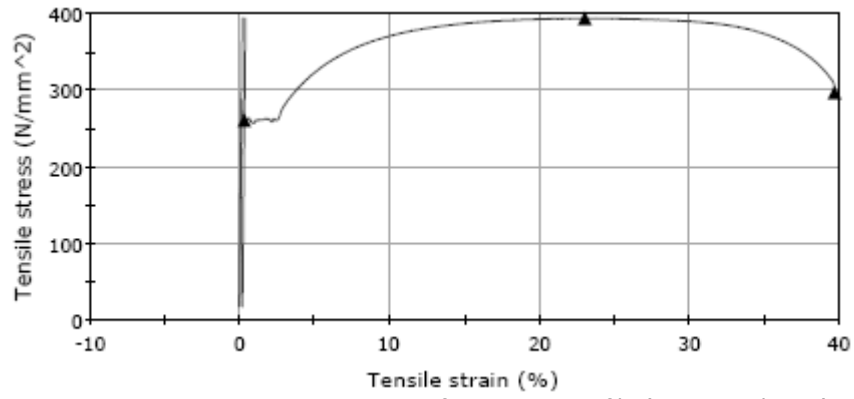Fig. A.10.   Stress-strain curve for HEA200 profile (link's flange)

Fig. A.11.   Stress-strain curve for HEA260 profile (MRF joint beam)
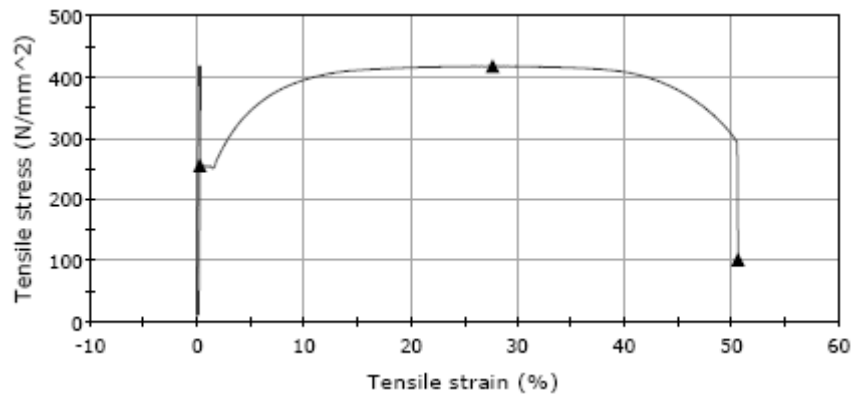

Fig. A.12.   Stress-strain curve for HEB260 profile (MRF joint column)

In this section are shown some representative details and the global behaviour of some specimens during the tests.

Fig. A.13. Instrumentation of the fixed link

Fig. A.14. EBF at the initiation of yield in link

Fig. A.15. EBF displacement during the test (ultimate state)

Fig. A.16.   Test setup for the EBF with composite beam

Fig. A.17.   Local damage of the concrete slab over the link

Fig. A.18. Cyclic testing of the joint with RBS

Fig. A.19.   Cyclic testing of the joint with RBS

Fig. A.20. Cyclic testing of the composite joint with RBS

Fig. A.21. Cyclic testing of the composite joint with RBS

Fig. A.22. Concrete cracking at the beam-to-column joint under positive bending